# MACHINE VISION INSPECTION OF DATE FRUITS

By

ABDULRAHMAN A. AL-JANOBI

Bachelor of Agriculture Science
King Saud University
Riyadh, Saudi Arabia
1986

Master of Science
Oklahoma State University
Stillwater, Oklahoma
1990

Submitted to the Faculty of the
Graduate College of the
Oklahoma State University
in partial fulfillment of
the requirements for
the Degree of
DOCTOR OF PHILOSOPHY
May, 1993

OKLAHOMA STATE UNIVERSITY

MACHINE VISION INSPECTION OF

DATE FRUITS

Thesis Approved:

Glenn A. Kranzler
Thesis Adviser

Kenneth A. Ingram

Gerald H. Brusewitz

Thomas C. Collins
Dean of the Graduate College

ACKNOWLEDGMENTS

I wish to express my sincere appreciation to Dr. Glenn Kranzler for serving as my major adviser; for his assistance, friendship, support, and patience. Without his guidance this project would never have been completed. I feel fortunate to have worked with him.

I would also like give my gratitude to Dr. Marvin Stone, Dr. Gerald Brusewitz, and Dr. Keith Teague for serving on my committee. Their suggestions and support were very helpful throughout this study.

Appreciation must be extended to Dole Dried Fruit and Nut Company for supplying date fruit samples. I also want to thank John Davies, manager Dole quality control for date operations, for his advice and support.

Thanks goes to Mike Rigney for his assistance with the IRI computer. Thanks also goes to my friends who made OSU such a rewarding experience.

A special thanks goes to my wife who made life easier in Stillwater. I appreciate her patience and support.

Finally, I would like to dedicate this work to my father and mother, my brothers and sisters, and all other members in my family for their support and encouragement throughout my study in the United States.

TABLE OF CONTENTS

LIST OF TABLES

LIST OF FIGURES

Figure Page

Figure Page

## NOMENCLATURE

| | |
|---|---|
| $\epsilon$ | Belongs to |
| $\theta$ | Angle |
| $\|COV\|$ | Determinant of covariance matrix |
| $\|a\|$ | Absolute value of a |
| A | Gray-level image |
| ACF | Autocorrelation function |
| C | Celsius |
| CCD | Charge-coupled device |
| CCM | Co-occurrence matrix |
| cm | Centimeter |
| $COV_i$ | Covariance matrix within-class, i |
| d | Distance, number of pixels |
| FOV | Field-of-view |
| FT | Fourier transform |
| G | Number of gray levels |
| GLRLM | Gray-level run-length matrix |
| HSI | Hue, saturation, intensity |
| K | Kelvin |
| kg | Kilogram |
| m | Meter |
| mm | Millimeter |
| nm | Nanometer |
| $N_{TU}$ | Texture unit number |

| | |
|---|---|
| P | Co-occurrence matrix |
| RGB | Red, green, blue |
| ROI | Region-of-interest |
| s | Second |
| SAR | Synthetic aperture radar |
| STD | Standard deviation |
| TS | Texture spectrum |
| USDA | United States Department of Agriculture |
| W | Watt |

# CHAPTER I

## INTRODUCTION

The date palm originated in Saudi Arabia, Iraq, Iran, and some of the northern African countries. The date is still the traditional agricultural product of its native countries. Spanish missionaries introduced the date palm to North America. In the United States, most date fruits are grown in California, with relatively limited production. The Kingdom of Saudi Arabia is the world's largest producer of dates, with an annual harvest of more than 480,000 tonnes from over 8 million trees representing more than 50 varieties (Saudi Arabia Ministry of Agr. & Water 1987). While most Americans have limited interest in date fruits, Saudians are the world's highest consumers. Annual per capita consumption averages over 40 kg.

In the United States, most date processing plants are located in California. Plants in Saudi Arabia and the United States differ in size and processing operations. Processing steps before washing such as harvesting, field grading, transportation to plants, and grading are called preprocessing. Processing includes the steps from washing to packaging.

There are hundreds of date fruit varieties which vary

in texture, color, moisture content, sugar content, size, and shape. Overall, date fruits can be categorized into three types by moisture content; soft, semi-dry, and dry.

In general, grading is based on color, size, surface defects, and texture. Color is an important factor in distinguishing between acceptable date fruits and damaged or immature dates. The color of acceptable dates is characteristic and relatively uniform. Size is affected by variety and the condition of the producing trees. Dates are rejected if they are significantly larger or smaller than the subjective average size of the dates or contain surface defects. Texture is a useful factor for identifying overdried "hard" dates. Moisture content is the main criterion in date grading in the United States. Uniformity of shape is also an important factor in identifying overdried dates and dates with surface defects.

The criteria for grading dates are based on visual judgment. Therefore, successful automation requires a system which can obtain results similar to those of manual graders. Early in the development of digital computers, researchers have attempted to design machines with "vision" capability (Horn 1987). Coupling a video camera with a specialized computer has enabled the development of machines capable of visual interpretation. Such machine vision systems have gained acceptance in food production industries. Many systems have been installed in food processing plants for inspection and grading.

Researchers continue to study the use of specialized machine vision for agricultural products that rely on visual inspection. Because color and texture are critical criteria in date grading, and since they are based on visual perception, color machine vision incorporating texture analysis is a potentially useful method for inspecting dates.

## Statement of Problem

In recent years, engineers have made substantial progress in automating inspection of fruits and vegetables. Date fruits, however, are still graded by hand.

Manual date inspectors use elasticity, surface texture, and color as the main grading criteria (Chesson et al. 1979). Elasticity is used as an indication of moisture content and is determined by touch. Surface texture and color indicate moisture and sugar content. These features are defined visually. Color is a difficult criterion, because perception is affected by lighting intensity and distribution, as well as the color spectrum of the light source (Davies and Perkins 1991).

Manual grading of dates carries disadvantages. Accuracy fluctuates during the workday as worker concentration varies. Cost is high and the labor supply is unstable. Automating the grading process is highly desired by the date industry.

## Objectives

The overall objective of this research is to investigate the potential of computer vision for inspecting and grading dates. Specific objectives are to:

1. Develop image processing techniques to grade dates into quality classes based on color and texture analysis,
2. Evaluate the accuracy of the techniques by comparison with manual inspection.

# CHAPTER II

# LITERATURE REVIEW

## Introduction

As background for the development of a machine vision approach to the grading of date fruits, literature was reviewed in a number of areas. Pertinent regions covered were computer vision applications, date fruits, color, and texture analysis.

## Computer Vision Applications

Over the last decade, computer vision has been used effectively in food processing applications. Sarkar and Wolfe (1985a, b) developed a method to sort fresh market tomatoes. They used an area-scan camera with a 530-nm interference filter to obtain images of stem and blossom ends of individual tomatoes. A light spot surrounded by a dark ring identified the stem end and distinguished it from the blossom end. Boundary chain code was used to define the shape of tomatoes. Size of tomatoes was calculated from the area within the chain-coded boundary. Tomato color was determined from gray levels within four windows. The system sorted tomatoes into two classes ("acceptable" or "reject"), with a 3.5% error rate. Error rate increased with more

classes or with small tomatoes.

Rehkughler and Throop (1985) used machine vision to sort apples for bruise defects. They used a line-scan camera to obtain images. Bruise shape analysis was performed by calculating a thinness ratio (ratio of area to the square of the perimeter). By thresholding thinness ratio between a minimum and a maximum value, clusters of circular shape were identified as apple bruises. Correlation between measured and predicted areas was 0.84. The system was able to classify 30 apples per minute into USDA standard grades (XFancy, Fancy, Utility, and Cull).

Davenel et al. (1988) developed a machine vision system to grade Golden Delicious apples for defects. An area-scan camera was used with a 550-nm band-pass filter to enhance the contrast between good and defective apples. The system operated at high speed (5 apples/s), but with a high overall error rate (31%).

Rehkughler and Throop (1989) used image thresholding techniques to segment bruised apple tissue. The system identified bruised areas with correlation coefficients of 0.64 to 0.73, with respect to human inspection. Using thresholding, the system was able to differentiate between bruises and other defects such as scab, bird pecks, insect stings, and hail damage.

Varghese et al. (1991) developed a comprehensive vision system to sort apples based on color, surface defects, shape, and size. Color classification accuracy was 100%.

Surface defects were detected with 85% accuracy.

Kaplan et al. (1984) describe a machine vision system for grading lemons. The system had nine production lines, each capable of grading 7.5 fruits per second. Grading decisions were based on lemon size, color, color contrast, and blemish size. The system was capable of grading lemons with 100% accuracy.

Sunkist developed a machine to grade oranges and lemons (Johnson 1985). The system used line-scan cameras to detect surface defects, analyze fruit color, and estimate fruit size. The system was capable of sorting ten fruits per second.

McClure and Morrow (1987) used a vision system to measure the size and shape of potatoes. The system measured the three axes with 1% error for the major axis, 0% error for the intermediate axis, and 2% error for the minor axis. Marchant et al. (1988) presented a machine vision system to sort potatoes for size and shape. The system was capable of sorting 40 potatoes per second. Tao et al. (1990) also described a machine vision system for grading potato size, shape, color, damage, disease, and blemishes. Two color cameras were used to collect images. Accuracy of the system was 90% for green grade detection and 89% for shape separation, compared to manual inspection.

Miller and Delwiche (1988) developed a machine vision system to identify maturity of peaches based on color. Accuracy of the system was 65%, compared with manual

inspection. They later used a machine vision system for detecting and identifying peach defects (Miller and Delwiche 1989). Sample correlation coefficients between predicted and measured defect areas ranged from 0.51 to 0.91 for surface cuts and scars, respectively. Overall error in identifying defects ranged from 26% to 43%.

Computer vision has been investigated as a method for grading bell peppers for orientation and shape (Wolfe and Swaminathan 1987). Six area-scan cameras were used to obtain six orthogonal views of samples. A Hough transform was applied to locate stem and blossom end centers. Accuracy of the Hough transform with preprocessing ranged from 81% to 95%. The system was capable of defining the shape with a 23% overall error rate. Wolfe and Hoernlein (1988) measured the ratio of red area to total area on bell peppers by using image processing techniques. Various band-pass filters were tested. Best performance was obtained at 650 nm, where the correlation coefficient between predicted and measured areas was 0.985.

Delwiche et al. (1990) developed a machine vision system to classify defective and acceptable prunes. A line-scan camera was used to collect images. Algorithms were simplified to achieve an inspection rate of 20 prunes per second. Classification error was 0% and 1.8% for acceptable and defective prunes, respectively.

A machine vision system for grading carrots for surface defects, size, and shape has been reported (Howarth and

Searcy 1989). Howarth et al. (1990) used machine vision techniques to identify tip shape. By using the Marquardt method (nonlinear least squares), tip shape was described by six parameters. The system was capable of grading carrots into five classes with a 14% error rate.

A raisin grading system using computer vision has been reported by Okamura et al. (1991). A gradient operator was used to detect edges. Texture was determined from wrinkle edge density. Angularity, elongation, size, area, and luminance were measured as grading criteria. Accuracy of the system for three grade classifications was 84% in grading substandard raisins, 66% in grading thin-fleshed raisins, and 78% in grading fine-wrinkled raisins. The accuracy of the system when using two grade classifications was 77% in grading thin-fleshed raisins and 78% in grading fine-wrinkled raisins.

## Date Fruits

Previous researchers have attempted to design methods to sort dry and semi-dry dates. Chesson et al. (1979) developed a vacuum system for separating dates. The system contained a press wheel and a drum with three zones of variable surface vacuum. The system was capable of separating 98% of high-moisture fruit from fresh dates. The accuracy of separating freshly harvested dates into three classes (Waxy, Number 1 Dry, and Number 2 Dry) was 65%, 70%, and 66%, respectively. The date industry requires a minimum

accuracy of 85%. Huxsoll and Reznik (1969) used mechanical methods to sort dates. Their system required that individual dates slide down a 1.5-m tube inclined at 40 to 50 degrees from horizontal, onto a metal impingement plate. Differences in sliding velocity related to lower friction and impingement reaction allowed dry dates to travel farther than soft dates and fall into different channels.

Davies and Perkins (1991) studied the effect of lighting intensity and color spectrum on manual grading of dates. They noted that increasing the illumination level from 62 to 140 footcandles enhanced the visual inspection of dates. The combination of cool white and daylight fluorescent lighting over a medium green background produced the best color contrast between different grades. Their previous work showed that using the upper red color spectrum for illumination enhanced the contrast between grades.

Dull et al. (1991) used near-infrared spectrophotometry to measure moisture content of whole dates (Deglet Noor variety). They measured the radiation that passed through the date samples and developed a relationship between transmittance and moisture content. Their method was capable of grading dates with 74% accuracy.

The earliest work on sorting dates with machine vision was done in 1986 by the VARTEC Co. in California. The algorithms in this project were developed to estimate moisture content from surface texture. Unfortunately, this work is undocumented and no longer active (Brown 1991).

Wulfsohn et al. (1989) studied the use of image processing techniques on two date varieties (Medjool and Zahidi). Their work addressed separating "good" dates from "defective" dates using thresholding techniques. A color camera was used to collect date images. They found that specular reflectance (glare) was a major problem. Relative reflectance was measured in the range of 400 to 1100 nm for good and defective dates. The largest differences between dry dates and dates with blister defects occurred at 600 nm for Medjools and in the 450-600 nm range for the Zahidi variety. An infrared cutoff filter was then used for obtaining images of both varieties, and an infrared cutoff filter combined with an optical filter for Medjools. They noted that the red-band image was most effective for detecting defective Medjool dates. The green-band image performed best with Zahidi dates.

## Color

Color is the basic description of the visible spectrum in terms of electromagnetic radiation. The visible spectrum comprises the wavelengths from 400 nm to 700 nm. The human eye perceives the color of an object by determining the nature of the light reflected from the object in view.

Sir Isaac Newton discovered the nature of color in 1704. He showed that sunlight consists of a spectrum of colors. The visible colors, so-called primary colors, are combinations of red, green, and blue. In 1931, the CIE

(Commission Internationle de l'Eclairage - the International Commission on Illumination) specified the wavelengths of primary colors to be 435.8, 546.1, and 700 nm for blue, green, and red, respectively. However, humans distinguish color based on intensity, hue, and saturation. Intensity refers to the brightness of chromatic light. Hue represents pure colors that the eye senses such as yellow, orange, red, green, etc. Saturation indicates the amount of white light mixed with hue. Colors such as lavender (violet + white) are less saturated, whereas the pure colors are totally saturated. Chromaticity refers to hue and saturation combined. In 1976, CIE developed a chromaticity scale.

RGB (red, green, blue) and HSI (hue, saturation, intensity) are the most commonly used color models. Figure 1 shows the RGB color cube. The color values have been normalized to present a unit cube. The RGB color values are at the axis-bound corners of the cube. Yellow, magenta, and cyan are at the extended corners. Black is at the origin, while white is at the far corner. The line between the black and white corners represents the gray scale.

The RGB color model is commonly used in cameras, television sets, and monitors. Color cameras work in the same way as black-and-white cameras, but the image is triplicated by separating red, green, and blue signals. The RGB model is desirable for obtaining and displaying images, but it is computationally intensive when processing the image. The RGB model does not represent the human visual

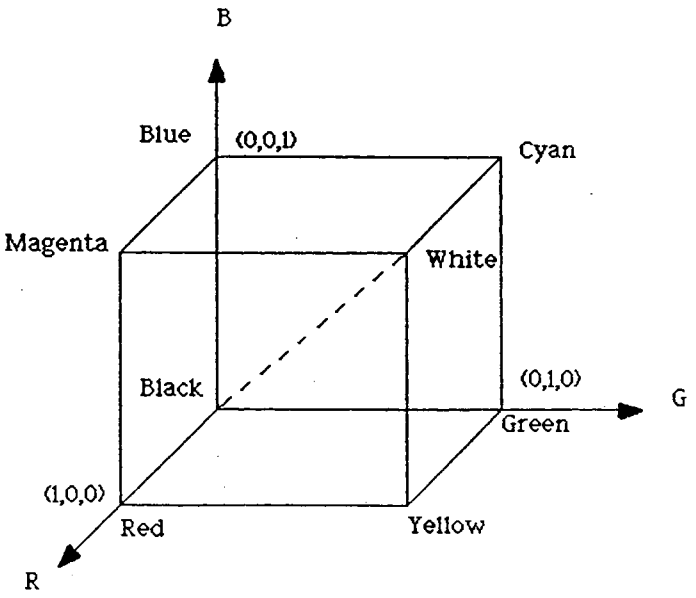


Figure 1. RGB Color Cube.

system. Therefore, processing one component of the RGB model to determine the color of an object is meaningless. For example, examining the green band of an RGB image of a violet object does not support specifying its color.

The HSI model mimics the human visual system. Figure 2 shows the color representation scheme. The hue, H, of color point P is the angle between the red axis and CP vector. Thus, when H = $0^{o}$, the color is red, when H is $120^{o}$ the color is green, when H is $240^{o}$ the color is blue, etc. Saturation, S, is proportional to the distance from the center of the triangle, C, and P. The color is fully saturated when the distance between C and P is at its maximum. The perpendicular line passing through the center of the HSI color triangle represents the intensity (Fig.2b).

Processing the HSI color images is faster and less complicated. Each band of HSI system contains meaningful information related to the human visual system. Therefore, each band can be processed separately. As an example of the HSI color model, consider pure red paint. Hue is the red color. Since the red is not diluted with white, the paint is fully saturated. By adding white color, the paint becomes less saturated. The red color becomes light red. Intensity of the paint can be controlled by dimming the lights in the room. The intensity decreases as the light dims until it becomes black.

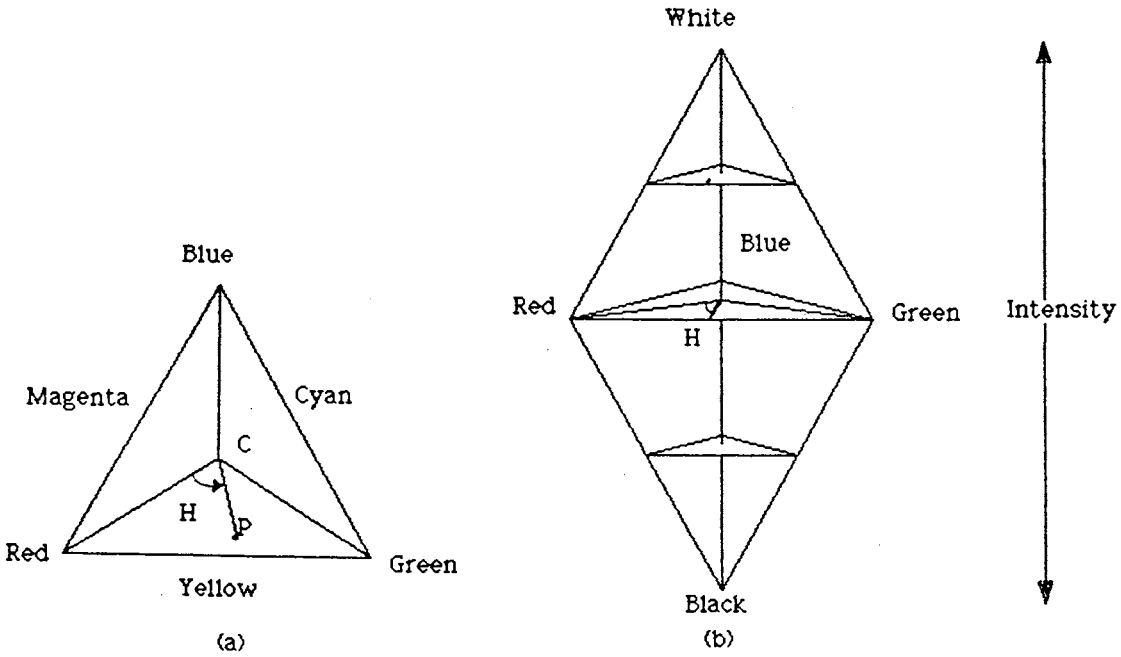


Figure 2. (a) HSI Color Triangle, (b) HSI Color Solid.

The RGB model can be converted to the HSI model. The following expressions show the relationship between HSI values and RGB values (Gonzalez and Woods 1992).

$$I = (1/3)*(R+G+B) \quad (1)$$

$$S = 1 - \{3\ [MIN\ (R,G,B)]\}/(R+G+B) \quad (2)$$

$$H = \cos^{-1}\left\{\frac{(0.5)*[(R-G)+(R-B)]}{[(R-G)^2 + (R-G)(G-B)]^{0.5}}\right\} \quad (3)$$

$$H = 360^{o} - H \ ;\ \text{if}\ [(B/I) > (G/I)\ ] \quad (4)$$

Color images contain more information than black-and-white images. However, color image processing is used less frequently than monochrome processing due to increased hardware cost, processing complexity, and greater processing time.

Monochrome systems are fully capable of meeting the needs of most industrial inspection applications. However, many agricultural inspection applications require color processing capabilities. Fruits and vegetables are typically inspected for color, shape, size, texture, defects, etc. Food inspection applications using both true color machine vision and black-and-white systems with color filters have been reported.

Unklesbay et al. (1986) studied the color distribution of beef ribeye steaks after heat processing. They classified steaks into five "doneness" categories (rare, medium-rare, medium, medium-well, and well) according to

traditional internal temperature specification. Images were obtained by using a black-and-white vision system through three color filters (red, green, blue). The mean, standard deviation, skewness, and kurtosis of the R, G, and B histograms were determined and used as grading criteria. The authors found that the mean and standard deviation were most successful in identifying steak doneness classes. Accuracy was 80%.

Meyer et al. (1988) compared the ability of a black-and-white and a color imaging system to determine the percent residue cover on the soil surface. Video and 35-mm film cameras were used to obtain field images on tape and slides. Images were then transferred to a computer vision system. Red and near-infrared high-pass filters were tested on the black-and-white system to provide better contrast. The authors found that the color system produced higher accuracy than the black-and-white system in all cases.

Ruzhitsky and Ling (1992) developed a machine vision system for tomato seedling inspection. A black-and-white camera was used with two color filters centered at 671 and 800 nm. The gray-level ratio from the two images $[I_{(x,y)800}/I_{(x,y)671}]$, called the radiant energy sensitivity, was used as a feature in classifying tomato seedlings.

Slaughter and Harrell (1987) reported the use of color vision to identify orange fruits in the tree canopy. The system was designed to control a picking arm for fruit harvest. They used a color decoder to transform recorded

video images into RGB images. Look-up tables for each of the three color images were developed to distinguish between oranges and background. Processing requirements were too demanding for real-time operation.

Color machine vision has been used for detection and classification of fungal-damaged soybeans (Wigger et al. 1988). Ratios of the red, green, and blue color bands were used to detect surface color differences. The system was able to differentiate between healthy and fungal-damaged soybeans with 98% accuracy. Comparing plant pathology classification with computer vision classification, fungal-damaged soybeans were correctly classified in 77 to 91% of tested samples.

Liao et al. (1991) used a color machine vision system to classify corn kernel hardness. The system correctly measured the vitreous and floury endosperm area of a corn kernel, which black-and-white images could not identify. The system was capable of classifying 4.3 kernels per minute. Ahmad and Reid (1991) reported the study of color representation, color calibration, and color quantification in corn due to water and nitrogen stress. They considered the correlation of color changes with stages of plant growth.

Singh et al. (1992) described a color machine vision system to evaluate peach maturity. Classification by color machine vision, manual inspection, and colorimeter were compared. Machine vision grading agreed with manual

classification in 46% of the tests, and with colorimeter results in 66% of the tests. A look-up table was designed using Bayes decision theory to partition the red-green plane of the RGB color space into six categories. Algorithms were developed for real-time inspection. The system was capable of classifying 5-10 fruits per second.

## Texture Analysis

For more than 25 years, texture analysis has been investigated by researchers. Texture analysis is a very important technique for characterizing digital images. Researchers have developed a number of techniques for texture analysis and classification. Their aim was to extract texture features for use in object classification.

Statistical and structural techniques are the two main approaches used to analyze texture. Both are based on characterization of the stochastic properties of the gray-level distribution. Statistical analysis characterizes texture as being fine, coarse, grainy, etc. The structural approach deals with the arrangement of image primitives, and is more difficult and complicated.

Several statistical approaches have been investigated, such as autocorrelation function, Fourier Transform, co-occurrence, gray-level run length, and texture spectrum.

The autocorrelation function is a feature which describes the size of the tonal primitives. It is defined as:

$$ACF(m,n) = \Sigma_i \Sigma_j A(i,j)\ A(i-m,j-n) \qquad (5)$$

where:

A(i,j) is the gray-level image,

T is the region length, $-T \leq (m,n) \leq T$.

As the autocorrelation function spreads (larger values of m and n), coarser textures are detected by the function. Pratt (1991) showed equations that measure the autocorrelation spread:

$$S(u,v) = \Sigma_{m=0}^{T} \Sigma_{n=-T}^{T} (m-\lambda_m)^u\ (n-\lambda_n)^v\ ACF(m,n) \qquad (6)$$

where:

$$\lambda_m = \Sigma_{m=0}^{T} \Sigma_{n=-T}^{T} m\ ACF(m,n)$$

$$\lambda_n = \Sigma_{m=0}^{T} \Sigma_{n=-T}^{T} n\ ACF(m,n)$$

S(1,1), S(2,2), and S(0,2) and S(2,0) represent the cross-relation, the second-degree spread, and the profile spreads, respectively. Resolution selection is critical in detecting texture. For example, a region may exhibit coarse texture at low resolution and fine texture at high resolution. The autocorrelation function is not a powerful procedure for classifying texture. It cannot accurately specify the texture of images, because different images may have the same autocorrelation function value.

The Fourier Transform (FT) is a well-known technique used in signal processing applications. Han and Feng (1991) extracted thirty-three features from the FT of egg shell images to detect cracks. The authors used multivariate discriminant analysis to analyze the 33 features. They

found that cracks were detected with an 88% success ratio. Han et al. (1992) used the same procedure for inspection of corn kernel stress cracks. Classification accuracy was 96%. Although the FT is a powerful technique, it is computationally intensive.

The number of edges per unit area has been used to classify textures. The approach can be implemented by producing an edge map array E(i,j) such that E(i,j) = 1 for a detected edge and E(i,j) = 0, otherwise. The following equation defines the texture measure:

$$T(i,j) = (1/W^2)\Sigma_{m=-w}^{w} \Sigma_{n=-w}^{w} E(i+m,j+n) \qquad (7)$$

where W is the width of the region. Okamara et al. (1991) used the edge density approach to classify raisins.

Haralick et al. (1973) presented the most commonly used texture features derived from the co-occurrence matrix. The co-occurrence matrix is known as a gray-tone spatially-dependent matrix.

The co-occurrence matrix can be specified according to relative frequencies. Assume the distance between two pixels A(j,k) and A(m,n) is d at angle $\theta$. Then, P(a,b;d,$\theta$) represents the co-occurrence matrix in which each pixel is quantified over a range $0<(a,b)<G-1$, where G is the gray level. It is necessary to limit the number of angles and distances to reduce computation. Figure 3 shows the geometry for measuring co-occurrence matrices for a unit distance and four angles: $0^{\circ}$, $45^{\circ}$, $90^{\circ}$, and $135^{\circ}$. Figure 4a

shows a gray-level image matrix with four gray tones. The co-occurrence matrices in four directions are illustrated in Figure 4b. The distance, d, is the measured distance between a pair of pixels. Thus, when d = 1, the texture-context information is extracted from the two nearest neighboring pixels [i.e. A(i,j) and A(i,j+1)], when d = 2, texture-context information is extracted from the two next neighboring pixels [i.e. A(i,j) and A(i,j+2)], etc. This method will be described in detail in Chapter VI.

The features of the co-occurrence matrix have been used successfully in many applications. For example, Han and Hayes (1988) used the co-occurrence matrix to measure crop cover based on the textural difference between soil and canopy.

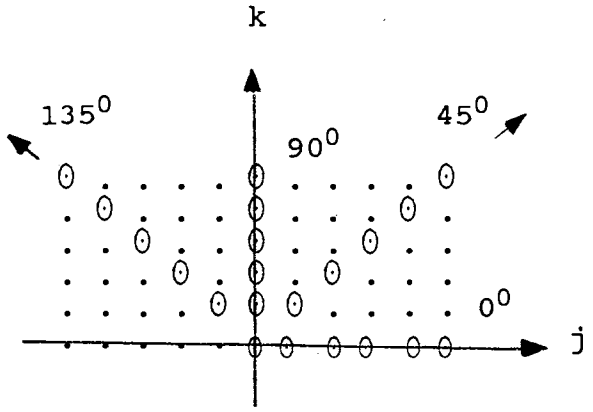


Figure 3. Four Directions of the Co-occurrence Matrix.

$$A(j,k) = \begin{vmatrix} 0 & 0 & 1 & 1 \\ 0 & 0 & 1 & 1 \\ 0 & 2 & 2 & 2 \\ 2 & 2 & 3 & 3 \end{vmatrix}$$

(a)

$$P(j,k;0^0) = \begin{vmatrix} 4 & 2 & 1 & 0 \\ 2 & 4 & 0 & 0 \\ 1 & 0 & 6 & 1 \\ 0 & 0 & 1 & 2 \end{vmatrix} \qquad P(j,k;45^\circ) = \begin{vmatrix} 4 & 1 & 0 & 0 \\ 1 & 2 & 2 & 0 \\ 0 & 2 & 4 & 1 \\ 0 & 0 & 1 & 0 \end{vmatrix}$$

$$P(j,k;90^0) = \begin{vmatrix} 6 & 0 & 2 & 0 \\ 0 & 4 & 2 & 0 \\ 2 & 2 & 2 & 2 \\ 0 & 0 & 2 & 0 \end{vmatrix} \qquad P(j,k;135^\circ) = \begin{vmatrix} 2 & 1 & 3 & 0 \\ 1 & 2 & 1 & 0 \\ 3 & 1 & 0 & 2 \\ 0 & 0 & 2 & 0 \end{vmatrix}$$

(b)

Figure 4. Obtaining the Co-occurrence Sets.
(a) Gray-level Image Matrix,
(b) Four Co-occurrence Matrices.

Galloway (1975) derived five texture features from a gray-level run-length matrix (GLRLM). Consecutive pixels with the same gray-level represent a run. The run length is the number of pixels in the run. The GLRLM can be defined in four directions: horizontal, +45°, vertical, and -45°. Figure 5 illustrates the GLRLM sets in the horizontal and vertical directions. The five features derived from GLRLM were used to measure the size of broccoli heads (Wilhoit et al. 1990). Wilhoit et al. applied a GLRLM to distinguish the broccoli head from leaves. An exponential relationship between head area and numerical texture measure was obtained. The error of head diameter measurement was less

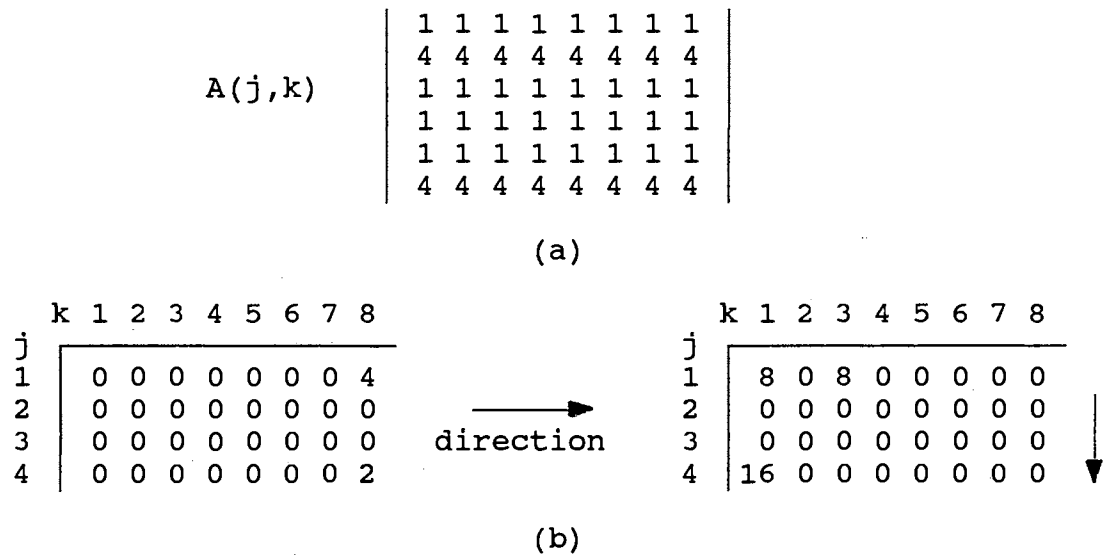


Figure 5. Obtaining the GLRLM Sets.
(a) Gray-level Image Matrix,
(b) Horizontal and Vertical Run-Length Matrices.

than 10%.

He and Wang (1991) proposed new features based on texture spectrum techniques. In this approach, a texture unit represents a pixel and its nearest neighbors. The texture spectrum is the distribution of texture units and characterizes the texture of an image. Figure 6 illustrates the development of a texture unit. The texture spectrum method will be described in detail in Chapter VI.

He and Wang (1991) evaluated the performance of texture spectrum features for discriminating images of six natural textures (beach sand, water, pressed cork, fur hide of an unborn calf, beach sand, and pressed calf leather). They found that the use of six texture features allowed discrimination of the six image categories.

Texture unit (TU) = $(E_1, E_2, \ldots, E_8)$

where:

$$Ei = \begin{cases} 0 & \text{if } Vi < V0 \\ 1 & \text{if } Vi = V0 \\ 2 & \text{if } Vi > V0 \end{cases}$$

| | | |
|---|---|---|
| V1 | V2 | V3 |
| V8 | V0 | V4 |
| V7 | V6 | V5 |

3x3 neighborhood

Texture unit number $(N_{TU}) = \sum_{i=1}^{8} E_i \, 3^{(i-1)}$

| | | |
|---|---|---|
| 63 | 28 | 45 |
| 88 | 40 | 35 |
| 67 | 40 | 21 |

→

| | | |
|---|---|---|
| 2 | 0 | 2 |
| 2 | | 0 |
| 2 | 1 | 0 |

→ 6095

V = (40,63,28,45,35,21,40,67,88) →
TU = (2,0,2,0,0,1,2,2) → $N_{TU}$=6095

Figure 6. Texture Unit.

Several researchers have studied different approaches to texture analysis in an attempt to identify the most effective method. Weszka et al. (1976) showed a comparative study of the Fourier spectrum, co-occurrence matrix, and GLRLM. They found that performance of the Fourier spectrum approach was significantly inferior to that of co-occurrence matrix and GLRLM. They also demonstrated that co-occurrence matrix was superior to GLRLM. He and Wang (1991) compared the performance of three texture spectrum features with that

of five features of the co-occurrence matrix on synthetic aperture radar (SAR) images. They concluded that for the example used, texture spectrum features performed more effectively in classifying textures.

## Color and Texture

Biological materials are rarely separated on the basis of one criterion. The classification usually depends on color, texture, shape, size, etc. Combining color and texture techniques, then, should improve classification, compared with either technique alone. Harms et al. (1986) extracted both co-occurrence matrix features and GLRLM features from RGB color images for blood cell analysis. They found that this combination provided more information and more accurate identification than texture analysis with a black-and-white system.

Krutz et al. (1991) showed the advantage of applying texture analysis to color images, as compared with gray-level images, for identifying weed seeds. Gray-level run-length features and twelve features of co-occurrence matrix were extracted from gray-level and RGB images. For one particular feature, identification accuracy increased from 43% using gray-level images to 90% when using RGB images. The best performance for a single feature was 88% correct identification when using gray-level images and 97% when using RGB images.

Shearer and Holmes (1987) used a co-occurrence matrix

to discriminate between plant cultivars. Eleven features were derived from HSI components. The classification accuracy was 81, 64, and 81% for intensity, saturation, and hue, respectively. Accuracy was increased to 90% by combining three features from the intensity with four features from the hue component.

# CHAPTER III

# DATE INSPECTION

## Introduction

The date palm originated in Saudi Arabia, Iraq, Iran, and some of the northern African countries. Spanish missionaries introduced the date palm to North America. In the United States, most date fruits are grown in California. The United States date production is about 18,000 tonnes, worth 14 million dollars annually (Wulfsohn et al. 1989).

Several date varieties are grown in the United States including Barhee, Khadrawy, Medjool, Zahidi, and Deglet Noor. Barhee is a soft date with a sweet taste. The popularity of this variety has increased in recent years. Annual production of a Barhee palm is about 300 pounds (136 kg). The Khadrawy variety is also a soft date, but not as popular. Khadrawy palm production ranges from 100 to 150 pounds (45 to 68 kg) per year. Medjool is a soft date from Morocco. It has the largest fruit size among commercial varieties. Annual production of this variety is 100 to 150 pounds (45 to 68 kg) per palm.

The Zahidi variety is a semi-dry date, popular in the United States. A Zahidi palm produces 200 to 300 pounds (91 to 136 kg) of dates per year. Deglet Noor, a semi-dry date,

is the most popular variety in the United States. It accounts for more than 80% of United States production. A single tree produces 200 to 300 pounds (91 to 136 kg) of dates annually.

## Date Identification

In the United States, date fruits are inspected and graded manually using United States Department of Agriculture (USDA) standards. The USDA grading standards define six classes of date fruits (USDA 1977): Natural, Waxy, Number 1 Dry, Number 2 Dry, Utility (substandard), and Cull. The United States date industry, however, uses only five classes (Chesson et al. 1979). Utility class is not recognized. The moisture content of each class varies with variety (soft, semi-dry, or dry) and seasonal weather conditions (wet or dry).

The description of date classes for the Deglet Noor variety follows USDA grading standards. Natural dates are soft and pliable, and have smooth skin with uniform color and little variation between dates. Moisture content is 23% or higher. They may require dehydration to prepare them for packing.

Waxy dates are generally firm, but slightly pliable. Waxy dates show mild surface wrinkles at the tips. Color of individual dates is uniform, but color among dates is quite varied (lighter or darker). Moisture content ranges from 20 to 23%.

Number 1 Dry dates are usually firm. Fruits of this class have a moisture content of 15-19%, with moderate surface wrinkle and a reasonably uniform color. They require hydration to prepare for packing.

Number 2 Dry dates are firm and contain less than 15% moisture content. The fruits have a very wrinkled surface, and show a fairly uniform color. Preparation for packing usually requires hydration.

Utility dates do not meet the characteristics of the above classes, but are still edible. This class is not used by the United States date industry.

Culls comprise dates with surface defects and poorly developed dates. These dates cannot be used for human consumption. Dates of this class can be used for animal feed or other production such as alcohol and inedible syrup.

The date industry occasionally combines two or more USDA classes into one grade. Dole Dried Fruit and Nut Company, Thermal, CA, for example, classifies Deglet Noors into three grades; A, B, and C. Grades A and C are Natural and Cull dates, respectively. Grade B includes Waxy, Number 1 Dry, and Number 2 Dry dates.

## Date Fruits

In this research, the Deglet Noor variety was examined. Dole Dried Fruit and Nut Company, Thermal, CA provided dates which were manually classified by a grading expert following USDA grading standards (Davies 1992). Dates from the 1991

and 1992 harvests were used. The 1991 crop was softer and more mature. The season was relatively cool. Date production was approximately 30% Grade A, 45% Grade B, and 25% Grade C (Davies 1992).

The 1992 growing season was hot. Fruit dried early, and the harvest was completed six weeks ahead of schedule. Date production was approximately 5% Grade A, 50% Grade B, and 45% Grade C (Davies 1992). Figures 7 and 8 show date fruits from the 1991 and 1992 crops.

Figure 7. Representative Dates From the 1991 Crop. Classes (from Left to Right) are Natural, Number 1 Dry, Number 2 Dry, and Cull.

Figure 8. Representative Dates From the 1992 Crop. Classes (from Left to Right) are Natural, Waxy, Number 1 Dry, Number 2 Dry, and Cull.

# CHAPTER IV

# EQUIPMENT

## Introduction

A computer vision system for automated date grading is composed of two functions: image acquisition and image analysis. This chapter describes hardware components used for images acquisition. The main components are the lighting system, camera, image digitization hardware, and microcomputer.

## Illumination

Lighting is one of the most important components in a machine vision system. Appropriate lighting reduces processing time and the use of expensive hardware and software. Lighting should enhance the acquired images in a way that simplifies later processing. High contrast between inspected features and their backgrounds is desired. Several illumination techniques have been defined which are generally useful for specific types of applications. These techniques include front lighting, back lighting, and structured lighting.

Front lighting is the most widely used method in machine vision applications. In this technique, the light

source and camera are on the same side of the target object. Front lighting is often used for texture or surface feature inspection. Back lighting is widely used for dimensional measurements. The object is positioned between the camera and a uniform light source. The camera views a sharp silhouette.

Structured lighting is most often used to extract three-dimensional information. The structured lighting can be achieved with directed light. In this technique, the camera and light source are on the same side of the target object. The light source projects a plane of light at an angle with respect to the camera line of sight. The line of light created traces the cross-sectional profile of the object. By moving the object or using a series of lines of light, the machine vision system can use triangulation to calculate a three-dimensional map of the object.

## Illumination Sources

Light source selection is an important factor in lighting system design. Illumination uniformity over the field-of-view (FOV) and spectral composition of the light are primary considerations. Various types of illumination sources are available. Incandescent, fluorescent, xenon strobe, and laser are the major illumination sources used in machine vision applications. Each of these sources has unique physical properties, including spectral distribution and color temperature. These properties are commonly used

for describing light sources. Color temperature of a light source is the temperature at which a blackbody radiator should be operated to have the same chromaticity as that of light source (North American Philips Lighting 1984).

Incandescent tungsten bulbs are widely used in machine vision applications. They operate at a color temperature of about 2850° K. Their highest radiant energy is in the infrared region (800-2000 nm). Tungsten halogen bulbs have a more constant visible output. Their color temperature is about 3200° K. In some applications, halogen bulbs are coupled with fiber-optic bundles to direct light to specific locations.

Fluorescent lamps are designed in various shapes and sizes. Fluorescent lamps generate more ultraviolet energy than incandescent bulbs. Their color temperature is about 3500° K (white). Generally, fluorescent lamps are useful in inspecting highly reflective parts, because they produce a diffuse light. The non-uniform spectral distribution of fluorescent lamps causes problems in color systems, because the relative outputs in the blue (350-480 nm) and green (480-600 nm) regions of spectrum are larger than the response of the red region (600-780 nm).

Xenon tubes are most widely used for inspecting moving parts. A xenon tube generates a 1 to 200-microsecond pulse which illuminates and freezes the motion of the objects. Spectral distribution ranges from 200 to 2000 nm. Color temperature is 6000-7000° K, which is similar to daylight

(about 6500° K).

Lasers are used mostly as structured light sources to project a line or spot on the target. The use of lasers has increased in recent years.

Lighting System

For this research, directional front lighting was configured to enhance the object surface texture. The light source consisted of two light projectors, each equipped with a 250W tungsten halogen bulb. The light projector generated a uniform light output.

Figure 9 shows the lighting system as a part of the machine vision system. The projectors were positioned on opposite sides of the object and inclined about $5^0$ above horizontal. Light projected slightly above parallel with an object surface causes surface depressions to appear dark with highlights from wrinkle ridges or raised points. A single light projector can illuminate only about half of the field-of-view (FOV) under $5^0$ orientation, because the date fruit is cylindrical in shape. Two light projectors were used to illuminate all of the FOV.

A natural wax coating on the surface of some dates caused specular reflection. A single polarizing filter placed in front of the camera was used to reduce the effect.

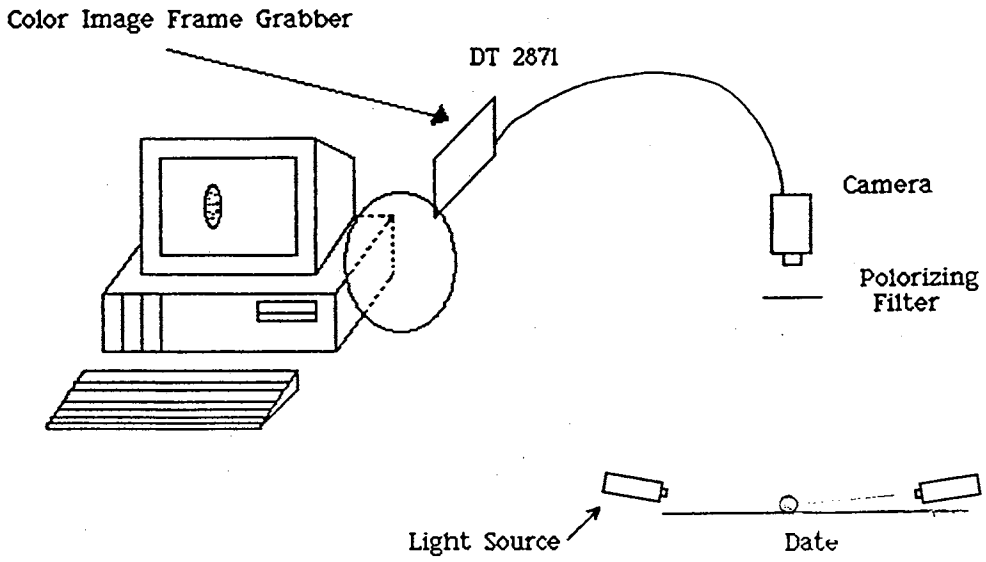


Figure 9. Block Diagram of Machine Vision System.

## Image Sensor

Image sensors used in machine vision applications fall into two general categories; Vidicon and solid-state cameras. A Vidicon camera utilizes an electron beam to scan a photoconductive layer onto which an optical image is formed. Solid-state devices consist of a monolithic array of closely spaced photodetectors, which are typically charge-coupled devices (CCDs). CCDs are manufactured in different geometric configurations ranging from linear arrays to matrices with various resolutions.

Color CCD cameras use either a single sensor overlaid with a primary color vertical stripe filter, or use three CCDs, one for each primary color. Color cameras with three CCDs are more accurate in terms of color separation.

For date inspection, a Sony Model XC-711 color camera was used. Red, Green, and Blue (RGB) outputs were available in parallel as RS-170 signals. The camera used a single CCD with 768 (horizontal) and 493 (vertical) pixels. A 50-mm (f/1.7) C-mount lens was used.

## Signal Digitization

A Data Translation Model DT2871 color frame grabber was used with an Everex 80486/33e microcomputer for image acquisition and processing. The DT2871 had three A/D converters which simultanensly digitized the RGB input signals into frames with 480 rows, 512 pixels per row, and 8 bits per pixel, in 1/30 s. The frame grabber was capable of converting the RGB signals into HSI (Hue, Saturation, and Intensity) signals in real time. A library of C language subroutines, Aurora, (Data Translation 1991) provided a variety of image processing functions, as well as control of image digitization and display.

# CHAPTER V

# IMAGE ANALYSIS

## Introduction

Image analysis encompasses the extraction and quantification of image features. The selected features should provide a useful description of the inspected object. The complexity and difficulty of image analysis can be reduced through optimization of the inspection environment. Environmental variables include the type of illumination and the object background.

Image analysis consists of three major functions (Jain 1989). These functions are image segmentation, feature extraction, and image classification. Image segmentation involves identifying the region-of-interest (ROI) and separating it from the background. The feature extraction technique calculates the properties (features) of the object. Image classification assigns the object to one of a set of classes, on the basis of measured features.

## Image Segmentation

Image segmentation involves the use of various techniques such as thresholding, boundary detection, filtering, template matching, and clustering to define a

meaningful region. In this study, image segmentation was defined by a 64x64-pixel ROI over the date surface. The ROI covered an area of 0.88 $cm^2$. Locations of the ROI are specified in the next chapter.

## Feature Extraction

Feature extraction is the procedure of generating descriptions of an object in terms of measurable features. A feature may be described as a parameter that characterizes the relationship between pixels. Extracted features utilize the relevant properties of the object, and may be used with a classifier to assign the object to a class or grade.

In this project, surface color and texture were the features of interest. Three different approaches to surface description were investigated. These approaches are the first-order histogram (Pratt 1991), the co-occurrence matrix, and the texture spectrum. The first-order histogram consists of simple statistical features such as the mean of histogram. The co-occurrence matrix is the most commonly used method for identifying texture (Haralick et al. 1973). Texture spectrum is a new technique, presented as a powerful texture analysis method by He and Wang (1991).

The aim of this research is to investigate the potential of machine vision color and texture measurements for use in automated date grading. Color and texture features may be extracted from the RGB component images or from the HSI representation. The HSI color system is

preferred, because it enables faster processing and mimics human visual perception. Each color component of the HSI image is processed separately.

In my preliminary work, Saudian dates (Sifri variety) were classified into four grades using thresholding techniques. I found that the red and green bands of the RGB color system were most effective for classifying dates. Processing RGB color system components has potential for good classification.

First-Order Histogram

First-order histogram features are of interest, because they can be computed quickly. The preliminary investigation showed that the mean of the histogram of red and green bands could be used to separate dates into four classes with 70% accuracy. The mean of each color band (H, S, I, R, G, and B) histogram was measured.

$$f_1 = (1/D) \sum_i \sum_j A(i,j) \qquad (8)$$

where A(i,j) is the image array and D (area) is 64x64 pixels.

Co-occurrence Matrix

The image, A, can be represented as a function in $L_x X L_y$; A: $L_x X L_y \rightarrow L_g$, where $L_x=(0,1,\ldots,N_x-1)$ and $L_y=(0,1,\ldots,N_y-1)$ are the horizontal and vertical spatial domains, respectively. $L_g=(0,1,\ldots,G-1)$ is the set of gray levels, $N_x$ and $N_y$ are the horizontal and vertical sizes of

the image, and G is the number of gray levels.

The texture-context information in an image, A, is specified by the matrix of relative frequencies, $P_{ab}$, with which two neighboring resolution cells separated by distance, d, occur on the image; one with gray level, a, and the other with gray level, b. The matrix of relative frequencies called the co-occurrence matrix is a function of the distance, d, between the neighboring resolution cells, as well as a function of the angular relationship, $\theta$, between them. The co-occurrence matrix, $P(a,b;d,\theta)$, can be considered as the joint probability distribution (Pratt 1991).

Feature values are dependent on the parameters d and $\theta$ used to compute the co-occurrence matrix. The direction of date surface texture (wrinkles) tends to parallel the major axis. Intensity variation is greatest perpendicular to surface texture, therefore, $\theta$ perpendicular to the major axis is preferred. The distance between neighboring resolution cells was selected to be one ($d = 1$), because it is the optimal distance (Haralick et al. 1973). Thus, when $d = 1$, the texture-context information is extracted from the two nearest neighbor pixels, i.e. $A(i,j)$ and $A(i,j+1)$. When $d = 2$, texture-context information is extracted from the next two neighboring pixels, i.e. $A(i,j)$ and $A(i,j+2)$, etc. The co-occurrence matrix was computed from:

$$P(a,b;d=1,\theta=0)=\#\{[(j,k),(m,n)]\epsilon(L_x \times L_y)\times (L_x \times L_y),\ j-m=0,\ |k-n|=d,\ A(j,k)=a,\ A(m,n)=b\} \quad (9)$$

where # denotes the number of elements in the set, and A(j,k) and A(m,n) are a pair of pixels separated by distance, d, at an angle, $\theta$. Size of the matrix, P, ranges from 0 to G-1, where G is the number of gray levels [0<(a,b)<G-1].

The processed matrix, P, should contain a reasonably large occupancy level in order to obtain sufficient statistical confidence in measuring the features of the co-occurrence matrix. This condition can be achieved either by selecting a large spatial region or restricting the number of gray levels. The first approach is susceptible to error if the texture changes over a large region. The second approach reduces accuracy in measurement of low gray-level texture. One heuristic approach is to use 16 gray levels in a region 30 to 50 pixels square (Pratt 1991). In this study, a 64x64-pixel region with 32 gray levels was used. This selection is more helpful in identifying tiny wrinkles on the date surface than Pratt's selection.

The co-occurrence matrix was normalized before texture extraction. Additional matrices were pre-computed for later use in computing texture features. These additions were marginal probability matrices and the sum and difference matrices.

Matrix normalization:

$$P(i,j) = \frac{P(i,j)}{\Sigma \Sigma P(i,j)} \tag{10}$$

Marginal probability matrices:

Row sum

$$P_x(i) = \Sigma_j P(i,j) \tag{11}$$

Column sum

$$P_y(i) = \Sigma_i P(i,j) \tag{12}$$

Sum & difference matrices:

$$P_{x+y}(k) = \sum_{k=i+j} \Sigma P(i,j); \; 0 \leq k \leq 2(N-1) \tag{13}$$

$$P_{x-y}(k) = \sum_{k=|i-j|} \Sigma P(i,j); \; 0 \leq k \leq (N-1) \tag{14}$$

The following texture features are computed from the above matrices (Haralick et al. 1973). These texture features ($f_2$ - $f_{14}$) are described in Table I.

Angular second moment:

$$f_2 = \Sigma_i \Sigma_j [P(i,j)]^2 \tag{15}$$

Correlation:

$$f_3 = \frac{\Sigma_i \Sigma_j (i\ j)\ P(i,j) - \mu_x\ \mu_y}{\sigma_x\ \sigma_y} \tag{16}$$

where $\mu_x$ and $\mu_y$, and $\sigma_x$ and $\sigma_y$ are the means and the standard deviations, respectively, of $P_x$ and $P_y$.

Variance:

$$f_4 = \Sigma (i - \mu_x)^2 P_x(i) \tag{17}$$

Inverse difference moment:

$$f_5 = \Sigma_i \Sigma_j \frac{P(i,j)}{1 + (i-j)^2} \tag{18}$$

Entropy:

$$f_6 = -\Sigma_i \Sigma_j P(i,j) \text{ Log}_2 P(i,j) \tag{19}$$

Sum entropy:

$$f_7 = -\Sigma_i^{2(N-1)} P_{x+y}(i) \text{ Log}_2 P_{x+y}(i) \tag{20}$$

Difference entropy:

$$f_8 = -\Sigma_i^{N-1} P_{x-y}(i) \text{ Log}_2 P_{x-y}(i) \tag{21}$$

Information measures of correlation:

$$f_9 = \frac{f_6 - HXY1}{MAX\ (HX, HY)} \tag{22}$$

$$f_{10} = \{1 - e^{[-2.0(HXY2 - f5)]}\}^{1/2} \tag{23}$$

Where:

$$HX \text{ (entropy of } P_x) = \Sigma_i P_x(i) \text{ Log}_2 P_x(i) \tag{24}$$

$$HY \text{ (entropy of } P_y) = \Sigma_i P_y(i) \text{ Log}_2 P_y(i) \tag{25}$$

$$HXY1 = -\Sigma \Sigma P(i,j) \text{ Log}_2 [P_x(i) P_y(j)] \tag{26}$$

$$HXY2 = -\Sigma \Sigma P_x(i) P_y(j) \text{ Log}_2 [P_x(i) P_y(j)] \tag{27}$$

Sum average:

$$f_{11} = \Sigma_i^{2(N-1)} i P_{x+y}(i) \tag{28}$$

Contrast:

$$f_{12} = \Sigma_n^{N-1} n^2 \left[\Sigma_{|i-j|=n}^{N-1} \Sigma_j^{N-1} P(i,j)\right] \tag{29}$$

Sum variance:

$$f_{13} = \sum_{i}^{2(N-1)} (i-f_{11})^2 \, P_{x+y}(i) \qquad (30)$$

Difference variance:

$$f_{14} = \text{variance of } P_{x-y} \qquad (31)$$

Texture Spectrum

Texture spectrum features have been applied successfully to the processing of radar images (He and Wang 1991), but have not been demonstrated for surface texture of biological materials. Texture spectrum is defined as the frequency of occurrence (histogram) of texture units in a region. Texture unit value is computed from the relationship between a central pixel and its eight nearest neighbors. There is no unique way to label the eight nearest neighbors. One approach is to select the eight pixels in a clockwise order (Fig. 10). This work employed eight ordering ways, 1 - 8, based on the starting neighbor [from top-left (a) to middle-left (h)]. Texture unit values vary, based on the ordering way, j, where j = 1,2,...,8 (the ordering ways a, b,...,h are represented, respectively, by j = 1,2,...,8). Figure 10 shows a method of computing texture units under the ordering ways, j = 1 and j = 3.

$$N_{TU;j=1} = (1x1)+(2x3)+(0x9)+(0x27)+(1x81)+(2x243) +(2x729)+(0x2187) = 2032$$

| a | b | c |
|---|---|---|
| h | Q | d |
| g | f | e |

Ordering way 1

| g | h | a |
|---|---|---|
| f | Q | b |
| e | d | c |

Ordering way 3

Texture unit number $(N_{TU}) = \sum_{i=1}^{8} E_i \, 3^{(i-1)}$

| 99 | 120 | 80 |
|---|---|---|
| 98 | 99 | 96 |
| 102 | 111 | 99 |

3x3 data image

→

| 1 | 2 | 0 |
|---|---|---|
| 0 | | 0 |
| 2 | 2 | 1 |

$E_1$ - $E_8$ values

$\rightarrow_{j=1}$ 2032

$\rightarrow_{j=3}$ 4219

Figure 10. Obtaining Texture Units Using Two Different Ordering Ways.

$$N_{TU;j=3} = (0x1)+(0x3)+(1x9)+(2x27)+(2x81)+(0x243)$$
$$+(1x729)+(2x2187) = 4219,$$

where $N_{TU;j=1}$ and $N_{TU;j=3}$ are texture units under ordering ways 1 and 3, respectively. A square region of 64x64 pixels and 256 gray levels was used in this work to obtain the texture spectrum.

The following texture spectrum features (He and Wang 1992) were extracted from date images.

Black-white symmetry:

$$f_{15} = [1- \frac{\sum_{i=0}^{3279} |S(i)-S(6560-i)|}{\sum_{i=0}^{6560} S(i)}]x100 \qquad (32)$$

where S(i) is the occurrence frequency of texture unit, i.

Geometric symmetry:

$$f_{16} = [1-(1/4)\ \Sigma_{j=1}^{4} \frac{\Sigma_{i=0}^{6560} |S_j(i)-S_{j+4}(i)|}{2 \times \Sigma_{i=0}^{6560} S_j(i)}]x100 \qquad (33)$$

where $S_j(i)$ is the occurrence frequency of the texture unit, i, in the texture spectrum under the ordering way, j.

Degree of direction:

$$f_{17} = [1-(1/6)\Sigma_{j=1}^{3}\ \Sigma_{k=j+1}^{4} \frac{\Sigma_{i=0}^{6560} |S_j(i)-S_k(i)|}{2 \times \Sigma_{i=0}^{6560} S_j(i)}]x100 \qquad (34)$$

Orientation features:

$$f_{18} = \Sigma\ S(i)*HM(i) \qquad (35)$$

$$f_{19} = \Sigma\ S(i)*VM(i) \qquad (36)$$

$$f_{20} = \Sigma\ S(i)*DM1(i) \qquad (37)$$

$$f_{21} = \Sigma\ S(i)*DM2(i) \qquad (38)$$

where HM(i) denotes the horizontal measure of the texture unit, i, computed by:

$$HM(i) = P(a,b,c) \times P(e,f,g)$$

where P(a,b,c) represents the number of elements having the same value in $E_a$, $E_b$, and $E_c$ (Figs. 6 and 10).

$$E_a = \begin{cases} 0 \text{ if value of a} < \text{value of Q} \\ 1 \text{ if value of a} = \text{value of Q} \\ 2 \text{ if value of a} > \text{value of Q.} \end{cases}$$

Similarly, VM(i), DM1(i), and DM2(i) denote the vertical,

first diagonal, and second diagonal measures of the texture unit, i, respectively. These measures can be computed from:

$$VM(i) = P(a,h,g) \times P(c,d,e)$$

$$DM1(i) = P(h,a,b) \times P(d,e,f)$$

$$DM2(i) = P(b,c,d) \times P(f,g,h).$$

Central symmetry:

$$f_{22} = \sum_{i=0}^{6560} S(i) \times [K(i)]^2 \qquad (39)$$

where K(i) is the number of pairs having the same value in elements ($E_a$, $E_e$), ($E_b$, $E_f$), ($E_c$, $E_g$), and ($E_d$, $E_f$) (Figs. 6 and 10).

The texture features described above were extracted from the color image components; R, G, B, H, S, and I. For example, the feature $f_{10}$ computed from the green band is denoted $G_{10}$. Table I lists the physical interpretation of each feature, given a 64x64-pixel region.

## Image Classification

Image classification is the most critical step in pattern recognition application. There are three main approaches. They are neural networks, syntactic, and statistical. Neural networks are based on a model of the brain's computational process. The syntactic approach utilizes the structure of a pattern in a discrimination process. The statistical approach can be subdivided into parametric and nonparametric methods. Parametric methods are appropriate when samples have an approximately normal

TABLE I

DESCRIPTION OF FEATURES

| Feature | Description |
|---|---|
| f1 | Mean is a measure of image brightness. |
| f2 | Angular second moment is a measure of the image homogeneity. It produces high values for high frequencies of occurrence in the matrix. |
| f3 | Correlation is a measure of the intensity of linear dependencies in the image. It gives high values if frequencies of occurrence are located in the (63,63) corner. Most of the contribution comes from the values close to the diagonal, (0,0) to (63,63). |
| f4 | Sum of squares (variance) is a measure of the variance of image intensity derived from the co-occurrence matrix. It gives zero value if the gray levels in the image have the same intensity. |
| f5 | Inverse difference moment measures image contrast. It gives high values if frequencies of occurrence are located around the (0,0) to (63,63) diagonal. |
| f6 | Entropy is a measure of the scattered patterns in the image. For example, an image with half black and half white has a lower entropy than an image with a black and white checker-board pattern. |
| f7 | Sum entropy is a measure of the scattered patterns in the right diagonal, (0,63) to (63,0). |
| f8 | Difference entropy is a measure of the scattered patterns in the left diagonal, (0,0) to (63,63). |
| f9-f10 | Information measures of correlation are a very complex measure and do not have a physical interpretation, except that (f9) is a ratio of entropies. |
| f11 | Sum average is a measure of frequencies of occurrence concentrated in the right diagonal, (0,0) to (63,63). It gives high values if the frequencies of occurrence are located in the (63,63) corner. |

TABLE I (Continued)

| Feature | Description |
|---|---|
| f12 | This feature measures the contrast in the co-occurrence matrix. It gives high values if most frequencies are concentrated in the two corners, (0,63) and (63,0). |
| f13 | Sum variance is a measure of the variance of the frequencies occurring around the right diagonal, (0,0) to (63,63). |
| f14 | Difference variance measures the variance of the frequencies occurring around the left diagonal, (0,63) to (63,0). |
| f15 | Black-white symmetry is a measure of the symmetry between the left half and the right half of the texture spectrum. The feature values were normalized from 0 to 100. This feature gives low value if the two halves are symmetrical. |
| f16 | Geometric symmetry is a measure of the shape regularity of the image. The feature values were normalized from 0 to 100. A value of 100 means that the image and its image rotated $180^0$ are identical. |
| f17 | Degree of direction measures the degree of linear structure within the image. The feature values were normalized from 0 to 100. A high value indicates that the image has some linear structure. |
| f18-f21 | Orientation features are measures of the image structure. The feature (f18) measures the micro-horizontal structure. A high value of (f18) means that the micro-structure of the image is horizontal. The same description can be applied to the other three features (f19-f21), which measure the vertical, first diagonal, and second diagonal micro-structure of the image, respectively. |
| f22 | This feature measures the central symmetry of texture unit. |

distribution within each class. The Bayes classifier is an example of a parametric classifier. Nonparametric methods are appropriate when data distributions are not normal. The SAS software package provides discriminant analysis procedures for both parametric and nonparametric methods (SAS Institute Inc. 1988).

Bayes Classifier

The Bayes classifier function is specified by the mean vector and the covariance matrix of each class (Gonzalez and Woods 1992). The Bayes decision function is

$$d_i(x)=\ln(q_i)-(1/2)\ln(|COV_i|) -(1/2)[(x-m_i)'COV_i^{-1}(x-m_i)] \quad (40)$$

where:

$q_i$ is the prior probability of membership in class, i,

$COV_i$ is the covariance matrix within class, i,

$|COV_i|$ is the determinant of $COV_i$,

p is the number of variables,

$m_i$ is the p-dimensional vector containing variable means in class, i,

x is the p-dimensional vector containing the variable of an observation,

ln() is the natural log,

The observation x is classified into class, i, when the value of decision function, $d_i(x)$, is the largest.

Nonparametric

Nonparametric classification functions are based on the estimated probability density of the class. The nearest-neighbor and the kernel are the two main methods used to estimate nonparametric probability density. The nearest neighbor and kernel densities at a point are estimated from cells located at that point. The nearest neighbor method fixes the number, k, of design set points and obtains the volume which contains the nearest k. From this number and volume, the probability density may be estimated. The kernel method, on the other hand, fixes the volume and obtains the value of k in this volume. Again, from the values of k and volume, the kernel probability density may be estimated (Hand 1982). The kernel method uses uniform, normal, Epanechnikov, biweight, or triweight kernels to estimate the nonparametric probability density.

Nonparametric probability density is used to generate a discriminant function for classifying observations into classes. Either within-class covariance matrices or the pooled covariance matrix can be used to compute the squared distance between two observations. An observation is assigned to class, i, when the value of the squared distance is the smallest.

# CHAPTER VI

# EXPERIMENTAL PROCEDURE

## Introduction

Experiments were conducted to assess the performance of machine vision date classification. More specifically, the classification performance of the co-occurrence matrix and texture spectrum method was investigated.

## Date Fruits

Manually inspected date fruits classified according to the USDA grading standards by an industry expert grader were provided by Dole Dried Fruit and Nut Company, Thermal, CA. Four classes from the 1991 crop (Waxy class unavailable) and five classes from the 1992 crop were received. Dole typically combines three USDA classes (Waxy, Number 1 Dry, and Number 2 Dry) into one grade (Grade B). Grades A and C are Natural and Cull dates, respectively.

The dates were stored at $5^{0}$C and 60% relative humidity. A sample of 100 fruits was randomly selected from each class, for a total of 400 and 500 fruits from the 1991 and 1992 crops, respectively.

## Image Acquisition

Groups of 40 or 50 dates (ten from each class) were removed from storage for image acquisition. Four representative images of the surface of each date were acquired, two from each of two opposite sides. Two images of the surface of a randomly selected side were obtained first. The date was then rotated $180^0$, and another pair of images was acquired (Fig. 11). Image FOV was approximately 8.0 by 6.6 cm, corresponding to a pixel resolution of 0.15 mm.

A region-of-interest (ROI) of 64 by 64 pixels was selected from each image to obtain color and texture features. This region covered an area of 0.88 $cm^2$. The ROI was small enough to fit within the date boundary in all images, accommodating size variation among date classes.

Location of the ROI was manually defined for each image, but was generally centered on the major axis (Fig. 11). The ROI was located above the minor axis of the date for the first and third images, and below the minor axis for the second and fourth images. Each ROI occupied approximately 15% of the total projected area of the date.

## Calibration

A square section of metal (25 $cm^2$) coated with barium sulfate was used as a reference for calibrating the machine vision system. Barium sulfate is a highly reflective material. Prior to image acquisition, HSI color images of

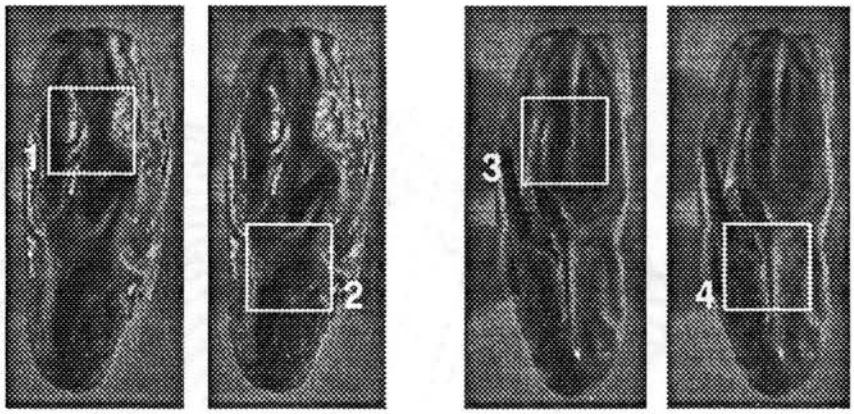


(a) (b)

Figure 11. Location of the ROI on Each Image. A Pair of Images of the Surface of a Randomly Selected Side Was Obtained (a), the Date Was Then Rotated $180^0$, and Another Pair of Images Was Acquired (b).

the reference were acquired to assign initial setpoints. These setpoints were the mean and standard deviation of the H, S, and I histograms. The HSI color system was used, because it is more sensitive to changes in light intensity than the RGB color system. HSI color images of the reference were repeated every two hours during image acquisition . If necessary, the position of the light source was adjusted, so that the mean and standard deviation of the H, S, and I histograms matched the initial setpoints.

## Feature Extraction

Twenty-two features were extracted from the ROI in each color band (H, S, I, R, G, and B) immediately after image

acquisition, for a total of 132 (22 x 6) features. The ROI in each color band was stored for future use. Features were combined and organized into SAS dataset files. The normality of the data was then checked. Bar graphs of each set of 400 regions-of-interest of within-class features were plotted to test the distribution. Also, a statistical test for normality was computed by applying the Univariate Procedure (SAS Institute Inc. 1988). This approach compares the shape of a normal distribution with the shape of the sample distribution. This comparison results in a p-value, which ranges from zero to one. A p-value close to zero indicates that the data distribution is not normal (Schlotzhauer and Littell 1987).

## Image Classification

Eighteen models, incorporating various subsets of the features, were investigated. The purpose of the models was to allow comparison of various features for classification accuracy. Two models used the mean of color band histograms, eight used features of the co-occurrence matrix, and eight used texture spectrum features. Table II summarizes the features used in each model.

SAS discriminant analysis was used to classify feature observations for each model into four or five classes (SAS Institute Inc. 1988). Discriminant analysis was used to obtain a function which could be used to classify additional observations. Figure 12 summarizes the overall procedure.

TABLE II

MODEL FEATURES

| Model | Features | Notes |
|---|---|---|
| HSI-1 | $H_1, S_1, I_1$ | Mean of H,S,and I histograms. |
| HSI-2 | $H_2$ - $H_{14}$ | Features of CCM extracted from H. |
| HSI-3 | $S_2$ - $S_{14}$ | Features of CCM extracted from S. |
| HSI-4 | $I_2$ - $I_{14}$ | Features of CCM extracted from I. |
| HSI-5 | $H_2$ - $H_{14}$<br>$S_2$ - $S_{14}$<br>$I_2$ - $I_{14}$ | Combination of HSI-2, HSI-3, and HSI-4. |
| HSI-6 | $H_{15}$ - $H_{22}$ | Features of TS extracted from H. |
| HSI-7 | $S_{15}$ - $S_{22}$ | Features of TS extracted from S. |
| HSI-8 | $I_{15}$ - $I_{22}$ | Features of TS extracted from I. |
| HSI-9 | $H_{15}$ - $H_{22}$<br>$S_{15}$ - $S_{22}$<br>$I_{15}$ - $I_{22}$ | Combination of HSI-6, HSI-7, and HSI-8. |
| RGB-1 | $R_1, G_1, B_1$ | Mean of R,G,and B histograms. |
| RGB-2 | $R_2$ - $R_{14}$ | Features of CCM extracted from R. |
| RGB-3 | $G_2$ - $G_{14}$ | Features of CCM extracted from G. |
| RGB-4 | $B_2$ - $B_{14}$ | Features of CCM extracted from B. |
| RGB-5 | $R_2$ - $R_{14}$<br>$G_2$ - $G_{14}$<br>$B_2$ - $B_{14}$ | Combination of RGB-2, RGB-3, and RGB-4. |
| RGB-6 | $R_{15}$ - $R_{22}$ | Features of TS extracted from R. |
| RGB-7 | $G_{15}$ - $G_{22}$ | Features of TS extracted from G. |
| RGB-8 | $B_{15}$ - $B_{22}$ | Features of TS extracted from B. |
| RGB-9 | $R_{15}$ - $R_{22}$<br>$G_{15}$ - $G_{22}$<br>$B_{15}$ - $B_{22}$ | Combination of RGB-6, RGB-7, and RGB-8. |

CCM : Co-occurrence matrix.
TS : Texture spectrum.

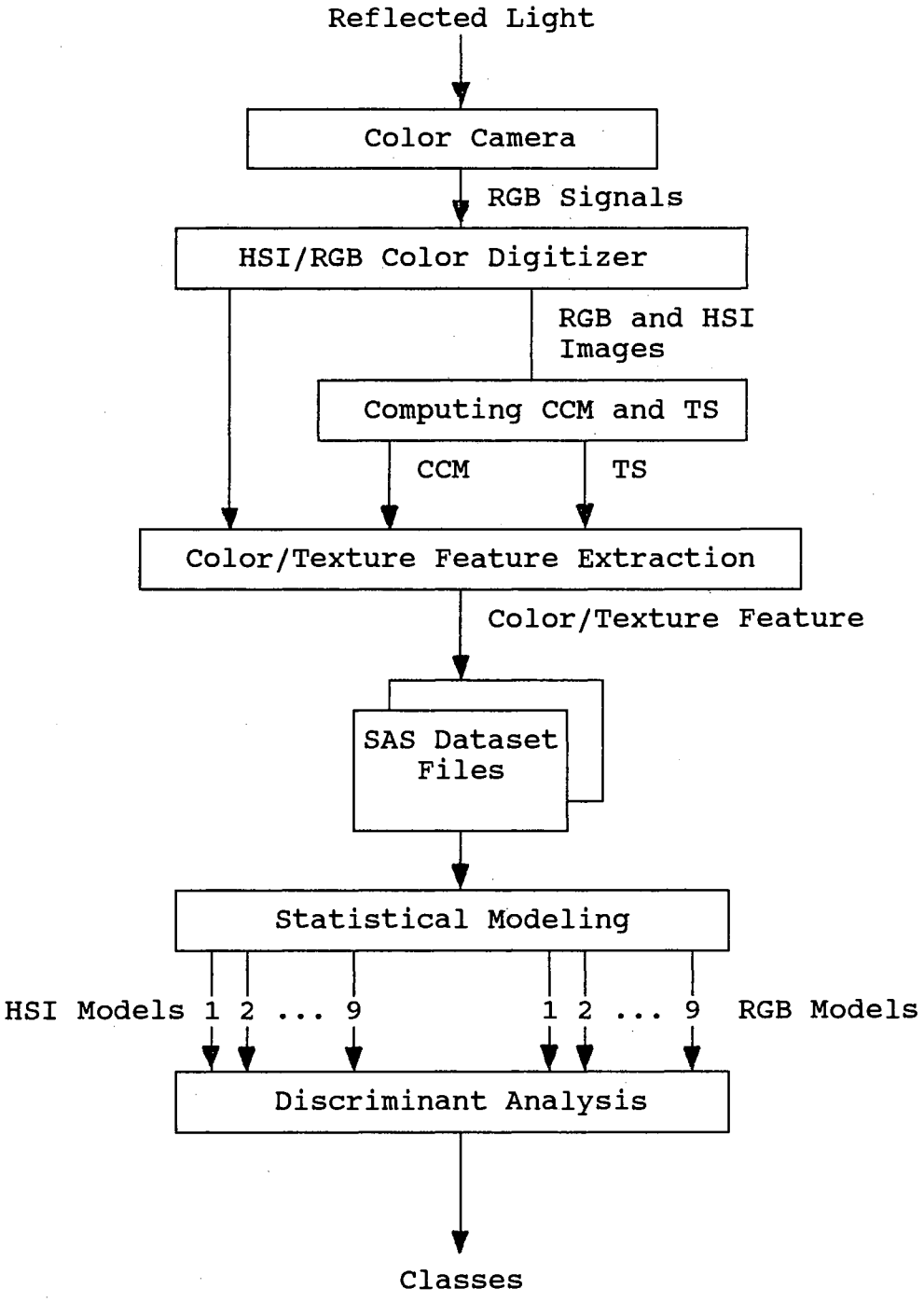


Figure 12. Color/Texture Date Classification Procedure. CCM and TS Denote the Co-occurrence Matrix and Texture Spectrum, Respectively.

# CHAPTER VII

# RESULTS AND DISCUSSION

## Introduction

A total of 900 date fruits from the 1991 and 1992 crops were tested. This consisted of 100 fruits in each of the 4 and 5 classes from the 1991 and 1992 crops, respectively. Four images were acquired from each individual date. A 64x64-pixel region-of-interest (ROI) was selected from each image, as described in Chapter VI. Each of the 3600 regions-of-interest (900 x 4) was processed for feature extraction. Twenty-two features were computed from six color bands (H, S, I, R, G, and B) of each ROI, for a total of 132 features (22 x 6).

Resulting feature values from the intensity band of the 100 regions-of-interest in the Natural Class of the 1992 crop are summarized in Table III as a representative example. This table consists of the minimum, maximum, mean, and standard deviation of each feature.

## Data Distribution

The SAS software package offers discriminant analysis procedures using both parametric and nonparametric methods (SAS Institute Inc. 1988). Parametric methods are

TABLE III

FEATURE SUMMARY STATISTICS

(Intensity Band, Natural Class)

| Features | MIN | MAX | MEAN | STD |
|---|---|---|---|---|
| I1 | 47.43 | 184.83 | 94.87 | 20.17 |
| I2 | 0.02 | 0.37 | 0.12 | 0.06 |
| I3 | 278.90 | 9,714.10 | 1,986.40 | 1,271.80 |
| I4 | 8.93 | 304.61 | 62.82 | 40.11 |
| I5 | 0.50 | 0.88 | 0.78 | 0.07 |
| I6 | 5.73 | 34.11 | 14.27 | 4.27 |
| I7 | 1.19 | 173.22 | 27.77 | 29.01 |
| I8 | 0.98 | 2.13 | 1.63 | 0.23 |
| I9 | 1.06 | 2.49 | 1.84 | 0.28 |
| I10 | 0.46 | 1.41 | 0.74 | 0.19 |
| I11 | 0.32 | 7.96 | 1.52 | 1.11 |
| I12 | 0.06 | 0.34 | 0.20 | 0.06 |
| I13 | 0.99 | 1.00 | 1.00 | 0.01 |
| I14 | 0.01 | 0.02 | 0.01 | 0.02 |
| I15 | 10.93 | 29.03 | 19.74 | 3.28 |
| I16 | 95.50 | 96.98 | 96.09 | 0.28 |
| I17 | 97.35 | 98.24 | 97.65 | 0.15 |
| I18 | 0 | 49,156,792 | 1,883,210 | 4,915,163 |
| I19 | 0 | 51,509,638 | 1,928,597 | 4,947,298 |
| I20 | 0 | 73,195,104 | 3,170,336 | 7,630,323 |
| I21 | 0 | 72,954,452 | 3,140,530 | 7,604,655 |
| I22 | 2,787 | 947,594,501 | 40,257,961 | 97,899,826 |

appropriate for data that have a normal distribution. Nonparametric methods are appropriate when data distributions vary from normal. Choice of appropriate method was based on analysis of the data distribution within each class.

Plotting the within-class data histogram is a visual method for presenting and estimating data distribution. Bar graphs of each set of 400 feature values (100 dates x 4 regions-of-interest within each class) were plotted to check

for normality. As an example, the data distribution of the feature values extracted from the intensity band in the Natural Class of the 1992 crop will be described in the following section.

Data distribution of the first feature, $I_1$, was found to be normal (Fig. 13), with a p-value of 0.85 (p-value close to one indicates normal distribution). Most of the features extracted from the co-occurrence matrices ($I_2$ - $I_{14}$) appeared normally distributed, with the exception of features such as $I_{13}$, which had skewed distributions. Figures 14 and 15 show the normal ($p = 0.93$) and skewed ($p = 0.46$) distributions of the data for features $I_{12}$ and $I_{13}$, respectively. Three of the texture spectrum features ($I_{15}$, $I_{16}$, and $I_{17}$) appeared normally distributed. The other five ($I_{18}$ - $I_{22}$) did not. Figures 16 and 17 show the distribution of features $I_{15}$ ($p = 0.93$) and $I_{21}$ ($p = 0.41$), respectively.

It appeared that the data distribution of some features changed from one class to another and from one color band to another. While the data from one date class appeared normally distributed, they were skewed in another class. The same condition existed among color bands. Therefore, nonparametric discriminant analysis was judged to be appropriate.

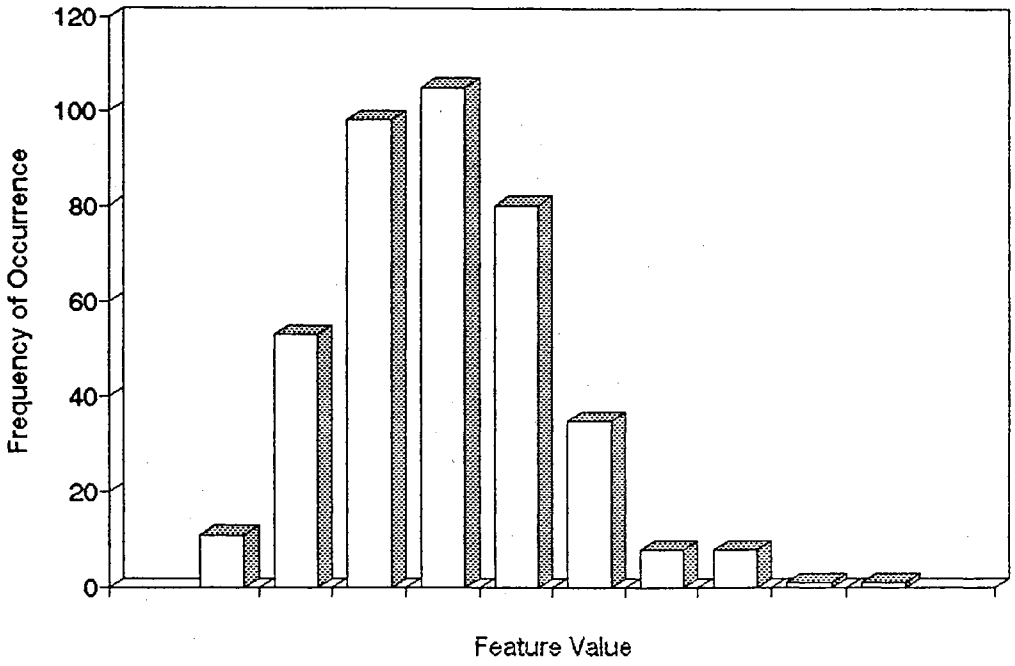


Figure 13. Data Histogram of the Feature, $I_1$, in the Natural Class of the 1992 Crop.

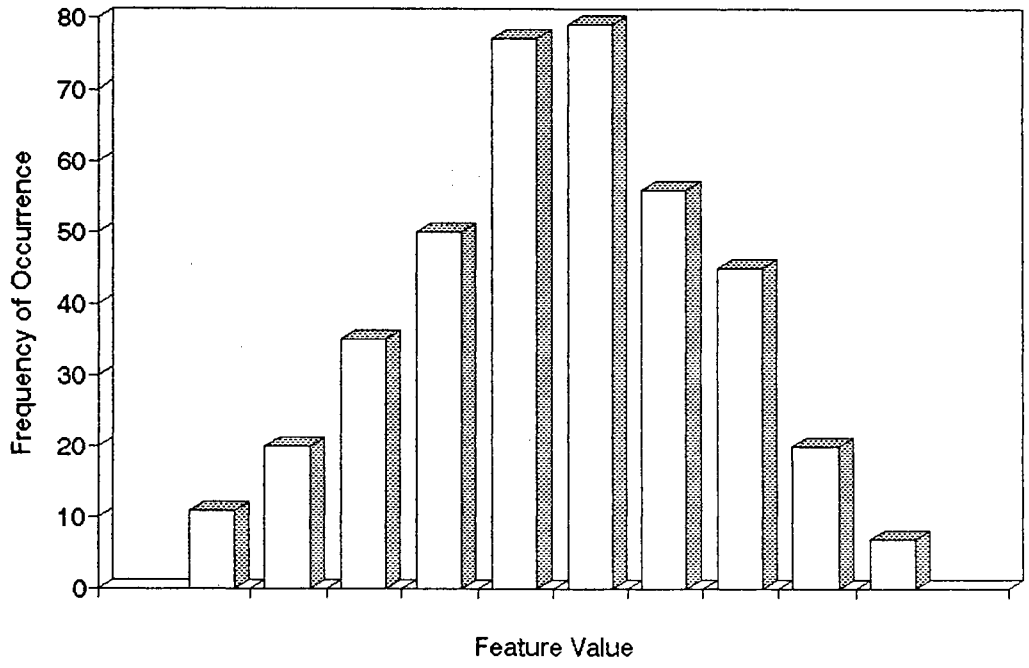


Figure 14. Data Histogram of the Feature, $I_{12}$, in the Natural Class of the 1992 Crop.

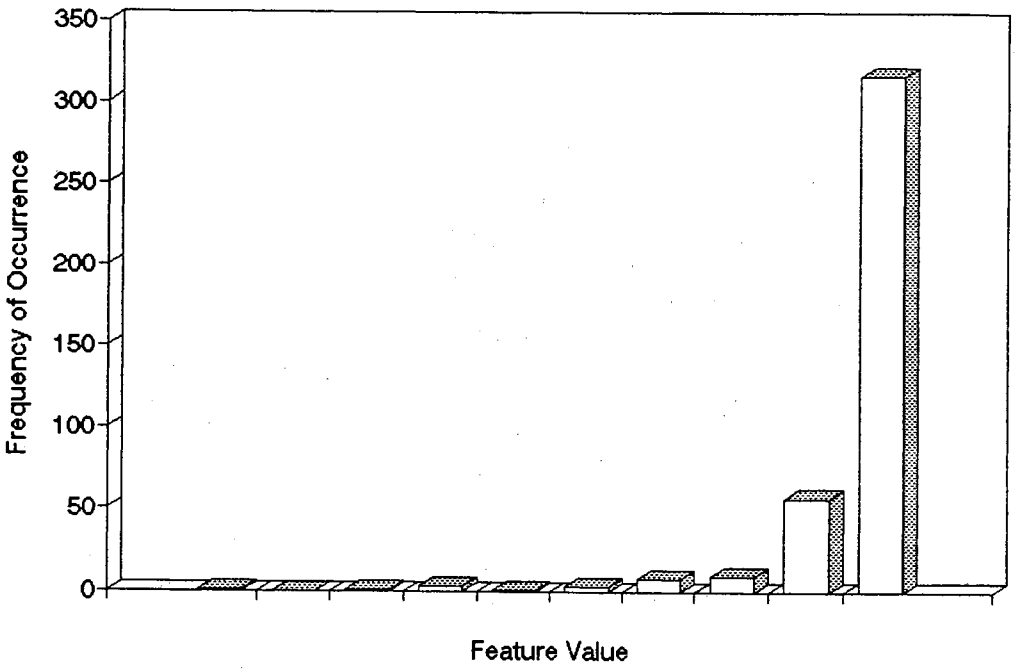


Figure 15. Data Histogram of the Feature, $I_{13}$, in the Natural Class of the 1992 Crop.

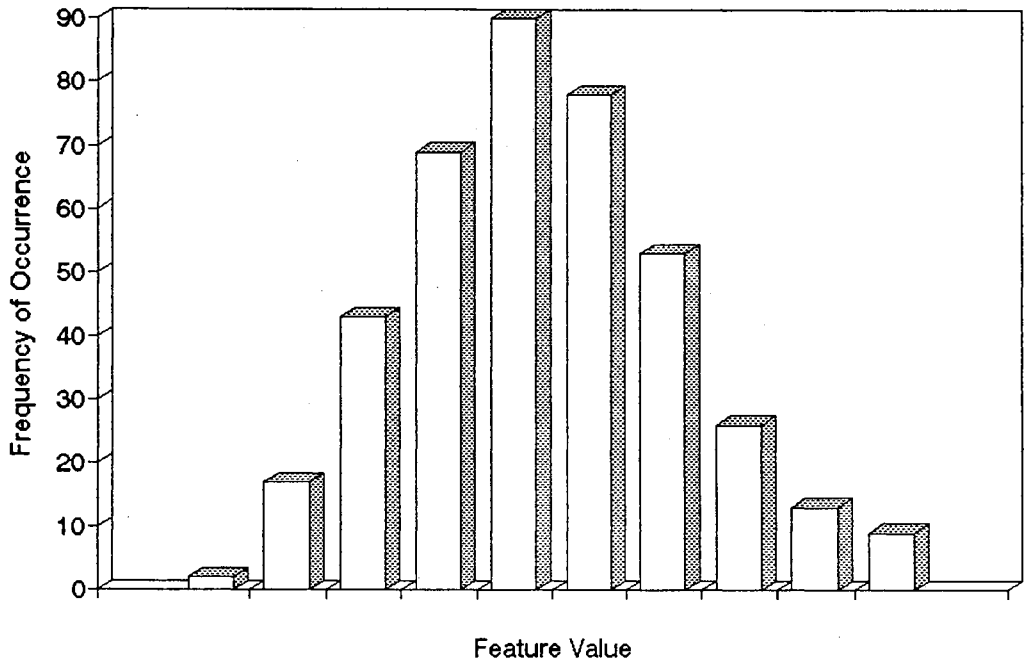


Figure 16. Data Histogram of the Feature, $I_{15}$, in the Natural Class of the 1992 Crop.

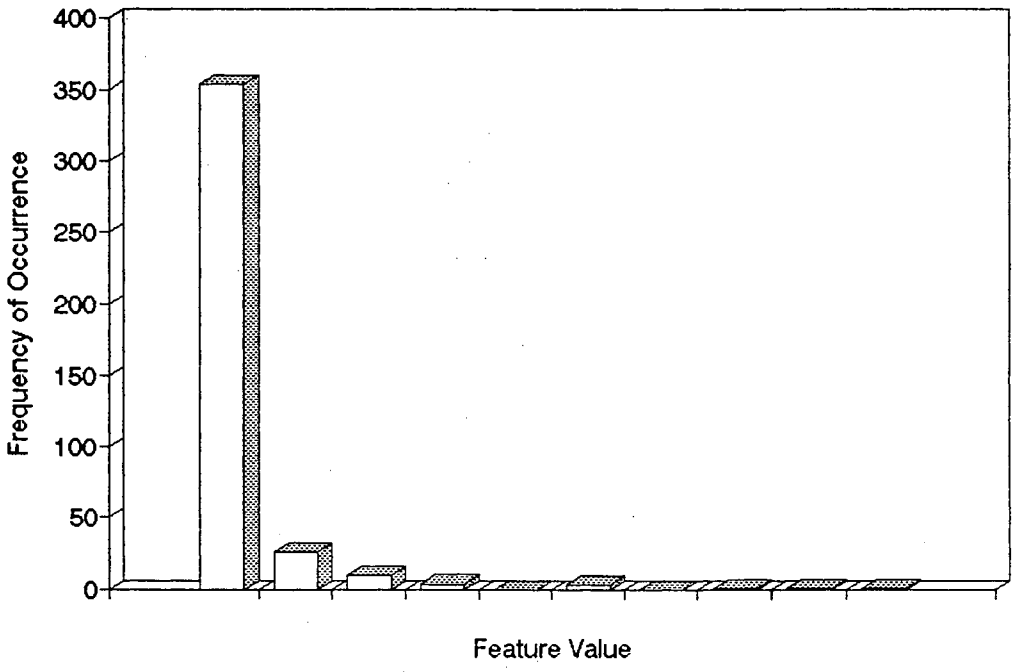


Figure 17. Data Histogram of the Feature, $I_{21}$, in the Natural Class of the 1992 Crop.

## Discriminant Analysis

The SAS software package provides a nonparametric discriminant analysis procedure under the DISCRIM option, using kernel methods (SAS Institute Inc. 1988). Several kernels presented by the SAS software package including uniform, normal, Epanechnikov, biweight, and triweight were used for classification. The multivariate discriminant procedure using the Epanechnikov kernel (Hand 1982) was the most effective, in terms of classification accuracy. Figure 18 shows a SAS program for the nonparametric discriminant procedure using the Epanechnikov kernel to classify date fruits into five classes.

```
PROC format;
     value classname
          1 = 'NATURAL  '
          2 = 'WAXY     '
          3 = 'DRY-NO.-1'
          4 = 'DRY-NO.-2'
          5 = 'CULL     ';
RUN;
DATA Int;
     INFILE 'A:DATE92.INT';
     INPUT features i2 i3 i4 i5 i6 i7 i8 i9
                   i10 i11 i12 i13 i14;
     FORMAT features classname.;

PROC discrim data = Int
     method = npar  kernel = epa  pool = yes  r = 3.03
     listerr;
  class features;
     var i2 i3 i4 i5 i6 i7 i8 i9 i10 i11 i12 i13 i14;
  title 'The features of CCM from Int band';
  titl2 'Using Epanechnikov-kernel Discriminant
                   Analysis';
RUN;
```

Figure 18. SAS program for nonparametric discriminant analysis.

In this program a nonparametric method (method = npar) was used to classify the 1992 crop into five classes (classname), using the Epanechnikov kernel (kernel = epa). The classification was based on the intensity features ($i_2$ - $i_{14}$) extracted from the co-occurrence matrix. The pooled covariance matrix was used in calculating the squared distances (pool = yes). An observation is assigned to class, i, when the value of squared distance is the smallest. The squared distance between two observation vectors, x and y, in class i was computed from:

$$d_i^2(x,y) = (x-y)' \ COV^{-1} \ (x-y) \tag{41}$$

where COV is the pooled covariance matrix. The value of smoothing parameter (r = 3.03) depends on kernel type, number of variables (features), and number of samples of the within-class data set. The smoothing parameter using the Epanechnikov kernel was computed from:

$$r = ( AK/n_i)^{1/(p+4)} \tag{42}$$

$$AK = \frac{2^{p+2} \ p^2 \ (p+2) \ (p+4) \ \Gamma(p/2)}{2p+1}$$

$$\Gamma(x) = \int_0^{\infty} t^{x-1} \ e^{-t} \ dt \tag{43}$$

Where:

p is number of variables (features),

$n_i$ is number of samples of within-class data set, and

$\Gamma$ is the gamma function.

Eighteen models were constructed using the features from the HSI and RGB color systems (Table II). Model HSI-1 consisted of three features; mean of the H, S, and I

histograms. Models HSI-2, HSI-3, and HSI-4 were composed of hue, saturation, and intensity features, respectively, extracted from the co-occurrence matrices. Each model consisted of 13 features. All the features (39) of Models HSI-2, HSI-3, and HSI-4 were included in Model HSI-5. Models HSI-6, HSI-7, and HSI-8 were composed of hue, saturation, and intensity features, respectively, extracted from the texture spectrum. Each model was constructed using 8 features. Model HSI-9 consisted of all the features (24) of Models HSI-6, HSI-7, and HSI-8. The same description can be applied to the RGB models (RGB-1 - RGB-9).

The nonparametric discriminant analysis procedure (Fig. 18) was applied to each model. Both the 1991 and 1992 crops were classified according to the USDA grading standards (five classes) and the Industry grading standards (three grades).

Comparison of Regions-of-Interest

The classification accuracy for data sets from the four regions of interest is summarized in Tables IV, V, VI, and VII. These tables present the classification accuracy of the 1991 and 1992 crops using the USDA and Industry grading standards, respectively. Tables XIV to XXIX (Appendix) list the specific classification accuracy of the 1991 and 1992 crops according to the USDA and Industry grading standards, respectively. Each table consists of the classification accuracy of each class or grade and the total

TABLE IV

CLASSIFICATION ACCURACY, 1991 CROP

(USDA Grading Standards)

| Model | ROI-1 | ROI-2 | ROI-3 | ROI-4 | MEAN | STD |
|---|---|---|---|---|---|---|
| HSI-1 | 60.5% | 60.3% | 60.0% | 60.8% | 60.4% | 0.3% |
| HSI-2 | 75.3% | 70.8% | 70.5% | 76.0% | 73.1% | 2.5% |
| HSI-3 | 70.5% | 75.5% | 70.5% | 73.5% | 72.5% | 2.1% |
| HSI-4 | 74.8% | 77.0% | 72.3% | 75.8% | 74.9% | 1.7% |
| HSI-5 | 91.0% | 94.3% | 90.5% | 95.3% | 92.8% | 2.0% |
| HSI-6 | 48.0% | 52.0% | 46.5% | 56.3% | 50.7% | 3.8% |
| HSI-7 | 44.3% | 48.0% | 46.5% | 47.5% | 46.6% | 1.4% |
| HSI-8 | 55.8% | 52.0% | 56.8% | 61.0% | 56.4% | 3.2% |
| HSI-9 | 76.0% | 75.3% | 74.3% | 87.8% | 78.3% | 5.5% |
| RGB-1 | 61.0% | 62.0% | 57.0% | 62.0% | 60.5% | 2.1% |
| RGB-2 | 72.0% | 75.3% | 70.3% | 76.8% | 73.6% | 2.6% |
| RGB-3 | 74.0% | 72.5% | 67.3% | 71.8% | 71.4% | 2.5% |
| RGB-4 | 74.3% | 74.5% | 66.0% | 73.0% | 71.9% | 3.5% |
| RGB-5 | 95.3% | 97.5% | 95.8% | 96.5% | 96.3% | 0.8% |
| RGB-6 | 54.3% | 56.0% | 59.3% | 56.3% | 56.4% | 1.8% |
| RGB-7 | 60.3% | 55.5% | 58.8% | 54.5% | 57.3% | 2.3% |
| RGB-8 | 51.0% | 58.0% | 51.8% | 55.8% | 54.1% | 2.9% |
| RGB-9 | 86.3% | 87.3% | 85.8% | 85.5% | 86.2% | 0.7% |

ROI-1 - Classification accuracy of first ROI.
ROI-2 - Classification accuracy of second ROI.
ROI-3 - Classification accuracy of third ROI.
ROI-4 - Classification accuracy of fourth ROI.
MEAN - Average classification accuracy of four regions-of-interest.
STD - Standard deviation.

TABLE V

CLASSIFICATION ACCURACY, 1992 CROP

(USDA Grading Standards)

| Model | ROI-1 | ROI-2 | ROI-3 | ROI-4 | MEAN | STD |
|---|---|---|---|---|---|---|
| HSI-1 | 66.0% | 67.8% | 63.8% | 65.6% | 65.8% | 1.4% |
| HSI-2 | 70.0% | 69.6% | 70.8% | 67.8% | 69.6% | 1.1% |
| HSI-3 | 69.2% | 73.2% | 69.6% | 77.0% | 72.3% | 3.2% |
| HSI-4 | 72.8% | 71.6% | 68.8% | 73.4% | 71.7% | 1.8% |
| HSI-5 | 92.8% | 94.0% | 92.8% | 90.4% | 92.5% | 1.3% |
| HSI-6 | 49.8% | 51.0% | 46.2% | 48.4% | 48.9% | 1.8% |
| HSI-7 | 42.6% | 39.2% | 41.4% | 42.8% | 41.5% | 1.4% |
| HSI-8 | 59.4% | 59.6% | 55.2% | 59.4% | 58.4% | 1.8% |
| HSI-9 | 85.8% | 81.2% | 80.0% | 74.8% | 80.5% | 3.9% |
| RGB-1 | 57.0% | 54.2% | 55.8% | 60.0% | 56.8% | 2.1% |
| RGB-2 | 77.8% | 79.2% | 79.6% | 75.8% | 78.1% | 1.5% |
| RGB-3 | 73.6% | 72.4% | 72.4% | 75.8% | 73.6% | 1.4% |
| RGB-4 | 74.8% | 78.4% | 76.6% | 77.6% | 76.9% | 1.3% |
| RGB-5 | 99.2% | 98.2% | 98.4% | 97.8% | 98.4% | 0.5% |
| RGB-6 | 46.8% | 59.8% | 47.4% | 53.4% | 51.9% | 5.3% |
| RGB-7 | 59.2% | 61.0% | 52.2% | 58.0% | 57.6% | 3.3% |
| RGB-8 | 52.4% | 53.4% | 50.4% | 49.8% | 51.5% | 1.5% |
| RGB-9 | 80.0% | 88.6% | 81.8% | 83.2% | 83.4% | 3.2% |

ROI-1 - Classification accuracy of first ROI.
ROI-2 - Classification accuracy of second ROI.
ROI-3 - Classification accuracy of third ROI.
ROI-4 - Classification accuracy of fourth ROI.
MEAN - Average classification accuracy of four regions-of-interest.
STD - Standard deviation.

TABLE VI

CLASSIFICATION ACCURACY, 1991 CROP

(Industry Grading Standards)

| Model | ROI-1 | ROI-2 | ROI-3 | ROI-4 | MEAN | STD |
|---|---|---|---|---|---|---|
| HSI-1 | 70.5% | 69.3% | 72.3% | 74.3% | 71.6% | 1.9% |
| HSI-2 | 80.8% | 76.0% | 75.7% | 84.5% | 79.3% | 3.7% |
| HSI-3 | 78.3% | 79.8% | 77.7% | 81.7% | 79.4% | 1.5% |
| HSI-4 | 81.5% | 83.7% | 81.3% | 83.0% | 82.4% | 1.0% |
| HSI-5 | 92.7% | 95.8% | 92.0% | 96.7% | 94.3% | 2.0% |
| HSI-6 | 55.8% | 55.5% | 50.2% | 64.2% | 56.4% | 5.0% |
| HSI-7 | 55.0% | 59.5% | 59.0% | 57.0% | 57.6% | 1.8% |
| HSI-8 | 65.5% | 59.3% | 65.8% | 66.3% | 64.3% | 2.9% |
| HSI-9 | 81.7% | 78.7% | 79.0% | 90.3% | 82.4% | 4.7% |
| RGB-1 | 69.0% | 70.7% | 65.7% | 74.8% | 70.0% | 3.3% |
| RGB-2 | 79.8% | 82.0% | 77.3% | 82.7% | 80.5% | 2.1% |
| RGB-3 | 81.8% | 79.5% | 75.5% | 81.0% | 79.5% | 2.4% |
| RGB-4 | 79.3% | 78.3% | 74.3% | 77.7% | 77.4% | 1.9% |
| RGB-5 | 97.2% | 97.5% | 97.0% | 97.8% | 97.4% | 0.3% |
| RGB-6 | 60.5% | 61.0% | 68.7% | 62.7% | 63.2% | 3.3% |
| RGB-7 | 68.3% | 61.3% | 65.0% | 59.5% | 63.5% | 3.4% |
| RGB-8 | 57.5% | 64.8% | 60.8% | 62.5% | 61.4% | 2.7% |
| RGB-9 | 90.8% | 89.5% | 89.2% | 88.5% | 89.5% | 0.8% |

ROI-1 - Classification accuracy of first ROI.
ROI-2 - Classification accuracy of second ROI.
ROI-3 - Classification accuracy of third ROI.
ROI-4 - Classification accuracy of fourth ROI.
MEAN - Average classification accuracy of four regions-of-interest.
STD - Standard deviation.

TABLE VII

CLASSIFICATION ACCURACY, 1992 CROP

(Industry Grading Standards)

| Model | ROI-1 | ROI-2 | ROI-3 | ROI-4 | MEAN | STD |
|---|---|---|---|---|---|---|
| HSI-1 | 77.2% | 78.3% | 74.9% | 79.8% | 77.6% | 1.8% |
| HSI-2 | 80.8% | 81.1% | 83.1% | 77.4% | 80.6% | 2.0% |
| HSI-3 | 79.2% | 83.9% | 80.0% | 86.9% | 82.5% | 3.1% |
| HSI-4 | 82.2% | 81.1% | 80.9% | 81.3% | 81.4% | 0.5% |
| HSI-5 | 96.4% | 96.1% | 96.6% | 94.1% | 95.8% | 1.0% |
| HSI-6 | 66.0% | 60.0% | 55.3% | 63.6% | 61.2% | 4.0% |
| HSI-7 | 56.8% | 54.8% | 56.7% | 59.6% | 56.9% | 1.7% |
| HSI-8 | 71.6% | 71.3% | 69.2% | 72.9% | 71.3% | 1.3% |
| HSI-9 | 91.9% | 86.2% | 89.3% | 83.3% | 87.7% | 3.2% |
| RGB-1 | 68.4% | 67.4% | 67.7% | 72.0% | 68.9% | 1.8% |
| RGB-2 | 86.7% | 89.6% | 88.1% | 85.8% | 87.5% | 1.4% |
| RGB-3 | 82.7% | 80.6% | 81.7% | 83.7% | 82.1% | 1.2% |
| RGB-4 | 85.7% | 87.8% | 86.6% | 88.9% | 87.2% | 1.2% |
| RGB-5 | 99.3% | 98.7% | 99.9% | 99.3% | 99.3% | 0.4% |
| RGB-6 | 64.7% | 73.2% | 61.9% | 68.8% | 67.1% | 4.3% |
| RGB-7 | 68.3% | 73.9% | 69.8% | 70.6% | 70.6% | 2.0% |
| RGB-8 | 68.8% | 68.8% | 64.3% | 63.9% | 66.4% | 2.3% |
| RGB-9 | 87.1% | 93.2% | 87.9% | 87.8% | 89.0% | 2.5% |

ROI-1 - Classification accuracy of first ROI.
ROI-2 - Classification accuracy of second ROI.
ROI-3 - Classification accuracy of third ROI.
ROI-4 - Classification accuracy of fourth ROI.
MEAN - Average classification accuracy of four regions-of-interest.
STD - Standard deviation.

classification from a set of regions-of-interest at one location on the date.

The classifications of date fruits from regions-of-interest at different locations on the date were inconsistent. While the classification of a set of regions-of-interest at one location was the highest in one model, it became the lowest in another. This variation existed among the models in one season, between models from two seasons, and between models from two classification standards (USDA or Industry). For example, the standard deviations of Models RGB-5 and RGB-6 of the 1992 crop were 0.5% and 5.3%, respectively. The standard deviations of Model RGB-9 were 0.7% and 3.2% for the 1991 and 1992 crops, respectively. While the standard deviation of Model HSI-6 for classifying the 1992 crop was 1.8% using the USDA grading standards, it increased to 4.0% using the Industry grading standards. Analysis of variance showed no significant difference at the 99% confidence level among classifications of the 1991 crop from regions-of-interest at different locations on the date using the USDA grading standards and the Industry grading standards (Table VIII). The same condition was true for the 1992 crop (Table VIII).

The U.S. date industry requires that the classification accuracy for all grades be no less than 85% (Chesson et al. 1979). Only two models, HSI-5 and RGB-5, achieved this requirement, using the USDA grading standards. The total classification accuracy of Model RGB-9 for the 1991 crop was

TABLE VIII

ANALYSIS OF VARIANCE FOR COMPARISON OF REGIONS-OF-INTEREST

| Source | DF | SS | MS | F | Pr>F |
|---|---|---|---|---|---|
| | | (USDA Grading Standards, 1991) | | | |
| ROI | 3 | 0.0132 | 0.0044 | 0.21## | 0.8882 |
| Error | 68 | 1.415 | 0.0208 | | |
| Total | 71 | 1.428 | | | |
| | | (USDA Grading Standards, 1992) | | | |
| ROI | 3 | 0.0068 | 0.0022 | 0.09## | 0.9644 |
| Error | 68 | 1.672 | 0.0246 | | |
| Total | 71 | 1.679 | | | |
| | | (Industry Grading Standards, 1991) | | | |
| ROI | 3 | 0.0104 | 0.0035 | 0.22## | 0.8809 |
| Error | 68 | 1.061 | 0.0156 | | |
| Total | 71 | 1.071 | | | |
| | | (Industry Grading Standards, 1992) | | | |
| ROI | 3 | 0.0032 | 0.0011 | 0.07## | 0.9736 |
| Error | 68 | 0.9818 | 0.0144 | | |
| Total | 71 | 0.9850 | | | |

DF : Degree of freedom.
SS : Sum of squares.
MS : Mean square.
## : Not significant at 1% level.

higher than the minimum, however, classification accuracy of some individual classes was not. Figure 19 shows the classification accuracy of Model RGB-9 with the 1991 crop, using the USDA grading standards. Note that the classification accuracy of the Natural and Cull Classes from the four regions-of-interest was higher than 85%, but it was less than 85% in Classes Number 1 Dry (N1D) and Number 2 Dry (N2D).

Using the Industry grading standards, the classification accuracy of Model RGB-9 for both crop seasons increased to 93.2%. The classification accuracy of each grade (Grade A, Grade B, and Grade C) was higher than 85% for the 1991 crop (Fig. 20). The same condition existed with the 1992 crop, with the exception of Grade C in the fourth ROI (Fig. 21). Figures 20 and 21 show the classification accuracy of RGB-9 using the Industry grading standards with the 1991 and 1992 crops.

Variations in color and surface texture within date classes were the main factors affecting classification accuracy. Figure 22 shows five representative dates from the Cull Class of the 1992 crop. This photograph illustrates the variation in brightness and surface texture within date classes. Variations in color cannot be seen directly in the black-and-white photograph, however, they can be detected from variations in overall brightness. As previously stated, date inspectors use surface texture, color, and firmness as grading criteria. These dates might

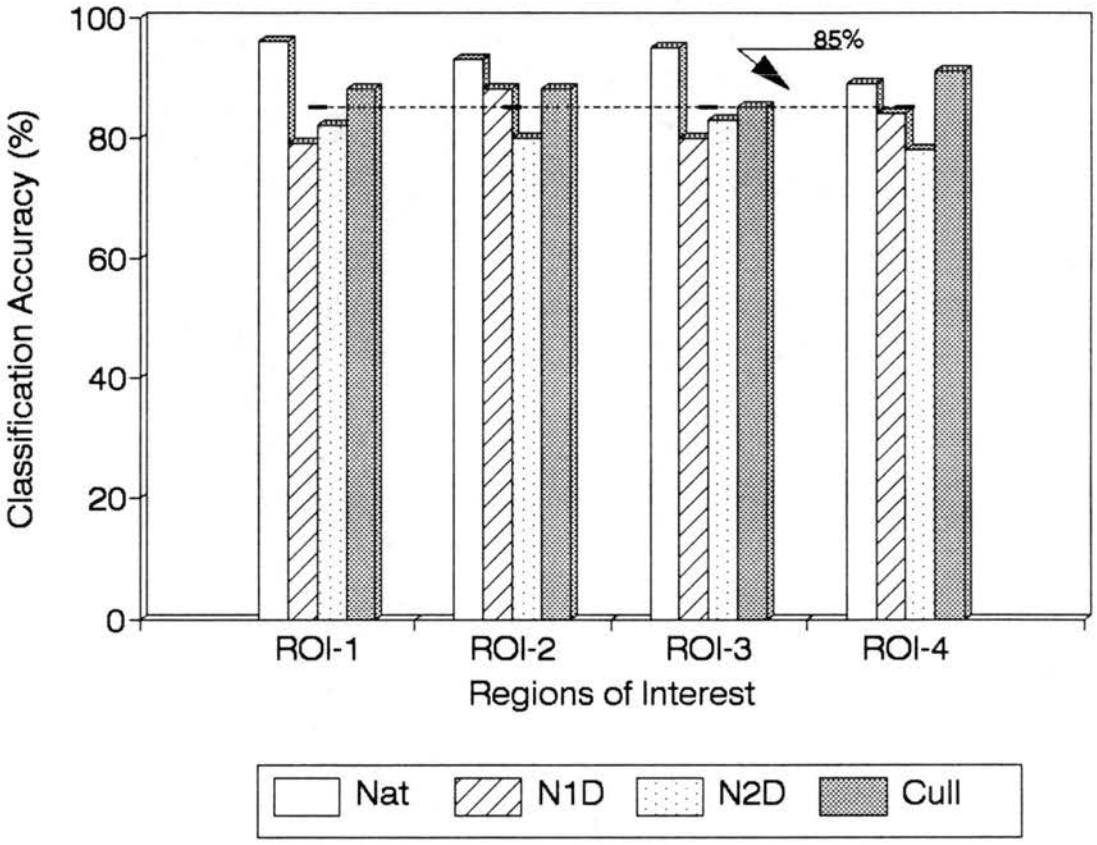


Figure 19. Model RGB-9 Classification of the 1991 Crop From the Four Sets of Regions-of-Interest, USDA Grading Standards.

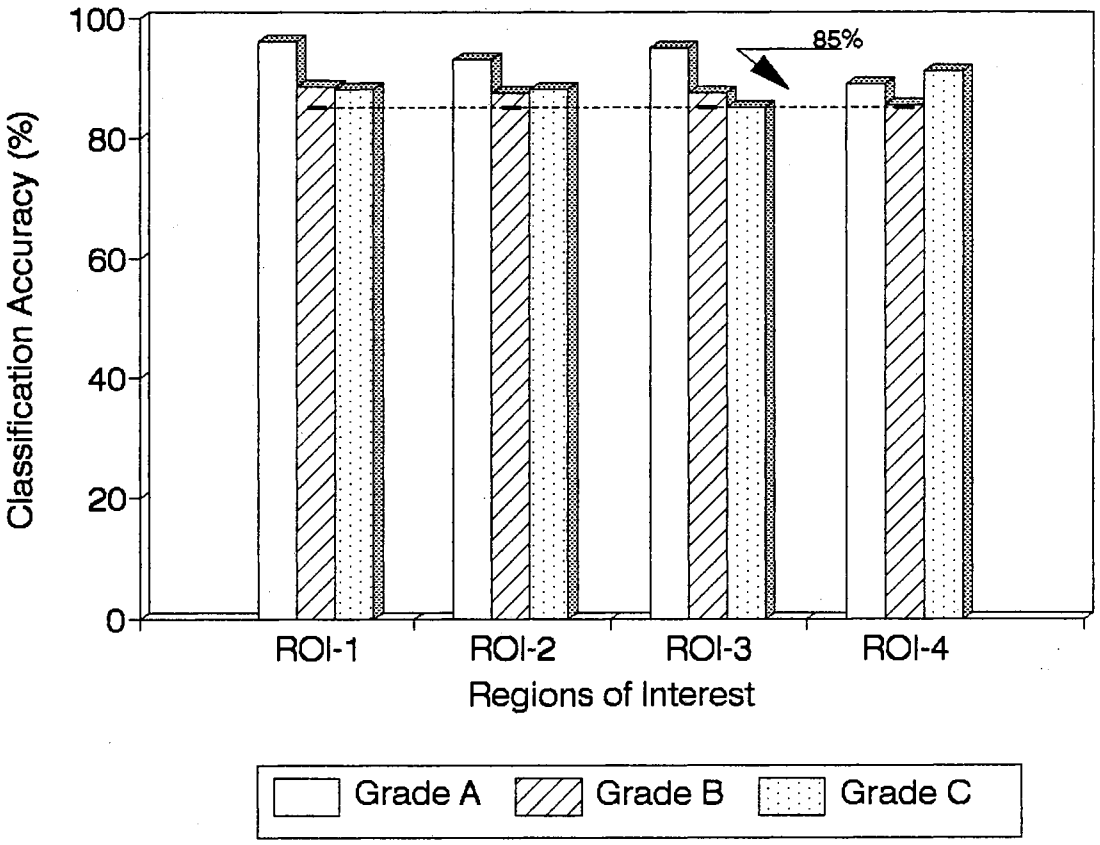


Figure 20. Model RGB-9 Classification of the 1991 Crop From the Four Sets of Regions-of-Interest, Industry Grading Standards.

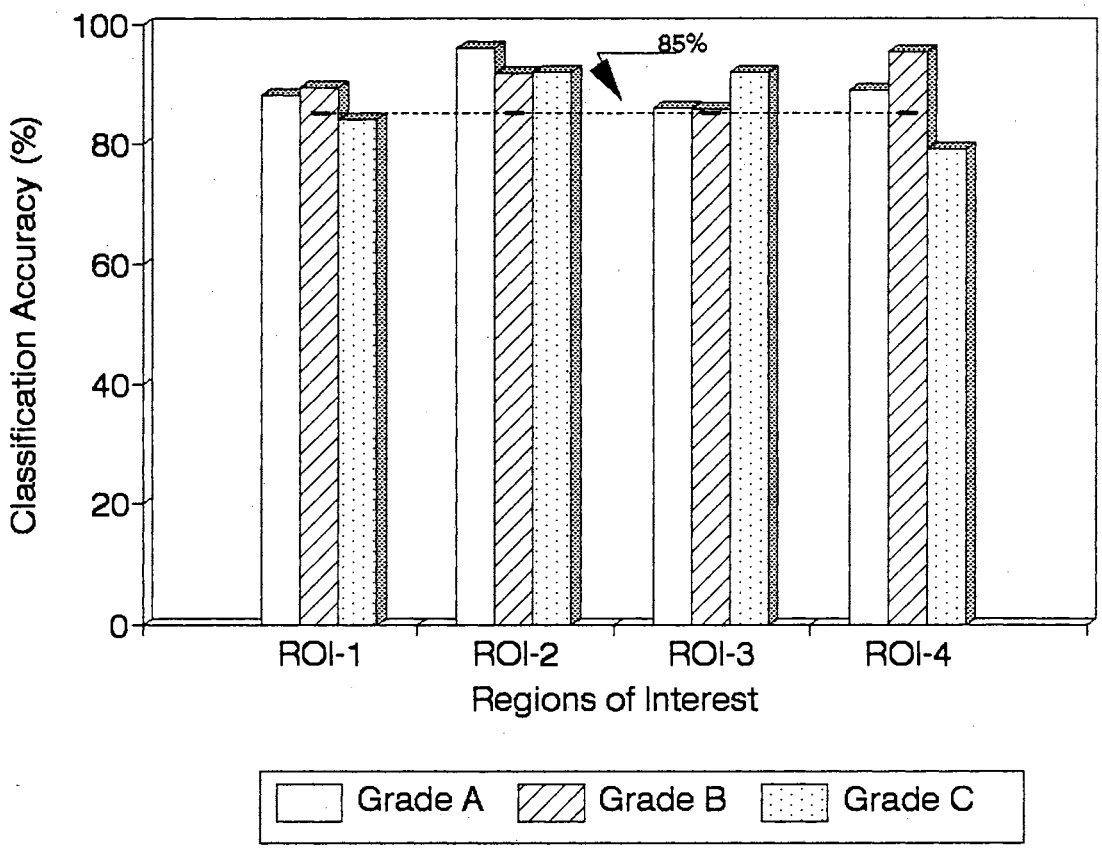


Figure 21. Model RGB-9 Classification of the 1992 Crop From the Four Sets of Regions-of-Interest, Industry Grading Standards.

Figure 22. Representative Dates From the Cull Class of the 1992 Crop.

be combined into one class on the basis of the firmness criterion, which was not used in this project.

Figure 23 consists of two photographs of a pair of dates. The first (a) was taken from one side. The dates were then rotated $180^0$, and the second photograph (b) was taken. It is clear that the brightness (an indication of color) and surface texture vary widely within a single date. The variations of color and surface texture over the surface of an individual fruit were the main cause of the differences among the classification of sets of four regions-of-interest.

(a) (b)

Figure 23. Opposite Sides of Two Individual Dates. Pair Shown in (a) were Rotated $180^0$, (b).

Comparison of HSI and RGB Color Systems

Using USDA grading standards, there was no significant difference between the classifications of the HSI and RGB models at the 99% confidence level for the 1991 and 1992 crops (Table IX). Figures 24 and 25 show the classification accuracy of the HSI and RGB models using the USDA grading standards for the 1991 and 1992 corps, respectively.

Using Industry grading standards, there was also no significant difference between the classifications of the HSI and RGB models at the 99% confidence level for the 1991 and 1992 crops (Table IX). Figures 26 and 27 show the classification accuracy of the HSI and RGB models using the Industry grading standards for the 1991 and 1992 crops, respectively. In general, classification accuracy of the RGB models was slightly higher than that of the HSI models.

It appeared that the RGB models extracted from the co-occurrence matrices and the texture spectrum were more accurate than the HSI models. However, the classification accuracy of HSI-1 was higher than that of RGB-1. Note that HSI-1 and RGB-1 consisted of the mean of the color band histograms.

The HSI color system yielded better performance than the RGB color system from the models using the mean of color bands histograms (HSI-1, RGB-1). On the other hand, the classification accuracy of features extracted from transformed data (i.e. the co-occurrence matrix or texture spectrum) is stronger using the RGB color system.

TABLE IX

ANALYSIS OF VARIANCE FOR COMPARISON OF HSI AND RGB COLOR SYSTEMS

| Source | DF | SS | MS | F | Pr>F |
|---|---|---|---|---|---|
| | | (USDA Grading Standards, 1991) | | | |
| Color | 1 | 0.0108 | 0.0108 | 0.53## | 0.4680 |
| Error | 70 | 1.4174 | 0.0202 | | |
| Total | 71 | 1.4282 | | | |
| | | (USDA Grading Standards, 1992) | | | |
| Color | 1 | 0.0169 | 0.0169 | 0.74## | 0.3931 |
| Error | 82 | 1.8756 | 0.0229 | | |
| Total | 83 | 1.8925 | | | |
| | | (Industry Grading Standards, 1991) | | | |
| Color | 1 | 0.0049 | 0.0049 | 0.32## | 0.5743 |
| Error | 70 | 1.0659 | 0.0152 | | |
| Total | 71 | 1.0708 | | | |
| | | (Industry Grading Standards, 1992) | | | |
| Color | 1 | 0.0122 | 0.0122 | 0.88## | 0.3516 |
| Error | 70 | 0.9728 | 0.0139 | | |
| Total | 71 | 0.9850 | | | |

DF : Degree of freedom.
SS : Sum of squares.
MS : Mean square.
## : Not significant at 1% level.

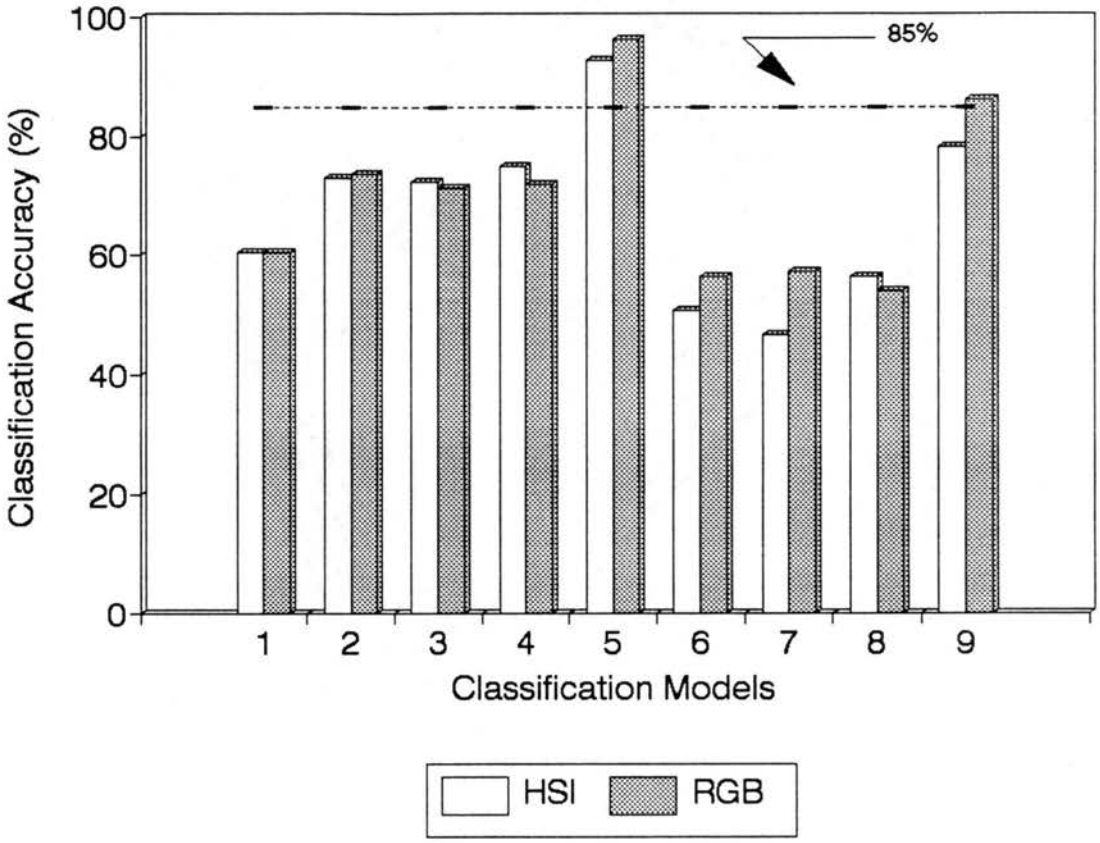


Figure 24. Classification by the HSI and RGB Models (9 Models From Each) of the 1991 Crop, USDA Grading Standards.

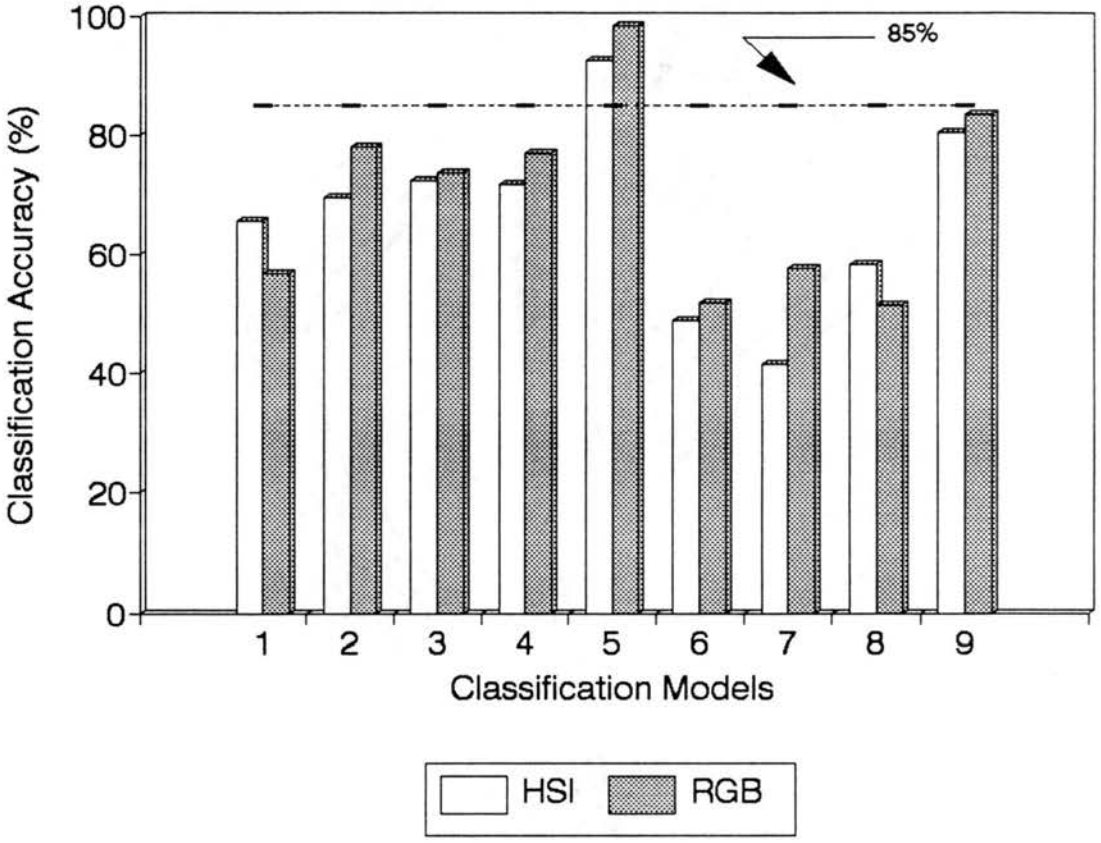


Figure 25. Classification by the HSI and RGB Models (9 Models From Each) of the 1992 Crop, USDA Grading Standards.

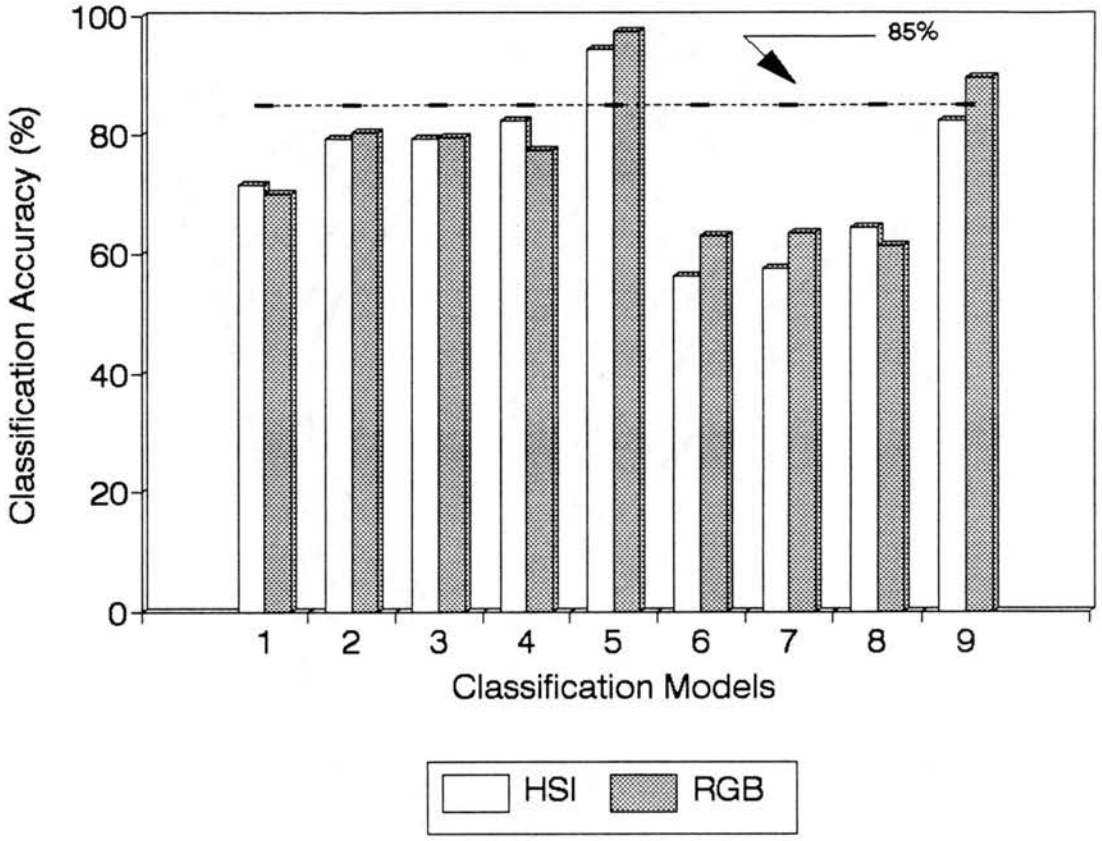


Figure 26. Classification by the HSI and RGB Models (9 Models from Each) of the 1991 Crop, Industry Grading Standards.

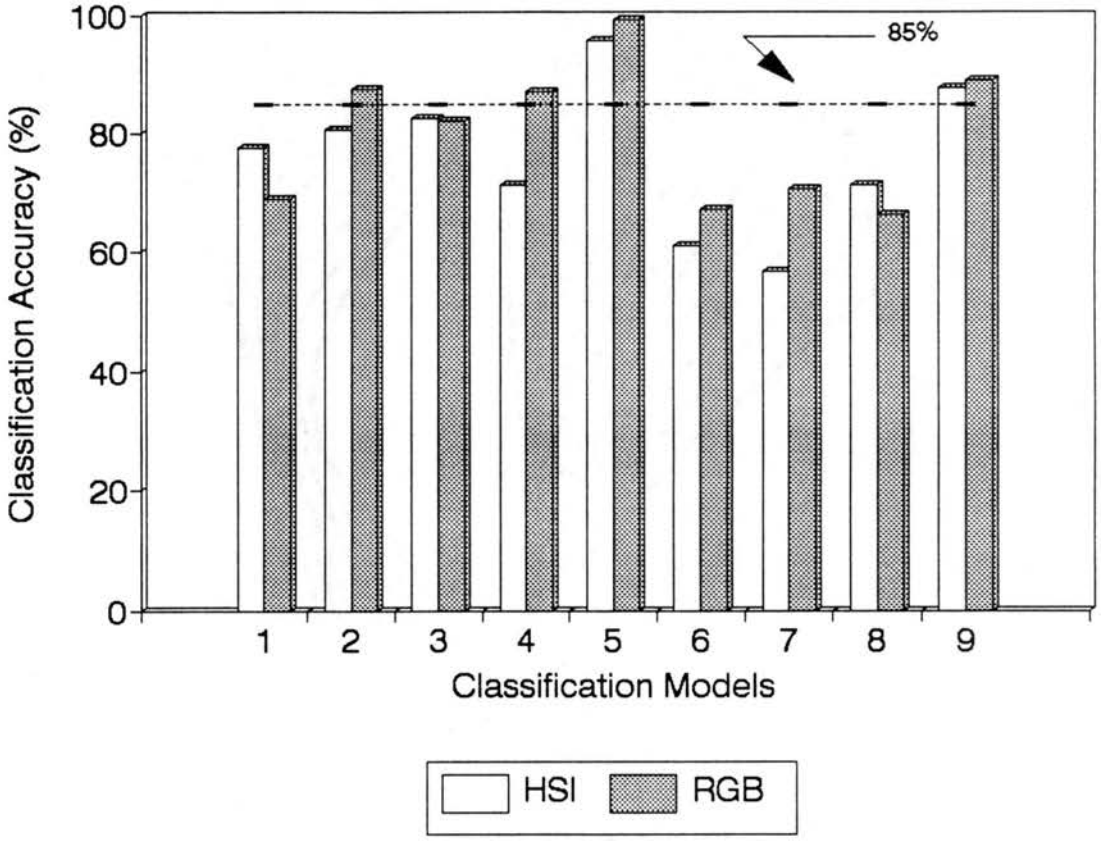


Figure 27. Classification by the HSI and RGB Models (9 Models from Each) of the 1992 Crop, Industry Grading Standards.

Comparison of Color and Black-and-White

Classification accuracy of color models extracted from the co-occurrence matrix (RGB-5) and from the texture spectrum (RGB-9) was compared with accuracy of black-and-white models (HSI-4 and HSI-8) represented by the intensity band of the HSI color system. Classification accuracy of the color and black-and-white models was found to be significantly different at 99% confidence level in both crop seasons, using the USDA grading standards and Industry grading standards (Table X). Figures 28 and 29 show the classification accuracy of the color model, RGB-5, and black-and-white model, HSI-4, for the 1991 and 1992 crops, using the USDA grading standards.

For the 1991 crop, the highest classification accuracy of the black-and-white model was 77%, which is less than the date industry requirement (85%), while accuracy of the color model was 97.5%. Classification accuracy of the black-and-white model increased to 83.7% using the Industry grading standards, but is still below the industry minimum (85%). Figures 30 and 31 show the classification accuracy of the color and black-and-white models using the Industry grading standards for the 1991 and 1992 crops, respectively. It appeared that color information is important for automated date inspection (Deglet Noor variety).

TABLE X

ANALYSIS OF VARIANCE FOR COMPARISON OF COLOR AND BLACK-AND-WHITE

| Source | DF | SS | MS | F | Pr>F |
|---|---|---|---|---|---|
| | | (USDA Grading Standards, 1991) | | | |
| System | 1 | 0.0907 | 0.0907 | 370.49** | 0.0001 |
| Error | 6 | 0.0015 | 0.0002 | | |
| Total | 7 | 0.0922 | | | |
| | | (USDA Grading Standards, 1991) | | | |
| System | 1 | 0.1431 | 0.1431 | 633.71** | 0.0001 |
| Error | 6 | 0.0014 | 0.0002 | | |
| Total | 7 | 0.1445 | | | |
| | | (Industry Grading Standards, 1991) | | | |
| System | 1 | 0.0450 | 0.0450 | 608.79** | 0.0001 |
| Error | 6 | 0.0004 | 0.00007 | | |
| Total | 7 | 0.0454 | | | |
| | | (Industry Grading Standards, 1992) | | | |
| System | 1 | 0.0643 | 0.0643 | 2258.08** | 0.0001 |
| Error | 6 | 0.0002 | 0.00003 | | |
| Total | 7 | 0.0644 | | | |

DF : Degree of freedom.
SS : Sum of squares.
MS : Mean square.
** : Significant at 1% level.

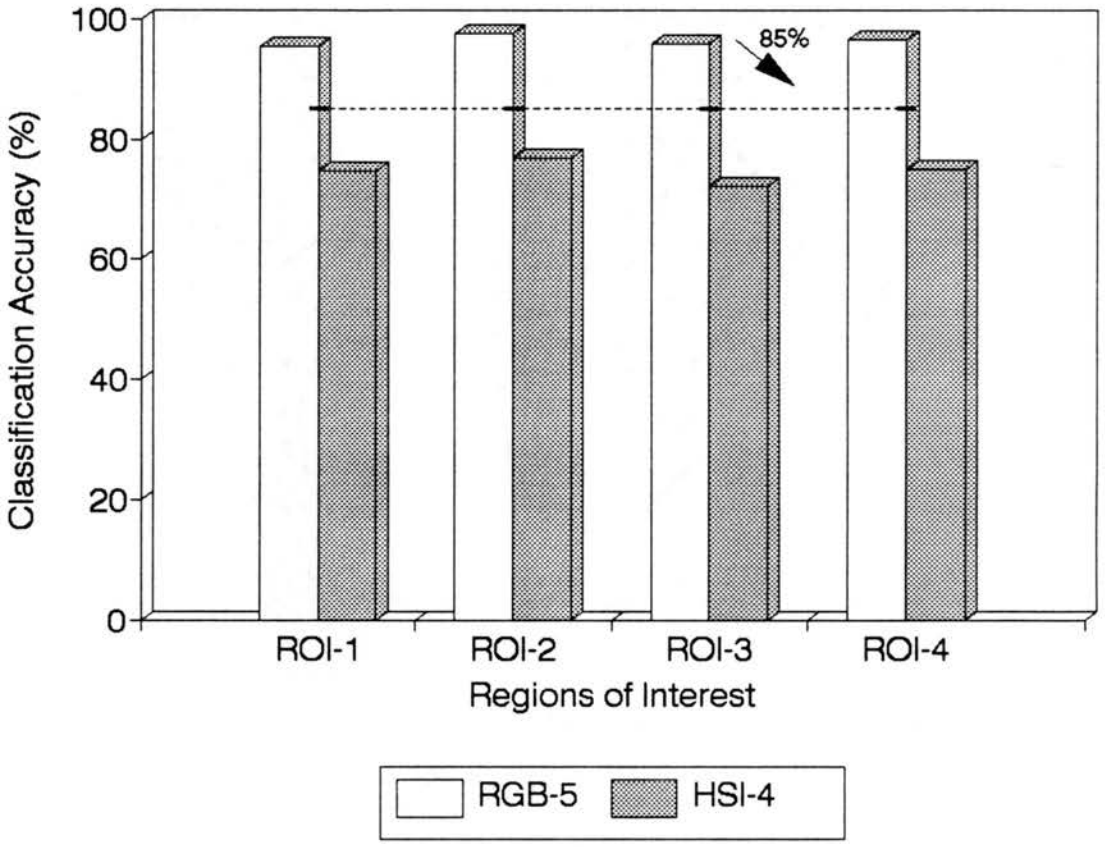


Figure 28. Classification of Color Model (RGB-5) and Black-and-White Model (HSI-4) for the 1991 Crop, USDA Grading Standards.

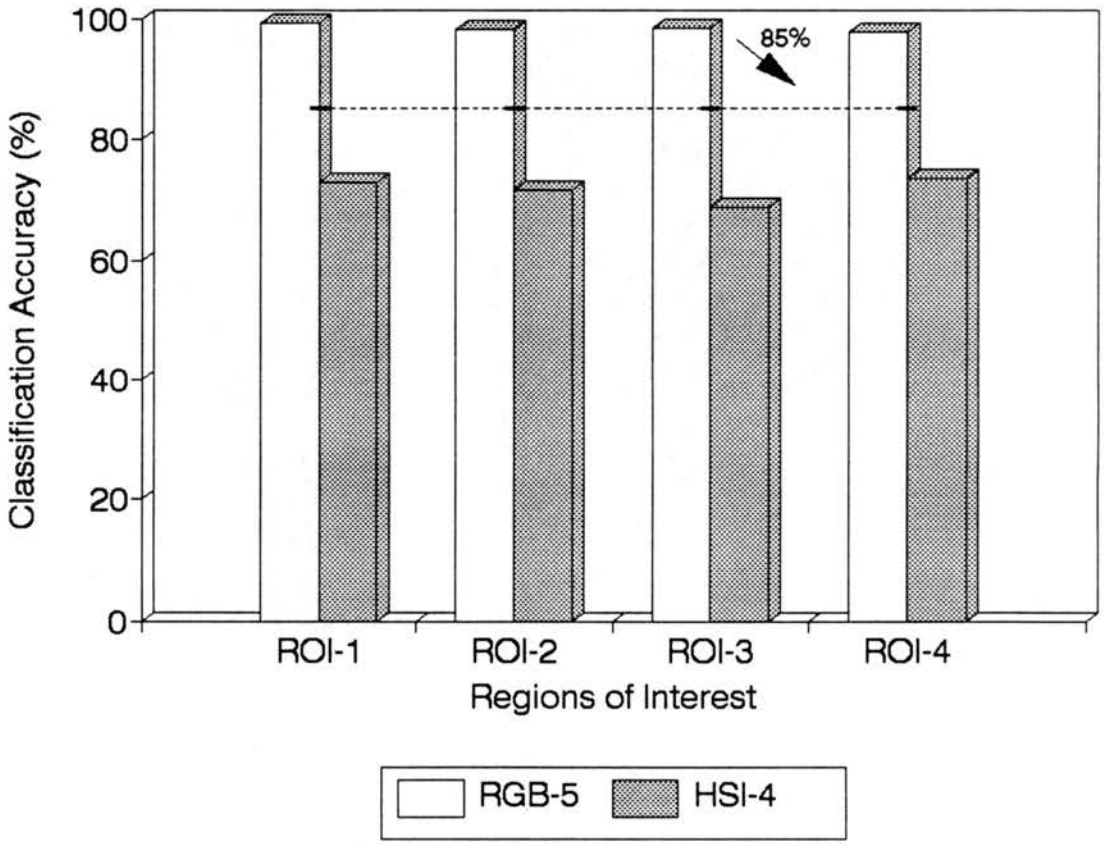


Figure 29. Classification of Color Model (RGB-5) and Black-and-White Model (HSI-4) for the 1992 Crop, USDA Grading Standards.

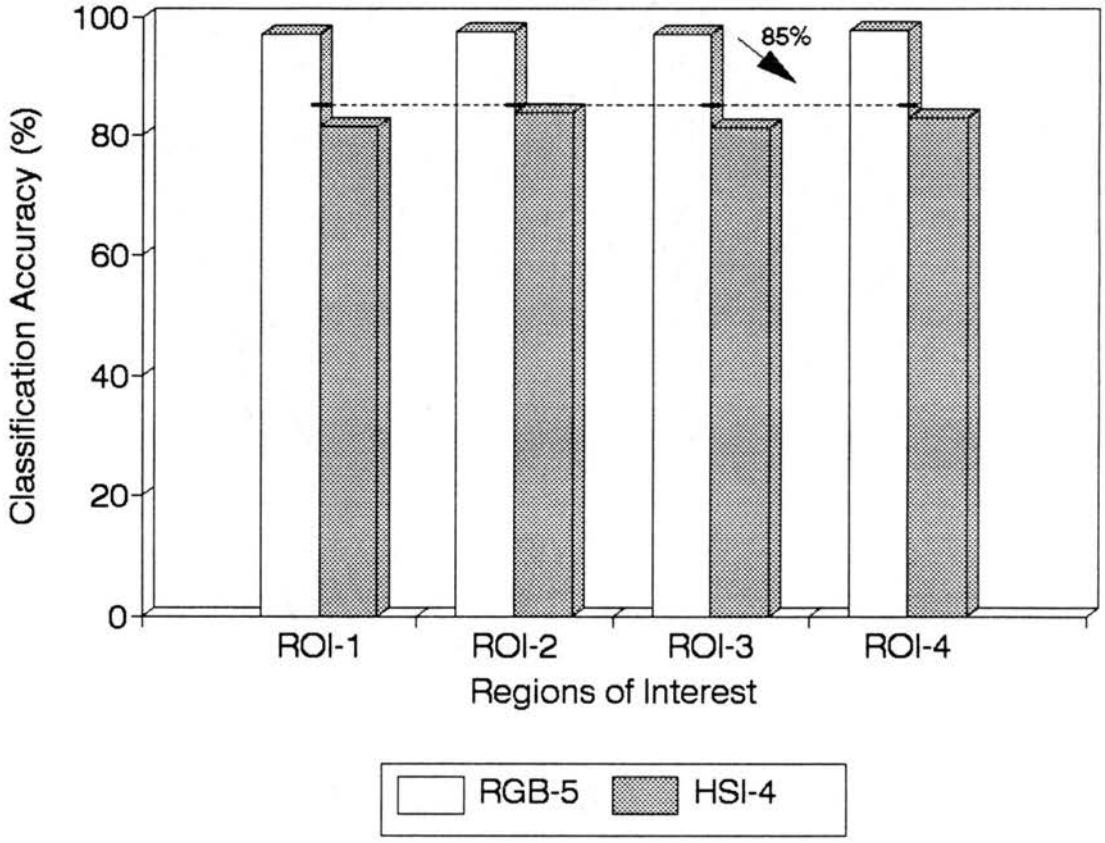


Figure 30. Classification of Color Model (RGB-5) and Black-and-White Model (HSI-4) for the 1991 Crop, Industry Grading Standards.

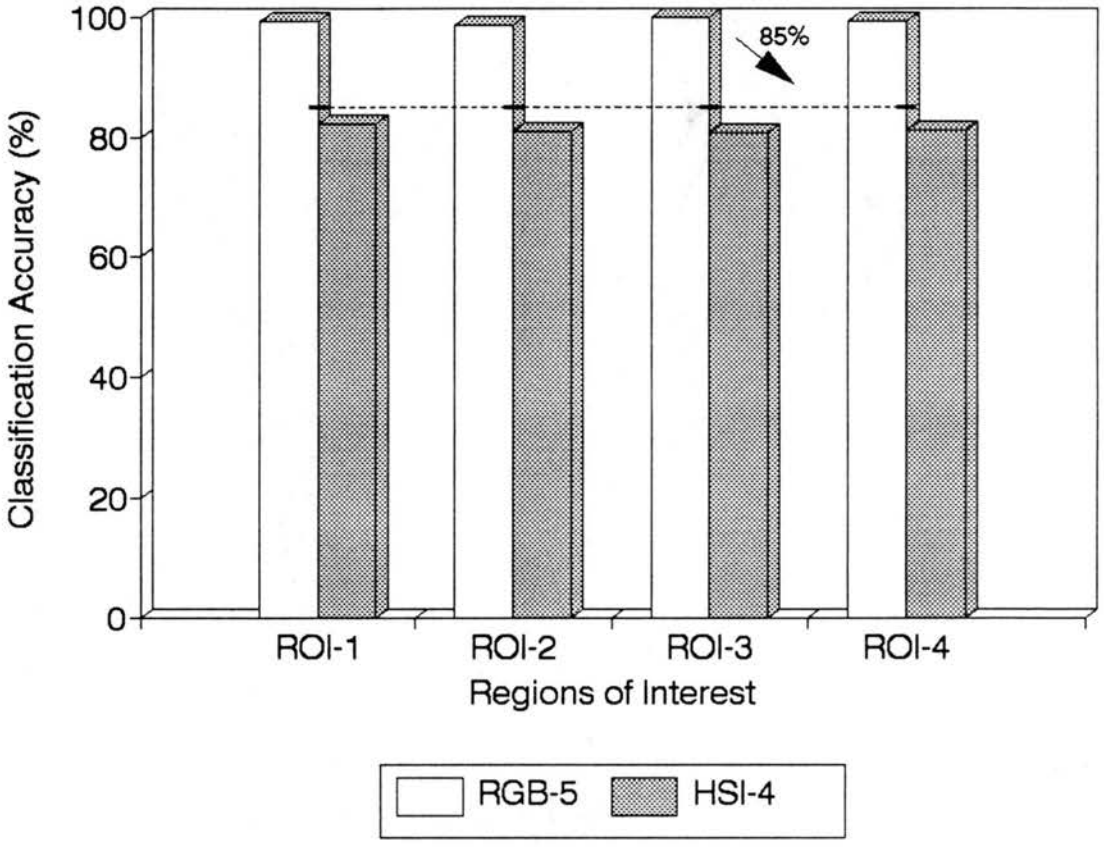


Figure 31. Classification of Color Model (RGB-5) and Black-and-White Model (HSI-4) for the 1992 Crop, Industry Grading Standards.

## Comparison of USDA Grading Standards and Industry Grading Standards

The USDA grading standards define six classes of date fruits, of which the U.S. date industry uses only five. The five classes are Natural, Waxy, Number 1 DRY, Number 2 Dry, and Cull. The Dole Dried Fruit and Nut Company combines Waxy, Number 1 Dry, and Number 2 Dry classes into one grade (Grade B) to form three grades; A, B, and C (Industry grading standards).

The classification accuracy of all eighteen models improved when applied to the Industry grading standards in the 1991 and 1992 crops. This improvement was significant at the 99% confidence level (Table XI). Figures 32 and 33 compare date classification accuracy using the USDA and Industry grading standards for the 1991 and 1992 crops, respectively. Classification improvement when using Industry grading standards ranged from 1.1 to 11.2 percentage points for the 1991 crop and from 1 to 16 percentage points for the 1992 crop. The greatest improvement occurred with the HSI-1 model for the 1992 crop, for which classification accuracy increased from 65.8% to 77.6%. It should also be noted that model HSI-1 included only three features.

TABLE XI

ANALYSIS OF VARIANCE FOR COMPARISON OF USDA GRADING STANDARDS AND INDUSTRY GRADING STANDARDS

| Source | DF | SS | MS | F | Pr>F |
|---|---|---|---|---|---|
| | | | (1991 Crop) | | |
| Season | 1 | 0.1503 | 0.1503 | 8.54** | 0.0040 |
| Error | 142 | 2.4990 | 0.0176 | | |
| Total | 143 | 2.6493 | | | |
| | | | (1992 Crop) | | |
| Season | 1 | 0.3778 | 0.3778 | 20.14** | 0.0001 |
| Error | 142 | 2.6641 | 0.0188 | | |
| Total | 143 | 3.0419 | | | |

DF : Degree of freedom.
SS : Sum of squares.
MS : Mean square.
** : Significant at 1% level.

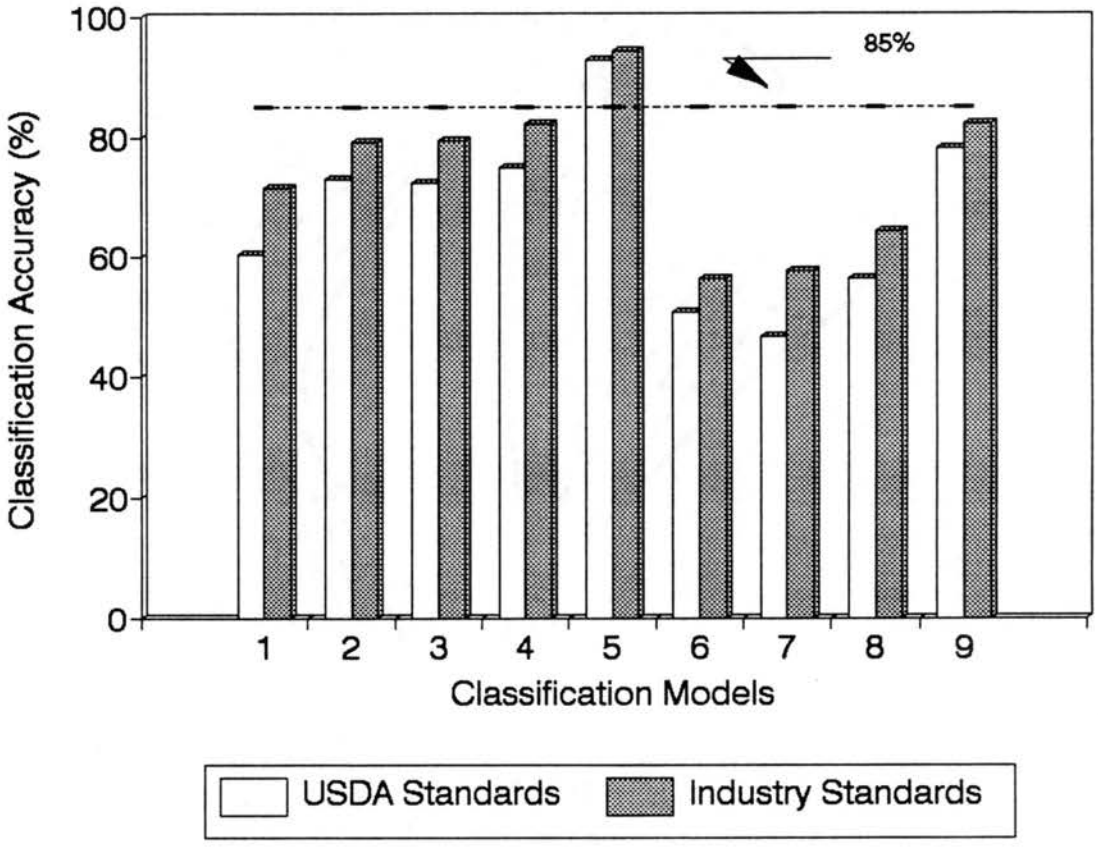


Figure 32. HSI Model Classification of the 1991 Crop Using the USDA Grading Standards and the Industry Grading Standards.

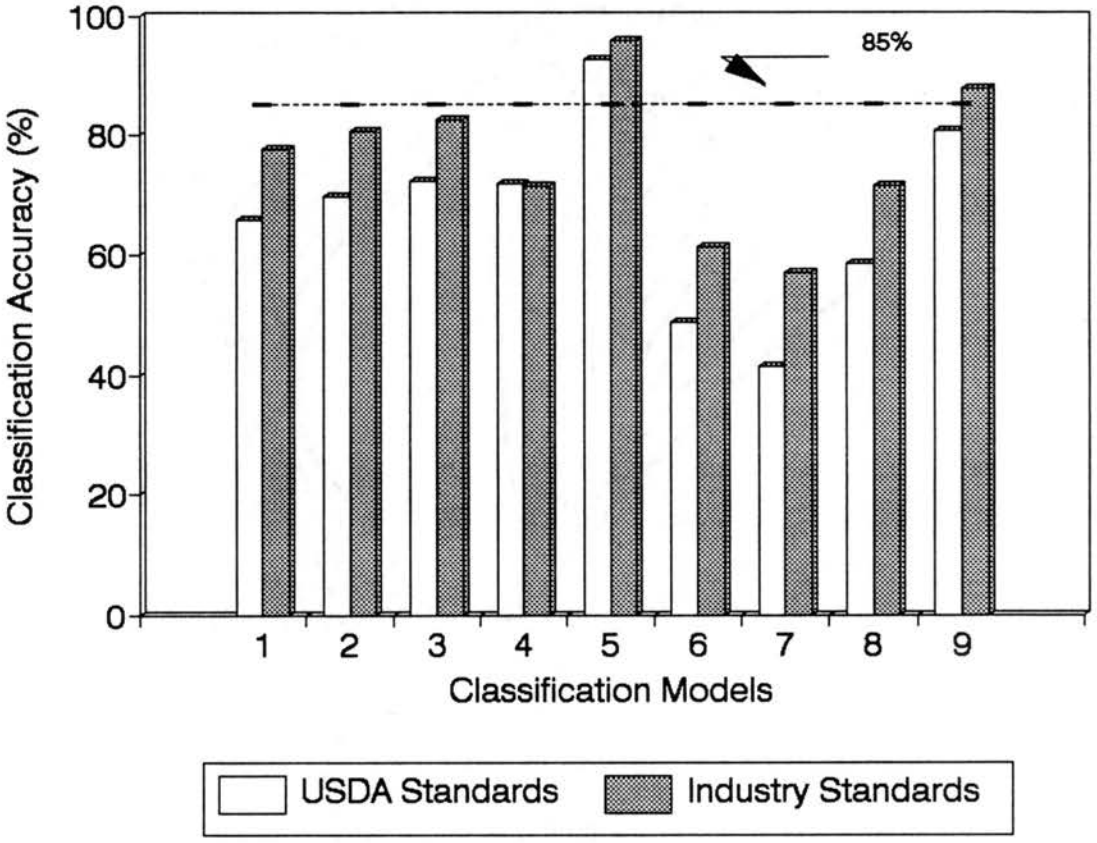


Figure 33. HSI Model Classification of the 1992 Crop Using the USDA Grading Standards and the Industry Grading Standards.

## Comparison of Co-occurrence Matrix and Texture Spectrum Models

The texture spectrum models (HSI-6 - HSI-9 and RGB-6 - RGB-9) performed poorly when compared with the co-occurrence matrix models (HSI-2 - HSI-5 and RGB-2 - RGB-5). Classification accuracy of the texture spectrum and the co-occurrence matrix models was found to be significantly different at the 99% confidence level for both crop seasons, using both USDA and Industry grading standards (Table XII). Figures 34 and 35 show the classification accuracy of the texture spectrum and the co-occurrence matrix models using the USDA grading standards for the 1991 and 1992 crops, respectively. The highest classification accuracy of a texture spectrum model was 86.2% (RGB-9) for the 1991 crop, while the accuracy of the corresponding co-occurrence matrix model was 96.3%.

Classification accuracy was slightly improved by using the Industry grading standards. Accuracy of the texture spectrum and co-occurrence matrix models increased to 89.5% and 97.4%, respectively. Figures 36 and 37 show the classification accuracy of the texture spectrum and the co-occurrence matrix models using the Industry grading standards for the 1991 and 1992 crops, respectively.

It should be noted that the texture spectrum Model RGB-9 included 24 features, while the co-occurrence matrix Model RGB-5 included 39 features. Only nine features of the RGB-9, ($R_{15}$- $R_{17}$, $G_{15}$- $G_{17}$, and $B_{15}$- $B_{17}$) had strong

TABLE XII

ANALYSIS OF VARIANCE FOR COMPARISON OF CO-OCCURRENCE MATRIX AND TEXTURE SPECTRUM

| Source | DF | SS | MS | F | Pr>F |
|---|---|---|---|---|---|
| | | (USDA Grading Standards, 1991) | | | |
| Approach | 1 | 0.4933 | 0.4933 | 34.99** | 0.0001 |
| Error | 62 | 0.8742 | 0.0141 | | |
| Total | 63 | 1.3676 | | | |
| | | (USDA Grading Standards, 1992) | | | |
| Approach | 1 | 0.6344 | 0.6344 | 40.07** | 0.0001 |
| Error | 62 | 0.9815 | 0.0158 | | |
| Total | 63 | 1.6159 | | | |
| | | (Industry Grading Standards, 1991) | | | |
| Approach | 1 | 0.4331 | 0.4331 | 43.61** | 0.0001 |
| Error | 62 | 0.6158 | 0.0099 | | |
| Total | 63 | 1.0489 | | | |
| | | (Industry Grading Standards, 1992) | | | |
| Approach | 1 | 0.3980 | 0.3980 | 45.36** | 0.0001 |
| Error | 62 | 0.5439 | 0.0088 | | |
| Total | 63 | 0.9419 | | | |

DF : Degree of freedom.
SS : Sum of squares.
MS : Mean square.
** : Significant at 1% level.

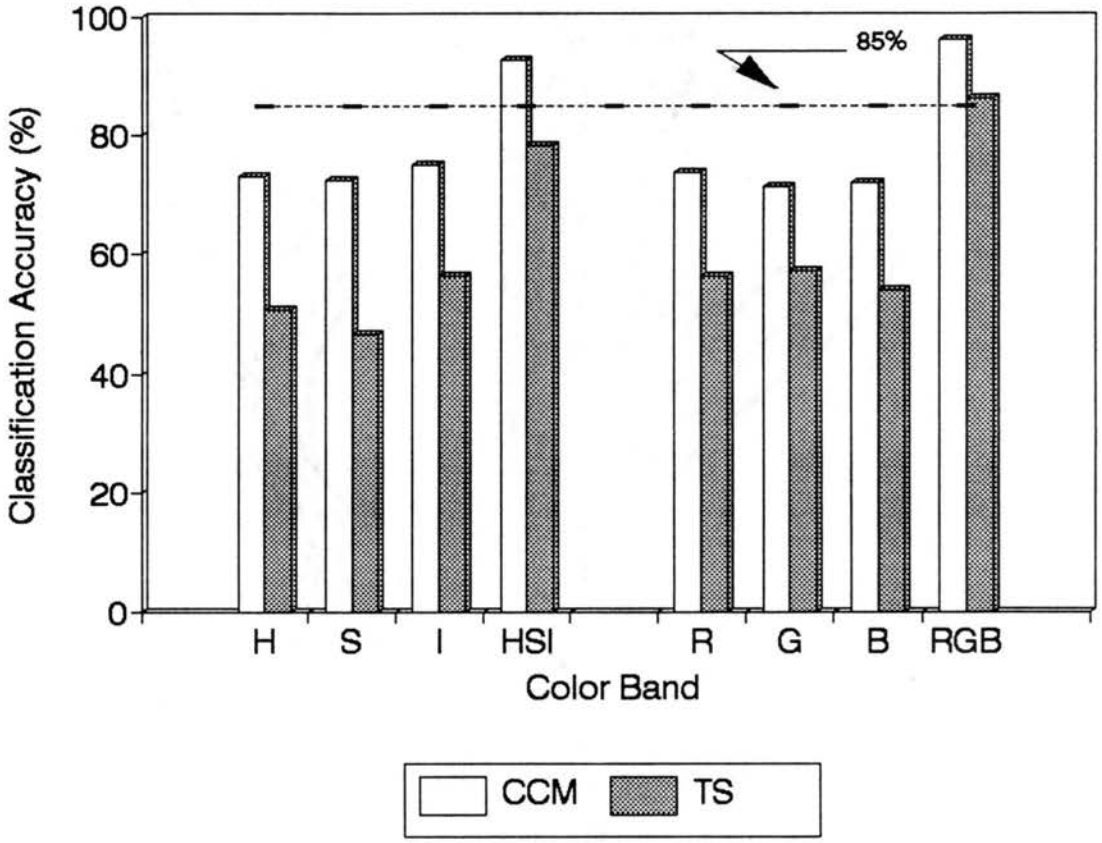


Figure 34. Classification Performance of the Co-occurrence Matrix and the Texture Spectrum Models for the 1991 Crop, USDA Grading Standards.

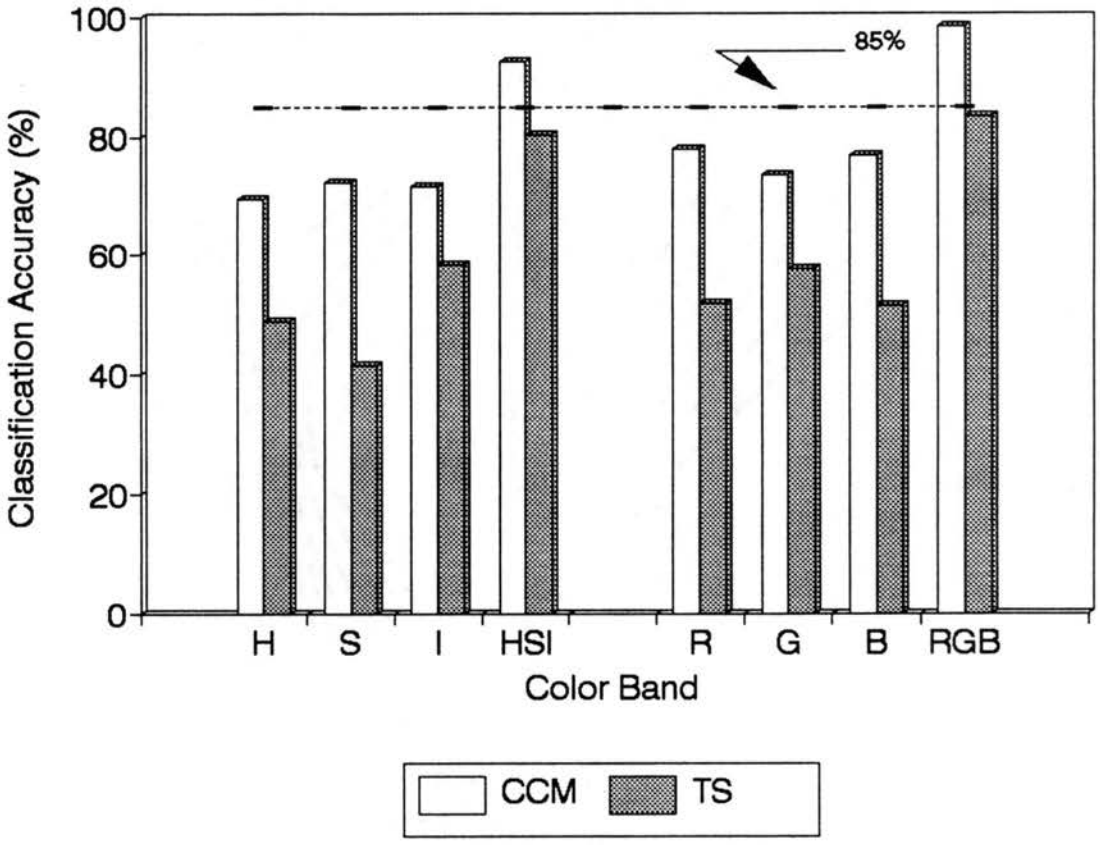


Figure 35. Classification Performance of the Co-occurrence Matrix and the Texture Spectrum Models for the 1992 Crop, USDA Grading Standards.

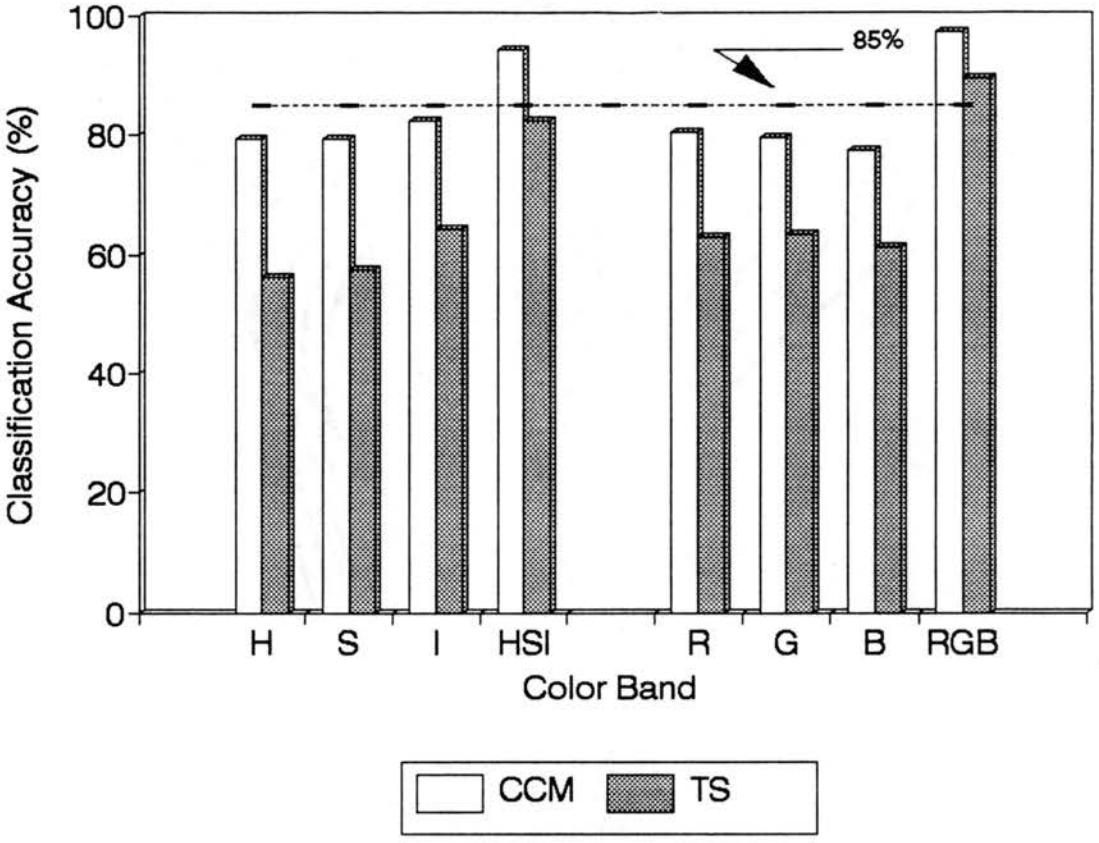


Figure 36. Classification Performance of the Co-occurrence Matrix and the Texture Spectrum Models for the 1991 Crop, Industry Grading Standards.

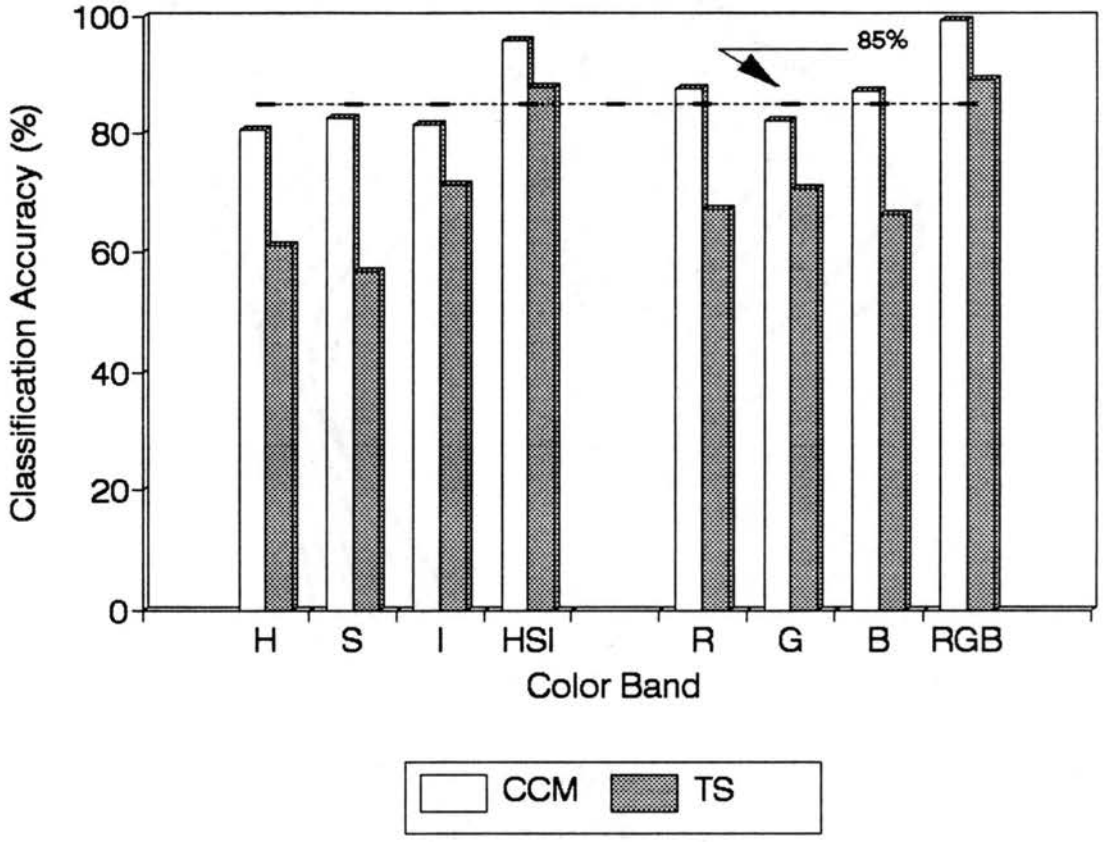


Figure 37. Classification Performance of the Co-occurrence Matrix and the Texture Spectrum Models for the 1992 Crop, Industry Grading Standards.

discriminating power. The discriminating power of the other fifteen features was very small. These features are sensitive to small changes in image data (equations 35 - 39). On the other hand, most of the features of the co-occurrence matrix Model RGB-5 had strong discriminating power.

It appeared that the weak discriminating power of texture spectrum features was due to the locality of texture-context, large range of texture unit values, and large number of gray levels (256). The texture spectrum method detects local texture. Texture unit computation considers only the eight nearest neighbors. The texture unit value ranged from 0 to 6560. This large range was very sensitive to small changes in image data. For example, the gray levels of the eight nearest neighbors of the pixel, Q = 99, in clockwise order a - h were 99, 120, 80, 96, 99, 111, 102, and 98, respectively (Fig. 10). The computed texture unit was 2032. Changing the value of the eighth neighbor from 98 to 99 would raise the texture unit to 4219.

It appeared that the sensitivity of the texture unit was reduced by changing the number of gray levels from 256 to 32. From the above example, if the value of the eighth neighbor was changed while using 32 gray levels, the texture unit value would be unchanged (4146). Accordingly, sensitivity of the texture spectrum features would be reduced.

In the work by He and Wang (1991), the texture spectrum

method performed more effectively in classifying radar images than the co-occurrence matrix. Each pixel in a radar image represents a relatively large area (hectares). Thus, texture-context extracted from the eight nearest neighboring pixels has meaningful information. In date images, the texture-context extracted from the eight nearest neighboring pixels has poorly defined information, because most of wrinkles (texture) have a width larger than 3 pixels. In general, by obtaining more texture spectrum features, using image data with 32 gray levels, and using large pixel resolution, performance of the texture spectrum method would be comparable to that of the co-occurrence matrix.

Comparison of 1991 and 1992 Crops

Using the USDA grading standards, there was no significant difference between the classifications of the 1991 and 1992 crops at the 99% confidence level (Table XIII). Note that the 1991 and 1992 crops were composed of 4 and 5 classes, respectively. The 1991 crop was softer and more mature, the result of a season which was relatively cool. The 1992 season, in contrast, was hot. Figure 38 shows the classification accuracy of the RGB models for the 1991 and 1992 crops, using the USDA grading standards. The highest classification accuracy was 96.3% and 98.4% (RGB-5) for the 1991 and 1992 crops.

Using the Industry grading standards, classification accuracy increased to 97.4% and 99.3% for the 1991 and 1992

TABLE XIII

ANALYSIS OF VARIANCE FOR COMPARISON OF 1991 AND 1992 CROPS

| Source | DF | SS | MS | F | Pr>F |
|---|---|---|---|---|---|
| | | (USDA Grading Standards) | | | |
| Season | 1 | 0.0002 | 0.0002 | 0.01## | 0.9154 |
| Error | 142 | 3.1072 | 0.0219 | | |
| Total | 143 | 3.1075 | | | |
| | | (Industry Grading Standards) | | | |
| Season | 1 | 0.0446 | 0.0446 | 3.08** | 0.0813 |
| Error | 142 | 2.0558 | 0.0145 | | |
| Total | 143 | 2.1005 | | | |

DF : Degree of freedom.
SS : Sum of squares.
MS : Mean square.
** : Significant at 1% level.
## : Not significant at 1% level.

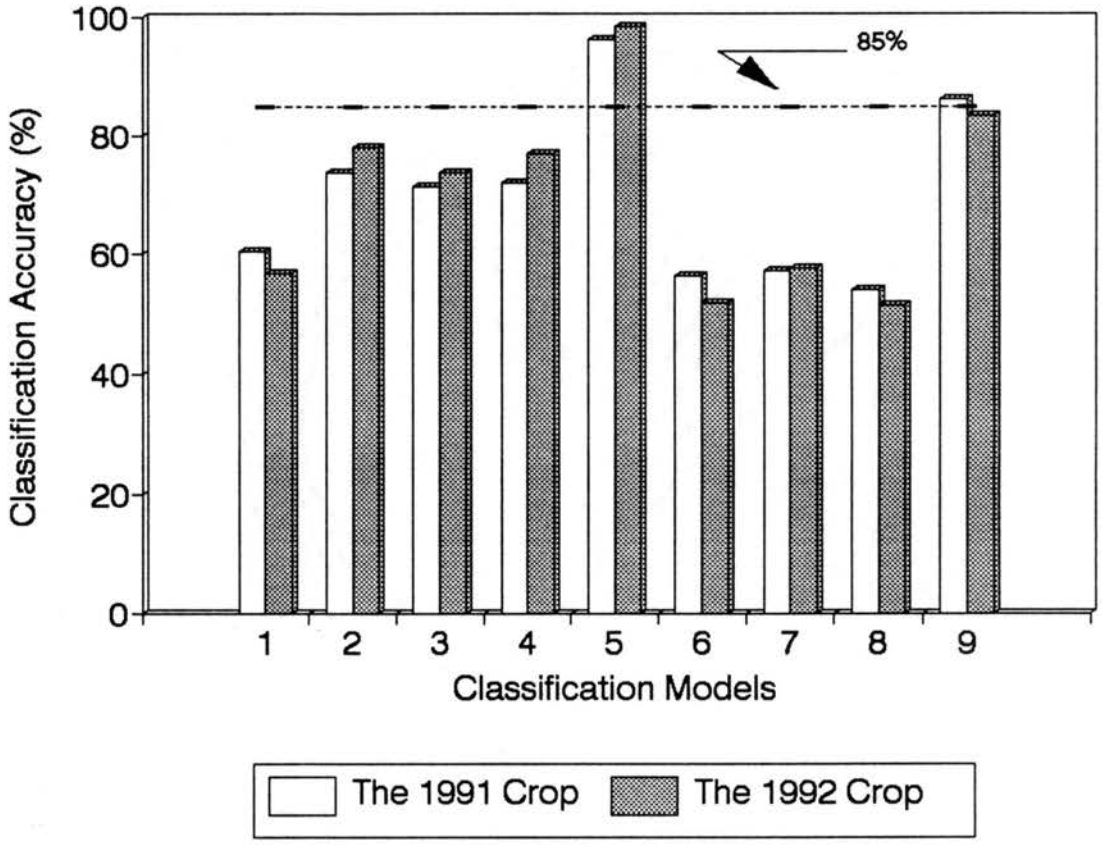


Figure 38. RGB Model Classification of the 1991 and 1992 Crops, USDA Grading Standards.

crops. However, the classification accuracy for both crop seasons was found to be significantly different at the 99% confidence level (Table XIII). Figure 39 shows the classification accuracy of the RGB models for the 1991 and 1992 crops, using the Industry grading standards. Accuracy with the 1992 crop was superior to that of the 1991 crop. Sample sizes for Grade B dates were 200 and 300 for the 1991 and 1992 crops, respectively, while sample sizes for Grade A and Grade C dates were 100. This difference was the main cause of the variation between the classification of the 1991 and 1992 crops.

## Performance

An Everex 486/33e microcomputer was used to compute the features of the first-order histogram, co-occurrence matrix, and texture spectrum. The features of the first-order histogram were processed in 0.09 s (666 fruits per minute). Features of the co-occurrence matrix (39) were computed in 4.2 s (14 fruits per minute). In a practical design, only the features which had the most discriminating power (less than ten features) should be used. Texture spectrum features (24) were processed in 5.1 s (11 fruits per minute). Only nine features had strong discriminating power. Processing time reduced to 3.2 s (18 fruits per minute) using only nine features.

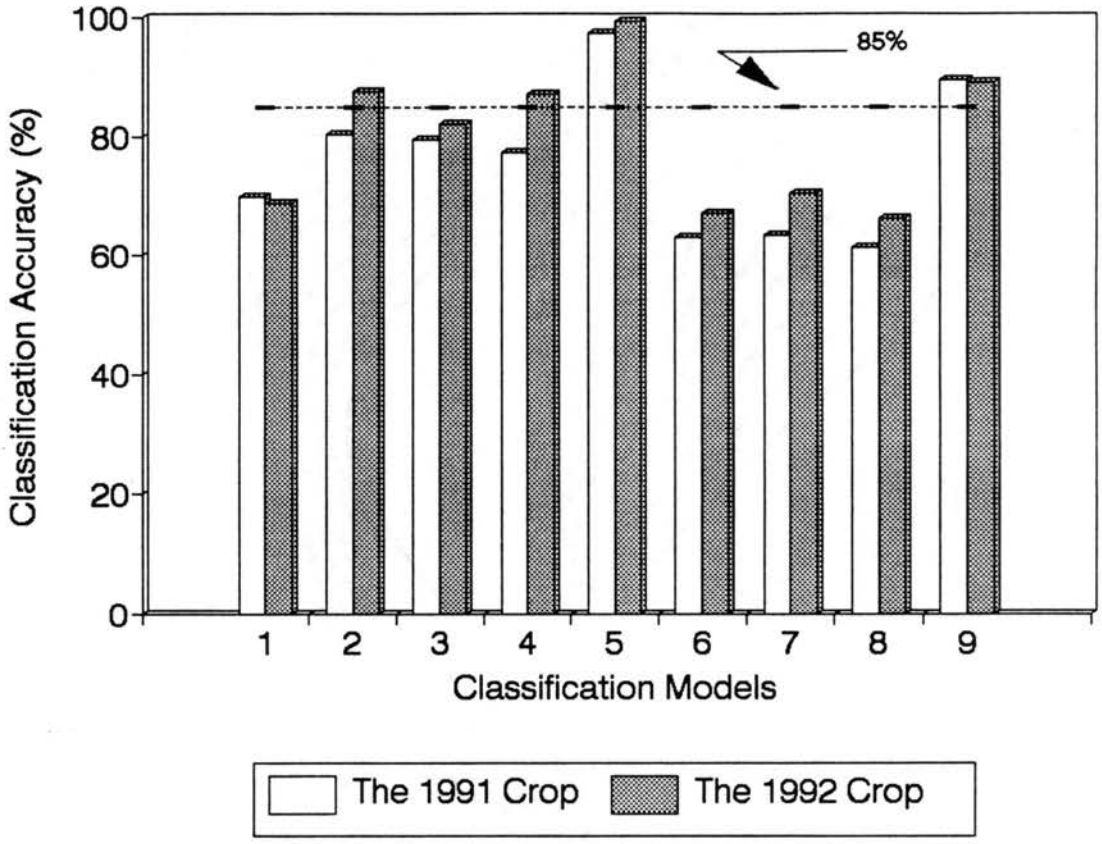


Figure 39. RGB Model Classification of the 1991 and 1992 Crops, Industry Grading Standards.

# CHAPTER VIII

# SUMMARY AND CONCLUSIONS

## Summary

Image processing techniques were developed to grade dates into quality classes based on color and texture analysis. Three surface color and texture approaches were investigated, namely; first-order histogram, co-occurrence matrix, and texture spectrum.

Date fruits manually classified according to the USDA grading standards (five classes) and Industry grading standards (three grades) from two crop seasons (1991 and 1992) were tested. Four images were acquired from each date. A 64x64-pixel region-of-interest (ROI) was selected from each image. Twenty-two features were extracted from the ROI in each color band of hue, saturation, and intensity (HSI) and red, green, and blue (RGB), for a total of 132 features.

Eighteen models were constructed. Two models used features of the first-order histogram, eight used features of the co-occurrence matrix, and eight used texture spectrum features. A nonparametric multivariate discriminant analysis procedure was used to classify feature observations for each model into classes or grades.

## Conclusions

Classification accuracy varied among the eighteen models. Highest classification accuracy was 65.8%, 98.4%, and 84.4% from the first-order histogram, co-occurrence matrix, and texture spectrum methods, respectively, using the USDA grading standards with the 1992 crop. Accuracy increased to 77.6%, 99.3%, and 89.0% using the Industry grading standards with the same crop. There was no significant difference at the 99% confidence level in classification accuracy of observations obtained from regions-of-interest at four different locations on the date, using either USDA grading standards or Industry grading standards. Processing only one ROI was sufficient to evaluate surface features. These results indicate that sufficient grading accuracy may be achieved by processing a relatively small percentage of the date surface.

There was no significant difference in classification accuracy of the RGB and HSI models for either crop season, using both USDA and Industry grading standards. In general, classification accuracy of the RGB models extracted from the co-occurrence matrix or texture spectrum was higher than that of the HSI models. RGB models extracted from the first-order histogram, on the other hand, performed less favorably than HSI models. Results suggest that the RGB color system should be used with models extracted from the co-occurrence matrix or texture spectrum. The HSI color system should be selected for models extracted from the

first-order histogram.

Accuracy of color and black-and-white models was significantly different. The highest classification accuracy of the black-and-white models represented by the intensity band of the HSI color system was 77%, which is below the date industry accuracy standard of 85%.

The classification accuracy of all models improved when applied to the Industry grading standards. The largest improvement was 16 percentage points. Several models met the date industry minimum accuracy standard (85%) using the Industry grading standards, while they did not when using the USDA grading standards.

Classification accuracy of the co-occurrence matrix models was significantly greater than that of the texture spectrum models. There was no significant difference in classification accuracy between the 1991 and 1992 crops, using USDA grading standards.

The features of the first-order histogram, co-occurrence matrix, and texture spectrum were processed in 0.09, 4.2, and 5.1 s, respectively.

## Recommendations For Further Research

The objectives of this project have been completed, and a foundation has been laid for future work. This section presents recommendations for additional research on the date grading system.

A 64x64-pixel (0.88 $cm^2$) ROI appears to be sufficient

for evaluation of date surface features. The texture spectrum features are sensitive to pixel spatial and intensity resolutions, which were 0.15 mm and 256 gray levels (8 bits), respectively. Improved accuracy from texture spectrum features might be achieved by lowering both spatial and intensity resolutions. A spatial resolution of 0.3 mm and intensity of 32 gray levels (5 bits) is suggested.

Classification accuracy of the HSI first-order histogram model was 65.8% and 77.6% using the USDA and Industry grading standards. This model consisted of the mean of the color band histograms. Fast computation (real time) is the main advantage of this model. Additional features, such as standard deviation and areas defined using thresholding techniques might allow classification accuracy of the model to meet the date industry requirment (85%).

Neural networks are an alternative method which has been applied to classification and pattern recognition. Comparing the performance of neural networks to that of the nonparametric multivariate discriminant method (using Epanechnikov kernel) is suggested.

## REFERENCES


Ahmad, S. I. and J. F. Reid. 1991. Computer vision technique for detecting color changes in stressed corn. ASAE Paper No. 91-3052, St. Joseph, MI.

Brown, G. K. 1991. Personal communication. Research Leader, USDA ARS, Agr. Eng. Dep., Michigan State Univ., East Lansing, MI.

Chesson, J. H., P. F. Burkner and R. M. Perkins. 1979. An experimental vacuum separator for dates. Transactions of the ASAE, 22(1):16-20.

Data Translation. 1991. Aurora User Manual. Data Translation Inc., 100 Locke Drive, Marlboro, MA 01752-1192.

Davenel, A., C. Guizard, T. Labarre and F. Sevila. 1988. Automatic detection of surface defects on fruit by using a vision system. Journal of Agricultural Engineering Research, 41(1):1-9.

Davies, J. 1992. Personal communication. Manager, Quality Control, Date Operations, Dole Dried Fruit and Nut Company, Thermal, CA.

Davies, J. and R. M. Perkins. 1991. Effect of illumination in grading dates. ASAE Paper No. 91-3547, St. Joseph, MI.

Delwiche, M. J., S. Tang and J. F. Thompson. 1990. Prune defect detection by line-scan imaging. Transactions of the ASAE, 33(3):950-954.

Dull, G. G., R. G. Leffler, G. S. Birth, A. Zaltzman and Z. Schmilovetch. 1991. The near infrared determination of moisture in whole dates. Hort. Science, 26(10):1303-1305.

Galloway, M. M. 1975. Texture analysis using gray level run length. Computer Graphics and Image Processing, 4:172-179.

Gonzalez, R. C. and R. E. Woods. 1992. Digital Image Processing. Addison-Wesley. Reading, MA.

Han, Y. J. and J. C. Hayes. 1988. Measuring crop residue cover using image processing. ASAE Paper No. 88-2137, St. Joseph, MI.

Han, Y. J. and Y. Feng. 1991. Feasibility of frequency domain inspection using Fourier transform. ASAE Paper No. 91-7541, St. Joseph, MI.

Han, Y. J., Y. Feng and C. L. Weller. 1992. Frequency domain inspection of corn kernal stress-cracks. ASAE Paper No. 92-7018, St. Joseph, MI.

Hand, D. J. 1982. Kernel Discriminant Analysis. Research Studies Press, Chichester, England.

Haralick, R. M., K. Shanmugam and I. Dinstein. 1973. Texture features for image classification. IEEE Tran. Syst. Man. Cybern. SMC-3:610-621.

Harms, H., U. Gunzer and H. M. Aus. 1986. Combined local color and texture analysis of stained cells. Computer Vision, Graphics, and Image Processing, 33:364-376.

He, D. C. and Li Wang. 1991. Texture features based on texture spectrum. Pattern Recognition, 24:391-399.

Horn, B. 1987. Robot Vision. The MIT Press, Cambridge, Massachusetts.

Howarth, M. S., J. R. Brandon, S. W. Searcy and N. Kehtarnavaze. 1990. Estimation of tip shape for carrot classification by machine vision. ASAE Paper No. 90-3530, St. Joseph, MI.

Howarth, M. S. and S. W. Searcy. 1989. Algorithms for grading carrots by machine vision. ASAE Paper No. 89-7502, St. Joseph, MI.

Huxsoll, C. C. and D. Reznik. 1969. Sorting and processing mechanically harvested dates. Date Grower's Institute Report, 46:8-10.

Jain, A. 1989. Fundamentals of Digital Image Processing. Prentice Hall, Englewood Cliffs, NJ.

Johnson, M. 1985. Automation in citrus sorting and packing. Proc. Agrimation I Conference and Exposition. ASAE Publication 01-85, pp. 63-68.

Kaplan, H. J., S. D. Scopatz and W. M. Miller. 1984. Analysis of manual and machine grading operations in California lemon packinghouses. Proc. Int. Soc. Citriculture, Vol. 1, pp. 532-537.

Krutz, G. W., P. E. H. Retersen, M. Rudemo and C. J. Precetti. 1991. Identification of weed seeds by color machine vision. ASAE Paper No. 91-7558, St. Joseph, MI.

Liao, K., J. F. Reid, M. R. Paulsen and E. E. Shaw. 1991. Corn kernel hardness classification by color segmentation. ASAE Paper No. 91-3504, St. Joseph MI.

Marchant, J. A., C. M. Onyango and M. J. Street. 1988. High speed sorting of potatoes using machine vision. ASAE Paper No. 88-3540, St. Joseph, MI.

McClure, J. E. and C. T. Morrow. 1987. Computer vision sorting of potatoes. ASAE Paper No. 87-6501, St. Joseph, MI.

Meyer, G. E., A. Stepanek, D. P. Shelton and E. C. Dickey. 1988. Electronic image analysis of crop residue cover on soil. Transactions of the ASAE, 31(3):968-973.

Miller, K. B. and M. J. Delwiche. 1988. A color vision system for peach grading. ASAE Paper No. 88-6025, St. Joseph, MI.

Miller, K. B. and M. J. Delwiche. 1989. Peach defect detection with machine vision. Transactions of the ASAE, 34(6):2588-2597.

North American Philips Lighting. 1984. Lighting Handbook. North American Philips Lighting Corporation, Bloomfield, NJ.

Okamura, K. Nancy, M. J. Delwiche and J. F. Thompson. 1991. Raisin grading by machine vision. ASAE Paper No. 91-7011, St. Joseph, MI.

Pratt, W. K. 1991. Digital Image Processing. John Wiley & Sons, New York.

Rehkugler, G. E. and J. A. Throop. 1985. Apple sorting with machine vision. ASAE Paper No. 85-3543, St. Joseph, MI.

Rehkugler, G. E. and J. A. Throop. 1989. Image processing algorithm for apple defect detection. Transactions of the ASAE, 32(1):267-272.

Ruzhitsky, V. N. and P. P. Ling. 1992. Machine vision for tomato seedling inspection. ASAE Paper No. 92-7020, St. Joseph, MI.

SAS Institute Inc. 1988. SAS/STAT User's Guide, Release 6.03 Edition. Cary, NC.

Sarkar, N. and R. R. Wolfe. 1985a. Feature extraction techniques for sorting tomatoes by computer vision. Transactions of the ASAE, 28(3):970-974.

Sarkar, N. and R. R. Wolfe. 1985b. Computer vision based system for quality separation of fresh market tomatoes. Transactions of the ASAE, 28(5):1714-1718.

Saudi Arabia Ministry of Agriculture & Water. 1987. Annual bulletin of current agricultural statistics ( sample survey). Department of Economic Studies & Statistics. Safir Press, Riyadh, Saudi Arabia (Arabic).

Schlotzhauer, S. D. and R. C. Littell. 1987. SAS System for Elementary Statistical Analysis. SAS Institute Inc. Cary, NC.

Shearer, S. A. and R. G. Holmes. 1987. Plant identification using color co-occurrence matrices. ASAE Paper No. 87-1534, St. Joseph, MI.

Singh, N., M. J. Delwiche, R. S. Johnson and J. Thompson. 1992. Peach maturity grading with color computer vision. ASAE Paper No. 92-3029, St. Joseph, MI.

Slaughter, C. D. and R. C. Harrell. 1987. Color vision in robotic fruit harvesting. Transactions of the ASAE, 30(4):144-148.

Tao, Y., C. T. Morrow, P. H. Heinemann and J. H. Sommer. 1990. Automated machine vision inspection of potatoes. ASAE Paper No. 90-3531, St. Joseph, MI.

United States Department of Agriculture - Agricultural Marketing Service. 1977. U. S. Standards for grades of dates. USDA, Washington, D.C.

Unklesbay, K., N. Unklesbay and J. Keller. 1986. Determination of internal color of beef ribeye steaks using digital image analysis. Food Microstructure, 5:227-231.

Varghese, Z., C. T. Morrow, P. H. Heinemann, H. J. Sommer, Y. Tao and R. M. Crassweller. 1991. Automated inspection of golden delicious apples using color computer vision. ASAE Paper No. 91-7002, St. Joseph, MI.

Weszka, J. S., C. R. Dyer and A. Rosenfeld. 1976. A comparative study of texture measures for terrain classification. IEEE Trans. on System, Man, and Cybernetics. SMC-6,4:269-285.

Wigger, W. D., M. R. Paulsen, J. B. Litchfield and J. B. Sinclair. 1988. Classification of fungal-damaged soybeans using color-image processing. ASAE Paper No. 88-3053, St. Joseph, MI.

Wilhoit, J. H., R. K. Byler, M. B. Koslav and D. H. Vaughan. 1990. Broccoli head sizing using image textural analysis. Transactions of the ASAE, 33(5):1736-1740.

Wolfe, R. R. and C. A. Hoernlein. 1988. Measurement of bell pepper coloration using machine vision. ASAE Paper No. 88-6018, St. Joseph, MI.

Wolfe, R. R. and M. Swaminathan. 1987. Determining orientation and shape of bell peppers by machine vision. Transactions of the ASAE, 30(6):1853-1856.

Wulfsohn, D., Y. Sarig and R. V. Algazi. 1989. Preliminary investigation to identify parameters for sorting of dates by image processing. ASAE Paper No. 89-6610, St. Joseph, MI.

# APPENDIX

## CLASSIFICATION ACCURACY OF CLASSES AND GRADES

TABLE XIV

CLASSIFICATION ACCURACY OF FIRST ROI

(1991 Crop, USDA Grading Standards)

| Model | Nat | N1D | N2D | Cull | TOTAL |
|---|---|---|---|---|---|
| HSI-1 | 84.0% | 44.0% | 62.0% | 52.0% | 60.5% |
| HSI-2 | 77.0% | 79.0% | 67.0% | 78.0% | 75.3% |
| HSI-3 | 87.0% | 77.0% | 60.0% | 58.0% | 70.5% |
| HSI-4 | 83.0% | 76.0% | 61.0% | 79.0% | 74.8% |
| HSI-5 | 94.0% | 96.0% | 87.0% | 87.0% | 91.0% |
| HSI-6 | 45.0% | 35.0% | 59.0% | 53.0% | 48.0% |
| HSI-7 | 76.0% | 18.0% | 48.0% | 35.0% | 44.3% |
| HSI-8 | 86.0% | 37.0% | 38.0% | 62.0% | 55.8% |
| HSI-9 | 88.0% | 62.0% | 77.0% | 77.0% | 76.0% |
| RGB-1 | 77.0% | 55.0% | 61.0% | 51.0% | 61.0% |
| RGB-2 | 84.0% | 71.0% | 57.0% | 76.0% | 72.0% |
| RGB-3 | 87.0% | 74.0% | 57.0% | 78.0% | 74.0% |
| RGB-4 | 89.0% | 69.0% | 69.0% | 70.0% | 74.3% |
| RGB-5 | 98.0% | 97.0% | 90.0% | 96.0% | 95.3% |
| RGB-6 | 85.0% | 29.0% | 71.0% | 32.0% | 54.3% |
| RGB-7 | 81.0% | 47.0% | 52.0% | 61.0% | 60.3% |
| RGB-8 | 69.0% | 56.0% | 51.0% | 28.0% | 51.0% |
| RGB-9 | 96.0% | 79.0% | 82.0% | 88.0% | 86.3% |

Nat - Classification accuracy of Natural Class.
N1D - Classification accuracy of Number 1 Dry Class.
N2D - Classification accuracy of Number 2 Dry Class.
Cull - Classification accuracy of Cull Class.
TOTAL - Average classification accuracy of all classes.

TABLE XV

CLASSIFICATION ACCURACY OF SECOND ROI

(1991 Crop, USDA Grading Standards)

| Model | Nat | N1D | N2D | Cull | TOTAL |
|---|---|---|---|---|---|
| HSI-1 | 74.0% | 48.0% | 62.0% | 57.0% | 60.3% |
| HSI-2 | 77.0% | 75.0% | 62.0% | 69.0% | 70.8% |
| HSI-3 | 85.0% | 81.0% | 73.0% | 63.0% | 75.5% |
| HSI-4 | 88.0% | 75.0% | 71.0% | 74.0% | 77.0% |
| HSI-5 | 97.0% | 94.0% | 95.0% | 91.0% | 94.3% |
| HSI-6 | 41.0% | 58.0% | 49.0% | 60.0% | 52.0% |
| HSI-7 | 78.0% | 17.0% | 34.0% | 63.0% | 48.0% |
| HSI-8 | 81.0% | 36.0% | 50.0% | 41.0% | 52.0% |
| HSI-9 | 86.0% | 72.0% | 75.0% | 68.0% | 75.3% |
| RGB-1 | 74.0% | 64.0% | 50.0% | 60.0% | 62.0% |
| RGB-2 | 85.0% | 70.0% | 67.0% | 79.0% | 75.3% |
| RGB-3 | 82.0% | 71.0% | 66.0% | 71.0% | 72.5% |
| RGB-4 | 86.0% | 76.0% | 77.0% | 59.0% | 74.5% |
| RGB-5 | 97.0% | 98.0% | 99.0% | 96.0% | 97.5% |
| RGB-6 | 60.0% | 53.0% | 53.0% | 58.0% | 56.0% |
| RGB-7 | 68.0% | 48.0% | 47.0% | 59.0% | 55.5% |
| RGB-8 | 86.0% | 49.0% | 59.0% | 38.0% | 58.0% |
| RGB-9 | 93.0% | 88.0% | 80.0% | 88.0% | 87.3% |

Nat - Classification accuracy of Natural Class.
N1D - Classification accuracy of Number 1 Dry Class.
N2D - Classification accuracy of Number 2 Dry Class.
Cull - Classification accuracy of Cull Class.
TOTAL - Average classification accuracy of all classes.

TABLE XVI

CLASSIFICATION ACCURACY OF THIRD ROI

(1991 Crop, USDA Grading Standards)

| Model | Nat | N1D | N2D | Cull | TOTAL |
|---|---|---|---|---|---|
| HSI-1 | 79.0% | 43.0% | 58.0% | 60.0% | 60.0% |
| HSI-2 | 75.0% | 68.0% | 76.0% | 63.0% | 70.5% |
| HSI-3 | 85.0% | 79.0% | 57.0% | 61.0% | 70.5% |
| HSI-4 | 85.0% | 67.0% | 62.0% | 75.0% | 72.3% |
| HSI-5 | 94.0% | 90.0% | 95.0% | 83.0% | 90.5% |
| HSI-6 | 24.0% | 48.0% | 61.0% | 53.0% | 46.5% |
| HSI-7 | 70.0% | 22.0% | 25.0% | 69.0% | 46.5% |
| HSI-8 | 83.0% | 42.0% | 50.0% | 52.0% | 56.8% |
| HSI-9 | 77.0% | 81.0% | 68.0% | 71.0% | 74.3% |
| RGB-1 | 72.0% | 40.0% | 47.0% | 69.0% | 57.0% |
| RGB-2 | 82.0% | 67.0% | 64.0% | 68.0% | 70.3% |
| RGB-3 | 75.0% | 80.0% | 46.0% | 68.0% | 67.3% |
| RGB-4 | 82.0% | 67.0% | 61.0% | 54.0% | 66.0% |
| RGB-5 | 98.0% | 95.0% | 94.0% | 96.0% | 95.8% |
| RGB-6 | 86.0% | 42.0% | 52.0% | 57.0% | 59.3% |
| RGB-7 | 66.0% | 63.0% | 56.0% | 50.0% | 58.8% |
| RGB-8 | 82.0% | 30.0% | 67.0% | 28.0% | 51.8% |
| RGB-9 | 95.0% | 80.0% | 83.0% | 85.0% | 85.8% |

Nat - Classification accuracy of Natural Class.
N1D - Classification accuracy of Number 1 Dry Class.
N2D - Classification accuracy of Number 2 Dry Class.
Cull - Classification accuracy of Cull Class.
TOTAL - Average classification accuracy of all classes.

TABLE XVII

CLASSIFICATION ACCURACY OF FOURTH ROI

(1991 Crop, USDA Grading Standards)

| Model | Nat | N1D | N2D | Cull | TOTAL |
|---|---|---|---|---|---|
| HSI-1 | 81.0% | 55.0% | 32.0% | 75.0% | 60.8% |
| HSI-2 | 84.0% | 72.0% | 67.0% | 81.0% | 76.0% |
| HSI-3 | 86.0% | 84.0% | 52.0% | 72.0% | 73.5% |
| HSI-4 | 81.0% | 83.0% | 56.0% | 83.0% | 75.8% |
| HSI-5 | 97.0% | 100.0% | 91.0% | 93.0% | 95.3% |
| HSI-6 | 56.0% | 52.0% | 40.0% | 77.0% | 56.3% |
| HSI-7 | 64.0% | 19.0% | 53.0% | 54.0% | 47.5% |
| HSI-8 | 70.0% | 64.0% | 58.0% | 52.0% | 61.0% |
| HSI-9 | 90.0% | 89.0% | 81.0% | 91.0% | 87.8% |
| RGB-1 | 81.0% | 55.0% | 39.0% | 73.0% | 62.0% |
| RGB-2 | 84.0% | 70.0% | 73.0% | 80.0% | 76.8% |
| RGB-3 | 88.0% | 73.0% | 54.0% | 72.0% | 71.8% |
| RGB-4 | 82.0% | 82.0% | 66.0% | 62.0% | 73.0% |
| RGB-5 | 100.0% | 95.0% | 95.0% | 96.0% | 96.5% |
| RGB-6 | 69.0% | 44.0% | 59.0% | 53.0% | 56.3% |
| RGB-7 | 72.0% | 49.0% | 56.0% | 41.0% | 54.5% |
| RGB-8 | 74.0% | 48.0% | 54.0% | 47.0% | 55.8% |
| RGB-9 | 89.0% | 84.0% | 78.0% | 91.0% | 85.5% |

Nat - Classification accuracy of Natural Class.
N1D - Classification accuracy of Number 1 Dry Class.
N2D - Classification accuracy of Number 2 Dry Class.
Cull - Classification accuracy of Cull Class.
TOTAL - Average classification accuracy of all classes.

TABLE XVIII

CLASSIFICATION ACCURACY OF FIRST ROI

(1991 Crop, Industry Grading Standards)

| Model | A | B | C | TOTAL |
|---|---|---|---|---|
| HSI-1 | 84.0% | 75.5% | 52.0% | 70.5% |
| HSI-2 | 77.0% | 87.5% | 78.0% | 80.8% |
| HSI-3 | 87.0% | 90.0% | 58.0% | 78.3% |
| HSI-4 | 83.0% | 82.5% | 79.0% | 81.5% |
| HSI-5 | 94.0% | 97.0% | 87.0% | 92.7% |
| HSI-6 | 45.0% | 69.5% | 53.0% | 55.8% |
| HSI-7 | 76.0% | 54.0% | 35.0% | 55.0% |
| HSI-8 | 86.0% | 48.5% | 62.0% | 65.5% |
| HSI-9 | 88.0% | 80.0% | 77.0% | 81.7% |
| RGB-1 | 77.0% | 79.0% | 51.0% | 69.0% |
| RGB-2 | 84.0% | 79.5% | 76.0% | 79.8% |
| RGB-3 | 87.0% | 80.5% | 78.0% | 81.8% |
| RGB-4 | 89.0% | 79.0% | 70.0% | 79.3% |
| RGB-5 | 98.0% | 97.5% | 96.0% | 97.2% |
| RGB-6 | 85.0% | 64.5% | 32.0% | 60.5% |
| RGB-7 | 81.0% | 63.0% | 61.0% | 68.3% |
| RGB-8 | 69.0% | 75.5% | 28.0% | 57.5% |
| RGB-9 | 96.0% | 88.5% | 88.0% | 90.8% |

A - Classification accuracy of Grade A.
B - Classification accuracy of Grade B.
C - Classification accuracy of Grade C.
TOTAL - Average classification accuracy of all grades.

TABLE XIX

CLASSIFICATION ACCURACY OF SECOND ROI

(1991 Crop, Industry Grading Standards)

| Model | A | B | C | TOTAL |
|---|---|---|---|---|
| HSI-1 | 74.0% | 77.0% | 57.0% | 69.3% |
| HSI-2 | 77.0% | 82.0% | 69.0% | 76.0% |
| HSI-3 | 85.0% | 91.5% | 63.0% | 79.8% |
| HSI-4 | 88.0% | 89.0% | 74.0% | 83.7% |
| HSI-5 | 97.0% | 99.5% | 91.0% | 95.8% |
| HSI-6 | 41.0% | 65.5% | 60.0% | 55.5% |
| HSI-7 | 78.0% | 37.5% | 63.0% | 59.5% |
| HSI-8 | 81.0% | 56.0% | 41.0% | 59.3% |
| HSI-9 | 86.0% | 82.0% | 68.0% | 78.7% |
| RGB-1 | 74.0% | 78.0% | 60.0% | 70.7% |
| RGB-2 | 85.0% | 82.0% | 79.0% | 82.0% |
| RGB-3 | 82.0% | 85.5% | 71.0% | 79.5% |
| RGB-4 | 86.0% | 90.0% | 59.0% | 78.3% |
| RGB-5 | 97.0% | 99.5% | 96.0% | 97.5% |
| RGB-6 | 60.0% | 65.0% | 58.0% | 61.0% |
| RGB-7 | 68.0% | 57.0% | 59.0% | 61.3% |
| RGB-8 | 86.0% | 70.5% | 38.0% | 64.8% |
| RGB-9 | 93.0% | 87.5% | 88.0% | 89.5% |

A - Classification accuracy of Grade A.
B - Classification accuracy of Grade B.
C - Classification accuracy of Grade C.
TOTAL - Average classification accuracy of all grades.

TABLE XX

CLASSIFICATION ACCURACY OF THIRD ROI

(1991 Crop, Industry Grading Standards)

| Model | A | B | C | TOTAL |
|---|---|---|---|---|
| HSI-1 | 79.0% | 78.0% | 60.0% | 72.3% |
| HSI-2 | 75.0% | 89.0% | 63.0% | 75.7% |
| HSI-3 | 85.0% | 87.0% | 61.0% | 77.7% |
| HSI-4 | 85.0% | 84.0% | 75.0% | 81.3% |
| HSI-5 | 94.0% | 99.0% | 83.0% | 92.0% |
| HSI-6 | 24.0% | 73.5% | 53.0% | 50.2% |
| HSI-7 | 70.0% | 38.0% | 69.0% | 59.0% |
| HSI-8 | 83.0% | 62.5% | 52.0% | 65.8% |
| HSI-9 | 77.0% | 89.0% | 71.0% | 79.0% |
| RGB-1 | 72.0% | 56.0% | 69.0% | 65.7% |
| RGB-2 | 82.0% | 82.0% | 68.0% | 77.3% |
| RGB-3 | 75.0% | 83.5% | 68.0% | 75.5% |
| RGB-4 | 82.0% | 87.0% | 54.0% | 74.3% |
| RGB-5 | 98.0% | 97.0% | 96.0% | 97.0% |
| RGB-6 | 86.0% | 63.0% | 57.0% | 68.7% |
| RGB-7 | 66.0% | 79.0% | 50.0% | 65.0% |
| RGB-8 | 82.0% | 72.5% | 28.0% | 60.8% |
| RGB-9 | 95.0% | 87.5% | 85.0% | 89.2% |

A - Classification accuracy of Grade A.
B - Classification accuracy of Grade B.
C - Classification accuracy of Grade C.
TOTAL - Average classification accuracy of all grades.

TABLE XXI

CLASSIFICATION ACCURACY OF FOURTH ROI

(1991 Crop, Industry Grading Standards)

| Model | A | B | C | TOTAL |
|---|---|---|---|---|
| HSI-1 | 81.0% | 67.0% | 75.0% | 74.3% |
| HSI-2 | 84.0% | 88.5% | 81.0% | 84.5% |
| HSI-3 | 86.0% | 87.0% | 72.0% | 81.7% |
| HSI-4 | 81.0% | 85.0% | 83.0% | 83.0% |
| HSI-5 | 97.0% | 100.0% | 93.0% | 96.7% |
| HSI-6 | 56.0% | 59.5% | 77.0% | 64.2% |
| HSI-7 | 64.0% | 53.0% | 54.0% | 57.0% |
| HSI-8 | 70.0% | 77.0% | 52.0% | 66.3% |
| HSI-9 | 90.0% | 90.0% | 91.0% | 90.3% |
| RGB-1 | 81.0% | 70.5% | 73.0% | 74.8% |
| RGB-2 | 84.0% | 84.0% | 80.0% | 82.7% |
| RGB-3 | 88.0% | 83.0% | 72.0% | 81.0% |
| RGB-4 | 82.0% | 89.0% | 62.0% | 77.7% |
| RGB-5 | 100.0% | 97.5% | 96.0% | 97.8% |
| RGB-6 | 69.0% | 66.0% | 53.0% | 62.7% |
| RGB-7 | 72.0% | 65.5% | 41.0% | 59.5% |
| RGB-8 | 74.0% | 66.5% | 47.0% | 62.5% |
| RGB-9 | 89.0% | 85.5% | 91.0% | 88.5% |

A - Classification accuracy of Grade A.
B - Classification accuracy of Grade B.
C - Classification accuracy of Grade C.
TOTAL - Average classification accuracy of all grades.

TABLE XXII

CLASSIFICATION ACCURACY OF FIRST ROI

(1992 Crop, USDA Grading Standards)

| Model | Nat | Waxy | N1D | N2D | Cull | TOTAL |
|---|---|---|---|---|---|---|
| HSI-1 | 87.0% | 41.0% | 85.0% | 60.0% | 57.0% | 66.0% |
| HSI-2 | 80.0% | 68.0% | 61.0% | 60.0% | 81.0% | 70.0% |
| HSI-3 | 87.0% | 67.0% | 64.0% | 68.0% | 60.0% | 69.2% |
| HSI-4 | 82.0% | 47.0% | 82.0% | 83.0% | 70.0% | 72.8% |
| HSI-5 | 94.0% | 86.0% | 96.0% | 92.0% | 96.0% | 92.8% |
| HSI-6 | 57.0% | 29.0% | 53.0% | 41.0% | 69.0% | 49.8% |
| HSI-7 | 74.0% | 9.0% | 38.0% | 65.0% | 27.0% | 42.6% |
| HSI-8 | 85.0% | 45.0% | 57.0% | 57.0% | 53.0% | 59.4% |
| HSI-9 | 94.0% | 73.0% | 89.0% | 84.0% | 89.0% | 85.8% |
| RGB-1 | 59.0% | 47.0% | 71.0% | 43.0% | 65.0% | 57.0% |
| RGB-2 | 89.0% | 53.0% | 83.0% | 88.0% | 76.0% | 77.8% |
| RGB-3 | 84.0% | 56.0% | 81.0% | 75.0% | 72.0% | 73.6% |
| RGB-4 | 91.0% | 54.0% | 77.0% | 79.0% | 73.0% | 74.8% |
| RGB-5 | 100.0% | 99.0% | 100.0% | 99.0% | 98.0% | 99.2% |
| RGB-6 | 64.0% | 47.0% | 23.0% | 30.0% | 70.0% | 46.8% |
| RGB-7 | 83.0% | 50.0% | 60.0% | 59.0% | 44.0% | 59.2% |
| RGB-8 | 57.0% | 25.0% | 60.0% | 46.0% | 74.0% | 52.4% |
| RGB-9 | 88.0% | 78.0% | 76.0% | 74.0% | 84.0% | 80.0% |

Nat - Classification accuracy of Natural Class.
Waxy - Classification accuracy of Waxy Class.
N1D - Classification accuracy of Number 1 Dry Class.
N2D - Classification accuracy of Number 2 Dry Class.
Cull - Classification accuracy of Cull Class.
TOTAL - Average classification accuracy of all classes.

TABLE XXIII

CLASSIFICATION ACCURACY OF SECOND ROI

(1992 Crop, USDA Grading Standards)

| Model | Nat | Waxy | N1D | N2D | Cull | TOTAL |
|---|---|---|---|---|---|---|
| HSI-1 | 83.0% | 44.0% | 82.0% | 62.0% | 68.0% | 67.8% |
| HSI-2 | 74.0% | 77.0% | 62.0% | 52.0% | 83.0% | 69.6% |
| HSI-3 | 86.0% | 81.0% | 60.0% | 66.0% | 73.0% | 73.2% |
| HSI-4 | 79.0% | 66.0% | 67.0% | 75.0% | 71.0% | 71.6% |
| HSI-5 | 95.0% | 95.0% | 91.0% | 95.0% | 94.0% | 94.0% |
| HSI-6 | 45.0% | 45.0% | 57.0% | 45.0% | 63.0% | 51.0% |
| HSI-7 | 75.0% | 27.0% | 26.0% | 41.0% | 27.0% | 39.2% |
| HSI-8 | 75.0% | 53.0% | 50.0% | 59.0% | 61.0% | 59.6% |
| HSI-9 | 83.0% | 72.0% | 81.0% | 86.0% | 84.0% | 81.2% |
| RGB-1 | 58.0% | 40.0% | 53.0% | 48.0% | 72.0% | 54.2% |
| RGB-2 | 94.0% | 76.0% | 69.0% | 75.0% | 82.0% | 79.2% |
| RGB-3 | 76.0% | 69.0% | 72.0% | 72.0% | 73.0% | 72.4% |
| RGB-4 | 90.0% | 65.0% | 78.0% | 80.0% | 79.0% | 78.4% |
| RGB-5 | 100.0% | 99.0% | 96.0% | 100.0% | 96.0% | 98.2% |
| RGB-6 | 68.0% | 34.0% | 59.0% | 60.0% | 78.0% | 59.8% |
| RGB-7 | 83.0% | 45.0% | 58.0% | 52.0% | 67.0% | 61.0% |
| RGB-8 | 64.0% | 31.0% | 48.0% | 55.0% | 69.0% | 53.4% |
| RGB-9 | 96.0% | 86.0% | 84.0% | 85.0% | 92.0% | 88.6% |

Nat - Classification accuracy of Natural Class.
Waxy - Classification accuracy of Waxy Class.
N1D - Classification accuracy of Number 1 Dry Class.
N2D - Classification accuracy of Number 2 Dry Class.
Cull - Classification accuracy of Cull Class.
TOTAL - Average classification accuracy of all classes.

TABLE XXIV

CLASSIFICATION ACCURACY OF THIRD ROI

(1992 Crop, USDA Grading Standards)

| Model | Nat | Waxy | N1D | N2D | Cull | TOTAL |
|---|---|---|---|---|---|---|
| HSI-1 | 82.0% | 46.0% | 82.0% | 50.0% | 59.0% | 63.8% |
| HSI-2 | 83.0% | 70.0% | 63.0% | 55.0% | 83.0% | 70.8% |
| HSI-3 | 87.0% | 73.0% | 61.0% | 65.0% | 62.0% | 69.6% |
| HSI-4 | 81.0% | 64.0% | 64.0% | 64.0% | 71.0% | 68.8% |
| HSI-5 | 96.0% | 94.0% | 89.0% | 90.0% | 95.0% | 92.8% |
| HSI-6 | 34.0% | 42.0% | 55.0% | 37.0% | 63.0% | 46.2% |
| HSI-7 | 76.0% | 19.0% | 32.0% | 59.0% | 21.0% | 41.4% |
| HSI-8 | 85.0% | 47.0% | 41.0% | 47.0% | 56.0% | 55.2% |
| HSI-9 | 94.0% | 73.0% | 71.0% | 72.0% | 90.0% | 80.0% |
| RGB-1 | 64.0% | 44.0% | 63.0% | 47.0% | 61.0% | 55.8% |
| RGB-2 | 96.0% | 77.0% | 70.0% | 80.0% | 75.0% | 79.6% |
| RGB-3 | 78.0% | 68.0% | 68.0% | 73.0% | 75.0% | 72.4% |
| RGB-4 | 89.0% | 73.0% | 71.0% | 71.0% | 79.0% | 76.6% |
| RGB-5 | 100.0% | 99.0% | 97.0% | 96.0% | 100.0% | 98.4% |
| RGB-6 | 49.0% | 24.0% | 47.0% | 48.0% | 69.0% | 47.4% |
| RGB-7 | 80.0% | 42.0% | 52.0% | 20.0% | 67.0% | 52.2% |
| RGB-8 | 56.0% | 38.0% | 43.0% | 48.0% | 67.0% | 50.4% |
| RGB-9 | 86.0% | 83.0% | 78.0% | 70.0% | 92.0% | 81.8% |

Nat - Classification accuracy of Natural Class.
Waxy - Classification accuracy of Waxy Class.
N1D - Classification accuracy of Number 1 Dry Class.
N2D - Classification accuracy of Number 2 Dry Class.
Cull - Classification accuracy of Cull Class.
TOTAL - Average classification accuracy of all classes.

TABLE XXV

CLASSIFICATION ACCURACY OF FOURTH ROI

(1992 Crop, USDA Grading Standards)

| Model | Nat | Waxy | N1D | N2D | Cull | TOTAL |
|---|---|---|---|---|---|---|
| HSI-1 | 84.0% | 37.0% | 76.0% | 56.0% | 75.0% | 65.6% |
| HSI-2 | 72.0% | 69.0% | 57.0% | 67.0% | 74.0% | 67.8% |
| HSI-3 | 90.0% | 75.0% | 64.0% | 77.0% | 79.0% | 77.0% |
| HSI-4 | 80.0% | 67.0% | 68.0% | 83.0% | 69.0% | 73.4% |
| HSI-5 | 94.0% | 94.0% | 81.0% | 93.0% | 90.0% | 90.4% |
| HSI-6 | 59.0% | 22.0% | 44.0% | 45.0% | 72.0% | 48.4% |
| HSI-7 | 62.0% | 12.0% | 40.0% | 55.0% | 45.0% | 42.8% |
| HSI-8 | 77.0% | 48.0% | 57.0% | 55.0% | 60.0% | 59.4% |
| HSI-9 | 78.0% | 57.0% | 80.0% | 82.0% | 77.0% | 74.8% |
| RGB-1 | 64.0% | 43.0% | 68.0% | 48.0% | 77.0% | 60.0% |
| RGB-2 | 90.0% | 59.0% | 76.0% | 82.0% | 72.0% | 75.8% |
| RGB-3 | 80.0% | 70.0% | 71.0% | 84.0% | 74.0% | 75.8% |
| RGB-4 | 95.0% | 63.0% | 76.0% | 76.0% | 78.0% | 77.6% |
| RGB-5 | 100.0% | 99.0% | 96.0% | 96.0% | 98.0% | 97.8% |
| RGB-6 | 70.0% | 40.0% | 33.0% | 62.0% | 62.0% | 53.4% |
| RGB-7 | 84.0% | 45.0% | 60.0% | 50.0% | 51.0% | 58.0% |
| RGB-8 | 48.0% | 22.0% | 58.0% | 61.0% | 60.0% | 49.8% |
| RGB-9 | 89.0% | 78.0% | 81.0% | 89.0% | 79.0% | 83.2% |

Nat - Classification accuracy of Natural Class.
Waxy - Classification accuracy of Waxy Class.
N1D - Classification accuracy of Number 1 Dry Class.
N2D - Classification accuracy of Number 2 Dry Class.
Cull - Classification accuracy of Cull Class.
TOTAL - Average classification accuracy of all classes.

TABLE XXVI

CLASSIFICATION ACCURACY OF FIRST ROI

(1992 Crop, Industry Grading Standards)

| Model | A | B | C | TOTAL |
|---|---|---|---|---|
| HSI-1 | 87.0% | 87.7% | 57.0% | 77.2% |
| HSI-2 | 80.0% | 81.3% | 81.0% | 80.8% |
| HSI-3 | 87.0% | 90.7% | 60.0% | 79.2% |
| HSI-4 | 82.0% | 94.7% | 70.0% | 82.2% |
| HSI-5 | 94.0% | 99.3% | 96.0% | 96.4% |
| HSI-6 | 57.0% | 72.0% | 69.0% | 66.0% |
| HSI-7 | 74.0% | 69.3% | 27.0% | 56.8% |
| HSI-8 | 85.0% | 76.7% | 53.0% | 71.6% |
| HSI-9 | 94.0% | 92.7% | 89.0% | 91.9% |
| RGB-1 | 59.0% | 81.3% | 65.0% | 68.4% |
| RGB-2 | 89.0% | 95.0% | 76.0% | 86.7% |
| RGB-3 | 84.0% | 92.0% | 72.0% | 82.7% |
| RGB-4 | 91.0% | 93.0% | 73.0% | 85.7% |
| RGB-5 | 100.0% | 100.0% | 98.0% | 99.3% |
| RGB-6 | 64.0% | 60.0% | 70.0% | 64.7% |
| RGB-7 | 83.0% | 78.0% | 44.0% | 68.3% |
| RGB-8 | 57.0% | 75.3% | 74.0% | 68.8% |
| RGB-9 | 88.0% | 89.3% | 84.0% | 87.1% |

A - Classification accuracy of Grade A.
B - Classification accuracy of Grade B.
C - Classification accuracy of Grade C.
TOTAL - Average classification accuracy of all grades.

TABLE XXVII

CLASSIFICATION ACCURACY OF SECOND ROI

(1992 Crop, Industry Grading Standards)

| Model | A | B | C | TOTAL |
|---|---|---|---|---|
| HSI-1 | 83.0% | 84.0% | 68.0% | 78.3% |
| HSI-2 | 74.0% | 86.3% | 83.0% | 81.1% |
| HSI-3 | 86.0% | 92.7% | 73.0% | 83.9% |
| HSI-4 | 79.0% | 93.3% | 71.0% | 81.1% |
| HSI-5 | 95.0% | 99.3% | 94.0% | 96.1% |
| HSI-6 | 45.0% | 72.0% | 63.0% | 60.0% |
| HSI-7 | 75.0% | 62.3% | 27.0% | 54.8% |
| HSI-8 | 75.0% | 78.0% | 61.0% | 71.3% |
| HSI-9 | 83.0% | 91.7% | 84.0% | 86.2% |
| RGB-1 | 58.0% | 72.3% | 72.0% | 67.4% |
| RGB-2 | 94.0% | 92.7% | 82.0% | 89.6% |
| RGB-3 | 76.0% | 92.7% | 73.0% | 80.6% |
| RGB-4 | 90.0% | 94.3% | 79.0% | 87.8% |
| RGB-5 | 100.0% | 100.0% | 96.0% | 98.7% |
| RGB-6 | 68.0% | 73.7% | 78.0% | 73.2% |
| RGB-7 | 83.0% | 71.7% | 67.0% | 73.9% |
| RGB-8 | 64.0% | 73.3% | 69.0% | 68.8% |
| RGB-9 | 96.0% | 91.7% | 92.0% | 93.2% |

A - Classification accuracy of Grade A.
B - Classification accuracy of Grade B.
C - Classification accuracy of Grade C.
TOTAL - Average classification accuracy of all grades.

TABLE XXVIII

CLASSIFICATION ACCURACY OF THIRD ROI

(1992 Crop, Industry Grading Standards)

| Model | A | B | C | TOTAL |
|---|---|---|---|---|
| HSI-1 | 82.0% | 83.7% | 59.0% | 74.9% |
| HSI-2 | 83.0% | 83.3% | 83.0% | 83.1% |
| HSI-3 | 87.0% | 91.0% | 62.0% | 80.0% |
| HSI-4 | 81.0% | 90.7% | 71.0% | 80.9% |
| HSI-5 | 96.0% | 98.7% | 95.0% | 96.6% |
| HSI-6 | 34.0% | 69.0% | 63.0% | 55.3% |
| HSI-7 | 76.0% | 73.0% | 21.0% | 56.7% |
| HSI-8 | 85.0% | 66.7% | 56.0% | 69.2% |
| HSI-9 | 94.0% | 84.0% | 90.0% | 89.3% |
| RGB-1 | 64.0% | 78.0% | 61.0% | 67.7% |
| RGB-2 | 96.0% | 93.3% | 75.0% | 88.1% |
| RGB-3 | 78.0% | 92.0% | 75.0% | 81.7% |
| RGB-4 | 89.0% | 91.7% | 79.0% | 86.6% |
| RGB-5 | 100.0% | 99.7% | 100.0% | 99.9% |
| RGB-6 | 49.0% | 67.7% | 69.0% | 61.9% |
| RGB-7 | 80.0% | 62.3% | 67.0% | 69.8% |
| RGB-8 | 56.0% | 70.0% | 67.0% | 64.3% |
| RGB-9 | 86.0% | 85.7% | 92.0% | 87.9% |

A - Classification accuracy of Grade A.
B - Classification accuracy of Grade B.
C - Classification accuracy of Grade C.
TOTAL - Average classification accuracy of all grades.

TABLE XXIX

CLASSIFICATION ACCURACY OF FOURTH ROI

(1992 Crop, Industry Grading Standards)

| Model | A | B | C | TOTAL |
|---|---|---|---|---|
| HSI-1 | 84.0% | 80.3% | 75.0% | 79.8% |
| HSI-2 | 72.0% | 86.3% | 74.0% | 77.4% |
| HSI-3 | 90.0% | 91.7% | 79.0% | 86.9% |
| HSI-4 | 80.0% | 95.0% | 69.0% | 81.3% |
| HSI-5 | 94.0% | 98.3% | 90.0% | 94.1% |
| HSI-6 | 59.0% | 59.7% | 72.0% | 63.6% |
| HSI-7 | 62.0% | 71.7% | 45.0% | 59.6% |
| HSI-8 | 77.0% | 81.7% | 60.0% | 72.9% |
| HSI-9 | 78.0% | 95.0% | 77.0% | 83.3% |
| RGB-1 | 64.0% | 75.0% | 77.0% | 72.0% |
| RGB-2 | 90.0% | 95.3% | 72.0% | 85.8% |
| RGB-3 | 80.0% | 97.0% | 74.0% | 83.7% |
| RGB-4 | 95.0% | 93.7% | 78.0% | 88.9% |
| RGB-5 | 100.0% | 100.0% | 98.0% | 99.3% |
| RGB-6 | 70.0% | 74.3% | 62.0% | 68.8% |
| RGB-7 | 84.0% | 76.7% | 51.0% | 70.6% |
| RGB-8 | 48.0% | 83.7% | 60.0% | 63.9% |
| RGB-9 | 89.0% | 95.3% | 79.0% | 87.8% |

A - Classification accuracy of Grade A.
B - Classification accuracy of Grade B.
C - Classification accuracy of Grade C.
TOTAL - Average classification accuracy of all grades.

VITA

Abdulrahman A. Al-Janobi

Candidate for the Degree of

Doctor of Philosophy

Thesis: MACHINE VISION INSPECTION OF DATE FRUITS

Major Field: Agricultural Engineering

Biographical:

Personal Data: Born in S. Alalaya, Saudi Arabia, January 1, 1963, the son of Abdulaziz AL-Janobi.

Education: Graduated from Almajmah High School, Almajmah, Saudi Arabia, in 1981; received Bachelor of Agriculture Science Degree from King Saud University at Riyadh, Saudi Arabia, in January, 1986; received Master of Science in Agricultural Engineering from Oklahoma State University at Stillwater in December, 1990; completed requirements for the Doctor of Philosophy degree at Oklahoma State University in May, 1993.

Professional Experience: Teaching Assistant, Department of Agricultural Engineering, King Saud University, January, 1986 to December, 1986.

Professional Organizations: Institute of Electrical and Electronic Engineers, The International Society for Optical Engineering.